

STUDIES TO ELUCIDATE THE MECHANISM OF REDUCED FLAVIN TRANSFER
IN THE ALKANESULFONATE MONOOXYGENASE SYSTEM
FROM ESCHERICHIA COLI

Except where reference is made to the work of others, the work described in this dissertation is my own or was done in collaboration with my advisory committee.
This dissertation does not include proprietary or classified information.

Kholis Abdurachim

Certificate of Approval:

Marie W. Wooten
Professor
Biological Science

Holly R. Ellis, Chair
Associate Professor
Chemistry and Biochemistry

Douglas C. Goodwin
Associate Professor
Chemistry and Biochemistry

Evert C. Duin
Assistant Professor
Chemistry and Biochemistry

George T. Flowers
Interim Dean
Graduate School

STUDIES TO ELUCIDATE THE MECHANISM OF REDUCED FLAVIN TRANSFER
IN THE ALKANESULFONATE MONOOXYGENASE SYSTEM
FROM ESCHERICHIA COLI

Kholis Abdurachim

A Dissertation

Submitted to

the Graduate Faculty of

Auburn University

in Partial Fulfillment of the

Requirements for the

Degree of

Doctor of Philosophy

Auburn, Alabama
December 17, 2007

STUDIES TO ELUCIDATE THE MECHANISM OF REDUCED FLAVIN TRANSFER
IN THE ALKANESULFONATE MONOOXYGENASE SYSTEM
FROM ESCHERICHIA COLI

Kholis Abdurachim

Permission is granted to Auburn University to make copies of this dissertation at its discretion, upon request of individuals or institutions and at their expense.
The author reserves all publication rights.

Signature of Author

Date of Graduation

VITA

Kholis Abdurachim Audah, son of Al-Hajj Abdurachim Audah and Khadijah Muhasim, was born in June 21, 1973, in Tangerang, Banten Province, the Republic of Indonesia. He did his undergraduate research at the Center for Biotechnology for Estate Crops, Indonesia under supervision of Dr. Hasim, DEA and Dr. Siswanto, DEA from September, 1995 to March, 1996. He graduated with a Bachelor of Science degree in Chemistry in 1996 from Bogor Agricultural University, Indonesia. He completed his M.S. degree in Molecular Biology (with Distinction) at University of Malaya, Malaysia in 2000 in Dr. Amir Feisal Merican laboratory. From 2000 to 2001, he worked as a research assistant in the same laboratory. He worked for Indonesian Government in the Nuclear Energy Control Board in 2002. He married Rifia Amalia, on January 14, 2000. They are blessed with three wonderful children, Hilyatushalihah Audah (daughter), Hanif Arkan Audah (son), and Hilwah Imani Audah (daughter). In spring 2003, he started his doctorate program at Auburn University in the Department of Chemistry and Biochemistry where he joined Dr. Holly R. Ellis laboratory for his research project towards the completion of his PhD degree.

DISSERTATION ABSTRACT

STUDIES TO ELUCIDATE THE MECHANISM OF REDUCED FLAVIN TRANSFER
IN THE ALKANESULFONATE MONOOXYGENASE SYSTEM
FROM ESCHERICHIA COLI

Kholis Abdurachim

Doctor of Philosophy, December 17, 2007
(M.S., University of Malaya, 2000)
(B.S., Bogor Agricultural University, 1996)

197 Typed Pages

Directed by Holly R. Ellis

The two-component alkanesulfonate monooxygenase system utilizes reduced flavin as a substrate to catalyze a unique desulfonation reaction during times of sulfur starvation. The flavin reductase (SsuE) provides reduced flavin for the monooxygenase (SsuD) reaction. The mechanism of reduced flavin transfer was analyzed in these studies. The results from affinity chromatography and cross-linking experiments support the formation of a stable complex between SsuE and SsuD enzymes. Interactions between the two proteins did not lead to overall conformational changes in protein structure, as indicated by the results from circular dichroism spectroscopy in the far-UV region. However, subtle changes in the flavin environment of FMN-bound SsuE that occur in the presence of SsuD were identified by circular dichroism spectroscopy in the

visible region. These data are supported by the results from fluorescent spectroscopy experiments, where a dissociation constant of $0.002 \pm 0.001 \mu\text{M}$ was obtained for the binding of SsuE to SsuD. A 1:1 stoichiometric ratio for monomeric binding between SsuE and SsuD supports a structural model involving four dimers of SsuE bound to a tetramer of SsuD.

The results from cross-linking experiments using a zero length cross-linker suggest that protein-protein interactions might occur between a negatively charge amino acid residue such as aspartate or glutamate of SsuE with a positively charge amino group of SsuD (arginine, lysine, or histidine). However, MALDI-TOF MS failed to determine the exact residues involved in protein-protein interactions due to the low amount of cross-linking products.

Rapid reaction kinetic analyses were performed to investigate the effect of protein-protein interactions between SsuE and SsuD on SsuE-catalyzed flavin reduction and charge transfer formation. The results showed that in the presence of SsuD the rate of the third phase of flavin reduction increased approximately 200-fold compared to the reaction by SsuE alone. Furthermore, in a coupled-enzyme system monitored at 550 nm, the rate for the second phase representing the charge transfer formation between FMNH₂ and NADP⁺ showed 10-fold increase compared to FMN reduction by SsuE alone. Taken together, these results suggest that SsuD is essential for efficient reduced flavin transfer. In this case, the reduced flavin may be rapidly transferred from SsuE to SsuD through a channeling mechanism. In addition, the results also suggest that SsuE-catalyzed flavin reduction is affected by the SsuD-catalyzed reaction through allosteric communication.

ACKNOWLEDGEMENTS

In the name of God, the Most Gracious, the Most Merciful. Praise be to God, the Lord of the universe and peace be upon the Prophet Muhammad.

First of all, I would like to express my highest appreciation to my advisor, Dr. Holly R. Ellis. I am greatly indebted to her for her invaluable guidance, support, encouragement and help throughout my study. Secondly, I would like to thank my committee members Dr. Marie W. Wooten, Dr. Douglas C. Goodwin, and Dr. Evert C. Duin for their help and constructive suggestion to my dissertation. I also want to thank my former and current lab members, Dr. Benlian Gao, Xuanzhi Zhan, Russell Carpenter, Honglei Sun, Erin Imsand, Mary Millwood, and Rajakumari Ramaswamy for their meaningful discussions and help. I would like to thank all professors and the administration assistants at the Department of Chemistry and Biochemistry, and all my friends at Auburn who directly or indirectly contribute to the success of my study. I would like to thank the Department of Chemistry and Biochemistry, Auburn University, and National Science Foundation for their funding for my research.

Last but not least, I would like to express my deepest gratitude to my beloved wife and my wonderful children, my parents Umi and Abah, and other family members for their understanding, love, help, and continuous prayers throughout these hard years. I would not be able to make it without their support.

Style manual used: The Journal of Bacteriology

Computer software used: Microsoft Word, ChemDraw, Microsoft Excel, and KaleidaGraph

TABLE OF CONTENTS

LIST OF TABLES.....	xii
LIST OF FIGURES.....	xiii
CHAPTER ONE: LITERATURE REVIEW.....	1
1.1 The role of sulfur in organisms.....	1
1.2 Primary sulfur sources and their assimilation in bacteria.....	6
1.3 Defense mechanism against sulfur starvation in bacteria.....	8
1.4 Alternative sulfur sources for bacteria during sulfate starvation.....	10
1.5 Gene clusters responsible for sulfate-starvation induced proteins in bacteria.....	10
1.6 Regulatory proteins of sulfur assimilation in <i>E. coli</i>	17
1.7 The alkanesulfonate monooxygenase system from <i>E. coli</i>	18
1.8 Flavins and flavoproteins.....	20
1.9 The Alkanesulfonate monooxygenase proteins.....	33
1.10 Reduced flavin and reduced flavin transfer in biological systems.....	42
1.11 Basic principles of protein-protein interactions.....	53
1.12 Research objectives.....	61

CHAPTER TWO: MATERIALS AND METHODS.....	63
2.1 Bacterial strains and plasmid vectors.....	63
2.2 Biochemical and chemical reagents.....	63
2.3 Construction and expression of double cloning expression system.....	65
2.4 Construction and expression of recombinant proteins.....	68
2.5 Affinity chromatography binding assay.....	69
2.6 Far-UV circular dichroism.....	70
2.7 Visible circular dichroism.....	70
2.8 Fluorescence spectroscopy.....	71
2.9 UV-visible spectroscopy of filtration of FMN-bound SsuE.....	73
2.10 Isothermal titration calorimetry.....	73
2.11 Chemical cross-linking.....	73
2.12 Pre-steady state kinetic experiments.....	80
2.13 UV-visible spectroscopy of FMNH ₂	83
CHAPTER THREE: RESULTS.....	84
3.1 Construction and expression of double cloning expression system in <i>E. coli</i>	84
3.2 Affinity chromatography.....	87
3.3 Secondary structure changes due to protein-protein interactions.....	93
3.4 Binding of SsuD to FMN-bound SsuE.....	97
3.5 Isothermal titration calorimetry.....	101
3.6 Trifunctional chemical cross-linking.....	101
3.7 Determination of amino acid residues involved in protein-protein	

interactions between SsuE and SsuD proteins.....	106
3.8 The effect of protein-protein interactions on SsuE-catalyzed flavin reduction.....	122
CHAPTER FOUR: DISCUSSION.....	136
4.1 Formation of insoluble proteins in the coexpression of SsuE and SsuD.....	137
4.2 Detection of protein-protein interactions in the alkanesulfonate monooxygenase system.....	139
4.3 Amino acid residues involved in protein-protein interactions between SsuE and SsuD.....	143
4.4 The importance of protein-protein interactions for efficient flavin reduction and reduced flavin transfer.....	147
4.5 Conclusion.....	156
REFERENCES.....	158

LIST OF TABLES

Table 1.1 Sulfate-regulated proteins of <i>E. coli</i> and <i>P. aeruginosa</i>	9
Table 1.2 Natural and synthetic sulfonates and sulfate ester.....	11
Table 1.3 Substrate for alkanesulfonate monooxygenase SsuD and α-KG-dependent taurine dioxygenase TauD.....	16
Table 1.4 Kinetic parameters of alkanesulfonate monooxygenase with various substrates.....	43
Table 2.1 Bacterial <i>E. coli</i> strains used for protein expression.....	64
Table 3.1 The molecular weight for the tryptically-digested SsuE peptide fragments.....	119
Table 3.2 The molecular weight for the tryptically-digested SsuD peptide fragments.....	121
Table 3.3 Rates for FMN reduction and charge transfer formation.....	126
Table 3.4 Rates for charge transfer formation in coupled-enzyme reactions with different oxygen concentration.....	131

LIST OF FIGURES

Figure 1.1 Structures of the sulfur-containing amino acids.....	2
Figure 1.2 Two major route of sulfur assimilation into microorganisms.....	7
Figure 1.3 Assimilation of sulfur from different sources in normal environment condition and during sulfate-starvation in <i>E. coli</i>	12
Figure 1.4 Gene clusters responsible for the synthesis of Ssi proteins in several bacterial species.....	13
Figure 1.5 Substrates uptake from different sulfur sources by TauABC and SsuABC transporter system in <i>E. coli</i> during sulfur starvation condition.....	15
Figure 1.6 Model for the regulation of sulfur assimilation by CysB and Cbl in <i>E. coli</i>	19
Figure 1.7 Overall reactions in the alkanesulfonate monooxygenase system from <i>E. coli</i>	21
Figure 1.8 Structures of Riboflavin, FMN, and FAD.....	22
Figure 1.9 The structures of flavin in three different oxidation states.....	24
Figure 1.10 The spectra of flavin in different oxidation states.....	26
Figure 1.11 Reactive by products generated from reaction between reduced flavin and molecular oxygen.....	31

Figure 1.12 Alignment of SsuE from <i>E. coli</i> (SsuE_Ecoli) with flavoprotein sequence from different bacterial species.....	35
Figure 1.13 Three dimensional structure of the alkanesulfonate monooxygenase monomer.....	38
Figure 1.14 The active-site pocket of alkanesulfonate monooxygenase in stick and space-filling model.....	39
Figure 1.15 Sequence alignment of SsuD from <i>E. coli</i> with its <i>Bacillus</i> <i>subtilis</i> homologue SsuD_Bs, <i>C. heintzii</i> nitrilotriacetate monooxygenase NtaA, <i>S. ristinaespiralis</i> pristinomycin synthase subunit A SnaA, <i>Rhodococcus sp.</i> IGTS8 dibenzothiophene desulfurization enzyme SoxA.....	41
Figure 1.16 Autoxidation reaction of reduced flavin with molecular oxygen.....	46
Figure 1.17 Mechanism of reduced flavin transfer through free diffusion between flavin oxidoreductase and flavin monooxygenase.....	48
Figure 1.18 Direct reduced flavin transfer through channeling mechanism between a dimeric flavin reductase and flavin monooxygenase.....	50
Figure 1.19 Mixed mechanism of reduced flavin transfer between NADH-specific flavin reductase (SMOB) to the FAD-specific styrene epoxidase (SMOA) from <i>Pseudomonas putida</i> S12.....	52
Figure 2.1 The pETDuet-1 vector expression system containing two multiple Cloning sites (MCS1 and MCS2).....	66
Figure 2.2 ProFound Label Transfer Sulfo-SBED {sulfosuccinimidyl[2,6 -(biotinamido)-2-(<i>p</i> -azidobenzamido)-hexanoamido]-ethyl-1,3'-	

dithiopropionate } Protein:Protein Interaction Agent.....	75
Figure 2.3 Cross-linking reagents used for determination of amino acid residues involved in protein-protein interactions between SsuE and SsuD.....	77
Figure 3.1 Subcloning of His-tagged <i>ssuE</i> and <i>ssuD</i> genes into double multiple cloning sites (MCS1 and MCS2) of pETDuet-1 plasmid.....	85
Figure 3.2 Agarose gel electrophoresis of double cloned of His-tagged <i>ssuE</i> and <i>ssuD</i> genes into pETDuet-1 plasmid expression system.....	86
Figure 3.3 Expression of pKAA-12 plasmid expression system containing SsuD and His-tagged SsuE in different <i>E. coli</i> K-12 strains.....	88
Figure 3.4 SDS-PAGE (10% acrylamide) from affinity chromatography experiments with SsuE and His-tagged SsuD.....	90
Figure 3.5 SDS-PAGE (10% acrylamide) from affinity chromatography experiments with SsuE in the absence of His-tagged SsuD.....	91
Figure 3.6 SDS-PAGE (10% acrylamide) from affinity chromatography experiments with rat cysteine dioxygenase and His-tagged SsuD.....	92
Figure 3.7 Far-UV CD spectroscopy of SsuE and SsuD.....	94
Figure 3.8 Visible CD spectra for FMN in the absence and presence of SsuE and SsuD.....	95
Figure 3.9 Visible CD spectra for FMN in the absence and presence of SsuD.....	96
Figure 3.10 Fluorometric titration of SsuE to FMN.....	98
Figure 3.11 Fluorometric titration of SsuD to FMN-bound SsuE and determination of binding constant between SsuE and SsuD.....	99
Figure 3.12 UV-visible spectra for filtration of FMN in the presence of SsuE	

and SsuD proteins.....	100
Figure 3.13 Isothermal titration calorimetry measurements to determine the thermodynamic properties of protein-protein interactions between SsuE and SsuD proteins.....	102
Figure 3.14 Complex formation between SsuE and SsuD by trifunctional cross-linking reagent. Biotin label was transferred from SsuE to SsuD following disulfide bond cleavage by DTT.....	104
Figure 3.15 Silver-stained gel electrophoresis of cross-linking experiments between SsuE and SsuD proteins.....	105
Figure 3.16 Silver-stained gel electrophoresis of DTT-treated cross-linked SsuE and SsuD.....	107
Figure 3.17 Reaction of EDC and sulfo-NHS cross-linking reagents with carboxyl group of protein 1 and amino group of protein 2.....	109
Figure 3.18 SDS-PAGE (10% acrylamide) from cross-linking experiments between SsuE and SsuD proteins with EDC and sulfo-NHS reagents.....	111
Figure 3.19 Reaction of EDC and sulfo-NHS cross-linking reagents with carboxyl groups of SsuE and amino groups of SsuD.....	112
Figure 3.20 MALDI-TOF MS spectra for protein standards.....	113
Figure 3.21 MALDI-TOF MS spectra for undigested SsuE protein.....	114
Figure 3.22 MALDI-TOF MS spectra for undigested SsuD protein.....	115
Figure 3.23 MALDI-TOF MS spectra for peptide standards.....	117
Figure 3.24 MALDI-TOF MS spectra for tryptically-digested SsuE.....	118
Figure 3.25 MALDI-TOF MS spectra for tryptically-digested SsuD.....	120

Figure 3.26 Charge transfer conversion between FMNH ₂ and NADP ⁺ in FMN reduction by SsuE.....	123
Figure 3.27 Spectra of FMN reduction and charge transfer formation in the absence and in the presence of SsuD.....	125
Figure 3.28 UV-visible spectra for free FMNH ₂ and FMNH ₂ -bound SsuD.....	128
Figure 3.29 Spectra of FMN reduction and charge transfer formation by SsuE in the presence of SsuD, octanesulfonate, and oxygen.....	130
Figure 3.30 Spectra of FMN reduction and charge transfer formation by SsuE in the presence of oxygen and octanesulfonate without SsuD	133
Figure 3.31 Spectra of FMN reduction and charge transfer formation by SsuE in the presence of SsuD and oxygen, but in the absence of octanesulfonate.....	135
Figure 4.1 Proposed model for protein complex formation between SsuE and SsuD Proteins.....	142
Figure 4.2 Charge-transfer complex of FMNH ₂ and NADP ⁺	150

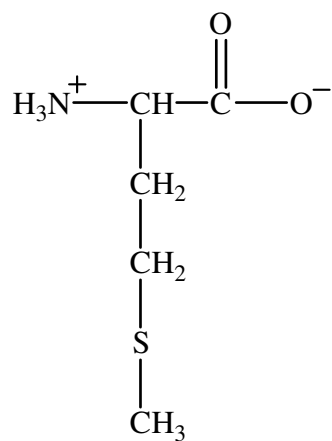
CHAPTER ONE

LITERATURE REVIEW

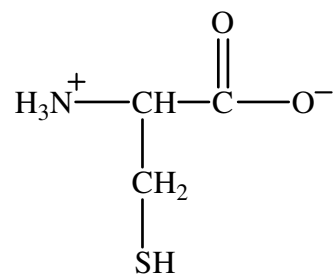
1.1 The role of sulfur in organisms

Sulfur is a primary element required for metabolic processes in all organisms. In bacteria, sulfur is one of the essential components that makes up of 0.5-1% of the cell dry weight [1]. Although sulfur belongs to the same group as oxygen, it has different physical characteristics. Sulfur is less electronegative, therefore, any molecules containing sulfur will have different redox properties compared to those containing oxygen. For example, sulfur-containing amino acids differ from hydroxyl-containing amino acids in several physicochemical properties, such as polarity, acidity or basicity, and chemical reactivity. Sulfur-containing amino acids are involved in a host of biological functions and their roles will be explained in more detail in the following section.

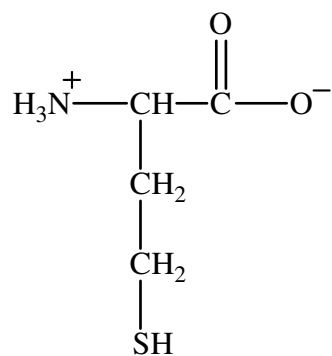
Sulfur plays an important role as an obligatory element of sulfur-containing amino acids. There are four sulfur-containing amino acids commonly found in organisms; cysteine, methionine, homocysteine, and taurine (Figure 1.1). Cysteine and methionine play critical roles in biological systems, not only as building blocks of proteins, but also as metabolites in a wide range of metabolic processes. There are some



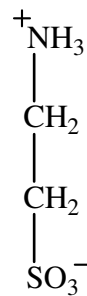
METHIONINE



CYSTEINE



HOMOCYSTEINE



TAURINE

Figure 1.1. Structures of the sulfur-containing amino acids.

unique characteristic associated with sulfur-containing amino acids, which distinguish these types of amino acids. For example, methionine and N-formylmethionine serve as the initiating amino acid for protein synthesis in all eukaryotic and prokaryotic cells, respectively. Methionine is also one of the most hydrophobic amino acids; therefore many methionine residues are buried in the hydrophobic core of soluble globular proteins. In non-polar environments methionine is found to interact with the lipid bilayer in membrane-spanning protein domains [2]. In some proteins, methionine residues are exposed on the surface of proteins and thus accessible to oxidation and serve as so-called endogenous antioxidants for the proteins [3]. In glutamine synthetase from *Escherichia coli*, the methionine residues are arrayed around the active site cavity and are believed to protect the active site from being oxidized by reactive oxygen species. Interestingly, the oxidation of these methionine residues often has little effect on the catalytic activity of the enzyme [4].

Sulfur-containing amino acids play a critical role in the stabilization of protein structures. Cysteine is involved in protein stability by forming inter- and intrasubunit disulfide bonds with other cysteine residues. In some proteins, proper protein folding is dependent on the formation of disulfide bonds leading to suitable protein structure-function relationships. In addition to its stabilizing role in protein structures, cysteine is a substrate for a variety of anabolic and catabolic enzymes. Cysteine serves as a precursor of coenzyme A, glutathione (GSH- γ -glutamyl-cysteinyl-glycine), and its catabolic products taurine and inorganic sulfur [5-11]. Therefore the cellular concentration of cysteine must be properly maintained [5]. In mammalian organisms, the concentration of cysteine is primarily regulated by hepatic cysteine dioxygenase (CDO).

The level of CDO is upregulated in a cysteine-responsive manner by a decrease in the rate of polyubiquitination and degradation by the 26S proteasome [5]. Thiol groups of cysteine and its derivative, by virtue of their ability to undergo reversible oxidation, are involved in redox sensitive reactions and are also recognized as key elements involved in the maintenance of redox balance. Under normal cellular conditions, most biological environments both cellular and extracellular, are maintained in a reduced state. When there is a perturbation to the environment such as an oxidative stress, reduced thiol compounds such as glutathione, act as an antioxidant to remove reactive oxygen species [5]. This defense mechanism allows the cell to remove, repair and control the normal reducing environment [6].

Taurine, 2-aminoethane sulfonic acid, is an amino acid which is not incorporated into proteins, however its role in metabolism is essential. Taurine is an essential nutrient and the most abundant free β -amino acid in mammalian tissues [2,12]. Taurine is synthesized from cysteine via the sequential actions of CDO, which gives rise to cysteinesulfinic acid, and cysteinesulfinic acid decarboxylase (CSD), which decarboxylates cysteinesulfinic acid to hypotaurine. Hypotaurine is further oxidized to taurine via an enzymatic reaction catalyzed by hypotaurine dehydrogenase [12]. The conversion of the cysteinesulfinic acid to hypotaurine/taurine is minimized by the active transamination of cysteinesulfinic acid to pyruvate and inorganic sulfur [5,13]. In mammalian cells, it has been established that taurine concentration is extremely high in the developing brain, liver, intestines, and skeletal muscles [14,15]. Taurine plays a wide range of physiological roles, therefore taurine deficiency leads to a variety of diseases [16-23].

Homocysteine is another amino acid which is not directly incorporated into protein but serves as a precursor for cysteine and methionine biosynthesis. In bacteria, the major route to methionine biosynthesis is through homocysteine and cysteine [24]. In higher organisms [25], the level of methionine is controlled by homocysteine, since methionine and homocysteine are readily interconvertible in the transsulfuration pathway [24]. A high amount of methionine is toxic whether derived from the diet or due to liver dysfunction [24]. Therefore, the levels of homocysteine are controlled to maintain proper methionine levels. Homocysteine is catabolized through an accelerated γ -cystathionase reaction when methionine is in excess, and homocysteine is re-methylated when methionine is needed [26].

In addition to the role of sulfur as a sulfur-containing amino acid, sulfur is also an essential component of a variety of enzyme cofactors such as Coenzyme A, Coenzyme M, biotin, lipoate, and as a component of iron-sulfur clusters. Coenzyme A is notable for its role as an acyl group carrier in the synthesis and oxidation of fatty acids [27,28], and the oxidation of pyruvate in the citric acid cycle [29]. Coenzyme M is a C1 carrier in methanogenesis, that assists in the conversion of 2-methylthioethanesulfonate to methane gas in microbial methanogens [30]. Biotin plays an important role as a carbon dioxide carrier in carboxylation reactions. It is an important prosthetic group of pyruvate carboxylase, an enzyme that catalyzes the ATP-dependent carboxylation of pyruvate to oxaloacetate in the gluconeogenesis pathway [31-33]. Lipoic acid or lipoate, the common form of lipoic acid under physiological conditions, is a cofactor that functions as an acyl carrier in enzymatic reactions [34]. In the pyruvate dehydrogenase complex, lipoic acid is a cofactor of dihydrolipoyl transacetylase (E_2) that catalyzes the transfer of

the acetyl group from acetyl-dihydrolipoamide to CoA to form acetyl-CoA and dihydrolipoamide. Sulfur, in the form of inorganic sulfide, is also incorporated into iron-sulfur clusters. More than 120 distinct types of enzymes and proteins are known to contain iron-sulfur clusters [35]. By virtue of their structural elasticity and versatility of their electronic and chemical properties, they are involved in a variety of biological processes. Some biological functions of iron-sulfur clusters include electron transfer, substrate binding and activation, iron-sulfur storage, and regulation of gene expression [35,36]. Considering the critical role of sulfur, the presence of sulfur is mandatory for all organisms either for cell growth or to perform various metabolic processes. In other words, the lack of sulfur can simply lead to the death of any organism.

1.2 Primary sulfur sources and their assimilation in bacteria

Cysteine and inorganic sulfate are two primary sulfur sources in bacteria [1]. However, in *E. coli* and many other bacterial species, cysteine is the preferred sulfur source, since the presence of cysteine in the medium represses the enzymes involved in sulfur assimilation from sulfate [37]. In bacteria, there are two major enzymatic routes for incorporation of sulfate into cysteine (reductive assimilation of sulfate): the APS (adenosine 5'-phosphosulfate) pathway (Figure 1.2, left pathway) and the PAPS (adenosine 3'-phosphate-5'-phosphosulfate) pathway (Figure 1.2, right pathway) [12]. In the APS assimilation pathway, ferredoxin and glutathione (GSH) react with APS to yield thiosulfate, GSSO_3^- (a Bunte salt), which is converted to GSS^- via a thiosulfate reductive reaction; GSS^- then reacts with *O*-acetylserine to yield L-cysteine. In the PAPS pathway, the conversion of PAPS to sulfite (HSO_3^-) requires thioredoxin-dependent PAPS

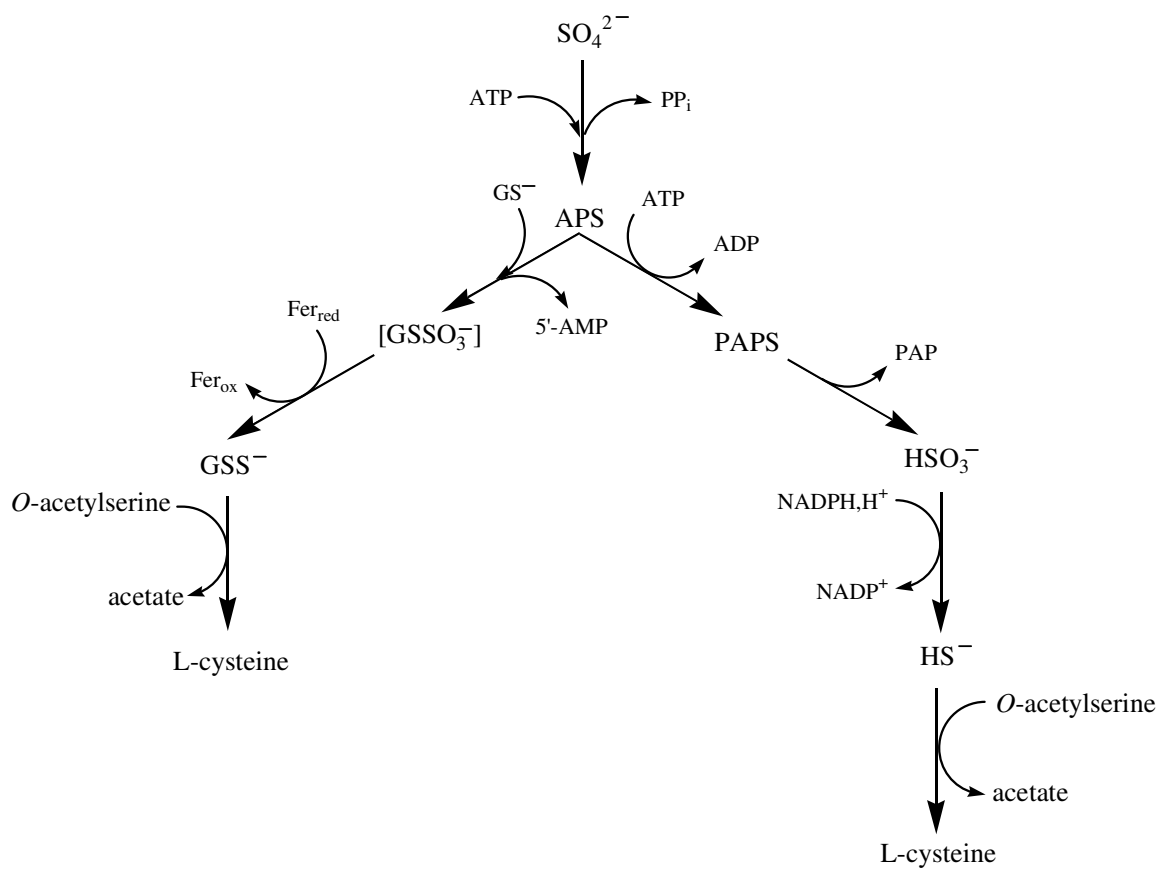


Figure 1.2. Two major route for sulfur assimilation in microorganisms [12].

reductase [37,38]. NADPH-dependent sulfite reductase converts HSO_3^- to sulfide (HS^-). Reaction of HS^- with *o*-acetylserine to form cysteine is catalyzed by *o*-acetylserine (thiol)-lyase or cysteine synthase [37,39-41].

1.3 Defense mechanism against sulfur starvation in bacteria

Sulfur starvation is defined as a condition when the amount of sulfate or cysteine is limiting in the environment [1]. Under these conditions, bacterial organisms are able to utilize alternative sulfur sources for their growth. This finding was first reported in 1955 when *E. coli* was able to grow when cysteine and inorganic sulfur were both absent from the growth medium but taurine was provided as a source of sulfur [42]. However, the enzymes responsible for the utilization of taurine and other aliphatic sulfonates were only identified four decades later [43]. The specific proteins that are synthesized only in the absence of primary sulfur sources are known as sulfate starvation-induced (Ssi) proteins [1,37,44-46]. Ssi proteins have been found in a wide variety of bacterial organisms. The Ssi proteins from *E. coli* and *Pseudomonas aeruginosa* have been identified by both N-terminal sequencing and mass spectrometric fingerprinting (Table 1.1) [1,44,46-48]. The Ssi proteins that have been identified can be categorized as follows: 1) enzymes and transport systems involved in utilizing alternative sulfur sources from the environment; 2) important cellular proteins with low-sulfur content, in which cysteine or methionine residues which are not critical for function have been replaced by other amino acid residues; 3) enzymes involved in mobilization of intracellular sulfur storage compounds [1]. In *E. coli*, the total sulfur content is reduced by half during sulfur starvation [42]. Ssi proteins are commonly found in aerobic bacteria and to date it is still unclear if

Table 1.1. Sulfate-regulated proteins of *E. coli* and *P. aeruginosa* [1].

Protein	Gene locus	Function
<i>E. coli</i>		
TauA, TauD	<i>tauABCD</i>	taurine desulfurization
SsuE, SsuD	<i>ssuEADCB</i>	alkanesulfonate desulfurization
Sbp	<i>sbp</i>	periplasmic sulfate binding protein
FliY	<i>fliY</i>	periplasmic cystine binding protein
AhpC	<i>ahpC</i>	alkylhydroperoxide reductase subunit
<i>P. aeruginosa</i>		
PA1	<i>sbp</i>	periplasmic sulfate binding protein
PA2, PA11, PA13	<i>ssuEADCBF, msuEDC</i>	alkanesulfonate desulfurization
PA11	<i>lsfA</i>	thiol-specific antioxidant
PA9	<i>tauABCD</i>	taurine desulfurization
PA7	<i>nlpA</i>	lipoprotein
PA4	<i>atsK</i>	unknown
PA19	similar to <i>E. coli fliY</i>	putative amino acid transport protein
PA17	similar to <i>P. putida asfC</i>	putative periplasmic sulfonate binding protein
PA14	similar to <i>E. coli ahpC</i>	alkylhydroperoxide reductase subunit
AtsA	<i>atsA</i>	arylsulfatase
AtsRBC	<i>atsR, atsBC</i>	transport of sulfate esters

similar proteins are found in strict anaerobes [49].

1.4 Alternative sulfur sources for bacteria during sulfate starvation

Since their identification, a large number of organosulfonates have been found as alternative sulfur sources for bacteria during sulfate starvation [1,37,42,46,49]. Organosulfonates, which include naturally occurring or xenobiotic sulfate esters are widespread in nature and are commonly subjected to desulfonation for sulfur acquisition by bacteria (Table 1.2) [1,49]. Xenobiotic sulfonates enter the environment through waste water and can be detected in rivers and soils. Some sulfonates in the environment are generated biologically from non-sulfonated xenobiotic compounds [49]. However, it is not clear whether all bacterial enzymes involved in desulfonation reactions have been identified.

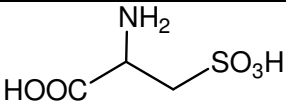
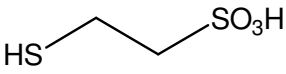
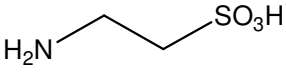
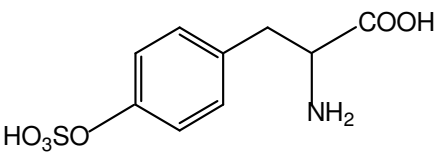
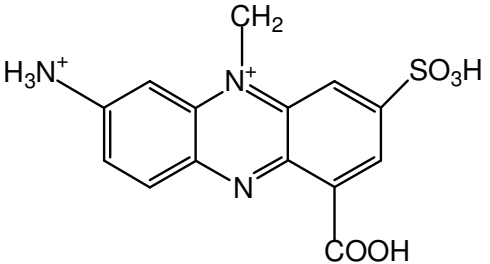
The assimilation of organosulfonates into bacterial cells employs a different set of enzymes and biochemical pathways from the assimilation of inorganic sulfate (Figure 1.3) [37]. These differences are due to the expression of Ssi proteins during sulfur starvation (Figure 1.3, upper left and right pathways), and the repression of proteins expressed under normal environment conditions (Figure 1.2 and Figure 1.3, bottom left pathway).

1.5 Gene clusters responsible for sulfate-starvation induced proteins in bacteria

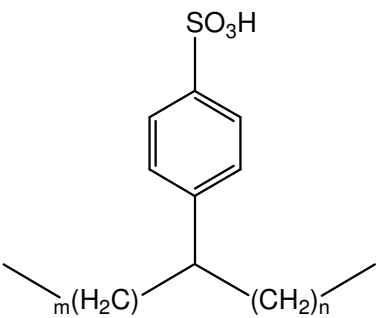
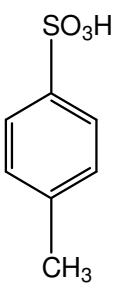
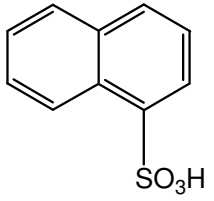
The gene clusters responsible for the synthesis of some Ssi proteins share a common operon and genetic organization (Figure 1.4) [1]. Both the *ssu* and *tau* operons are found on the *E. coli* and *P. aeruginosa* chromosome. An additional operon, *msu*, is

Table 1.2. Natural and synthetic sulfonates and sulfate ester [49,1].

Natural sulfates and sulfonates

Structure	Compound	Source
	cysteate	wool
	coenzyme M	methanogenic archaea
	taurine	mammals
$R-(CH_2)_n-SO_3H$	alkanesulfonate	oil-contaminated soil (natural oil)
	tyrosine sulfate	eukaryotic proteins
	aeruginosin	<i>Pseudomonas aeruginosa</i>

Xenobiotic sulfates and sulfonates

		$C_{12}H_{25}-OSO_3H$	
Linear Alkylbenzenesulfonate (LAS)	Toluenesulfonate (surfactant)	Dodecyl sulfate (surfactant)	Naphthalenesulfonate (substituted compounds)

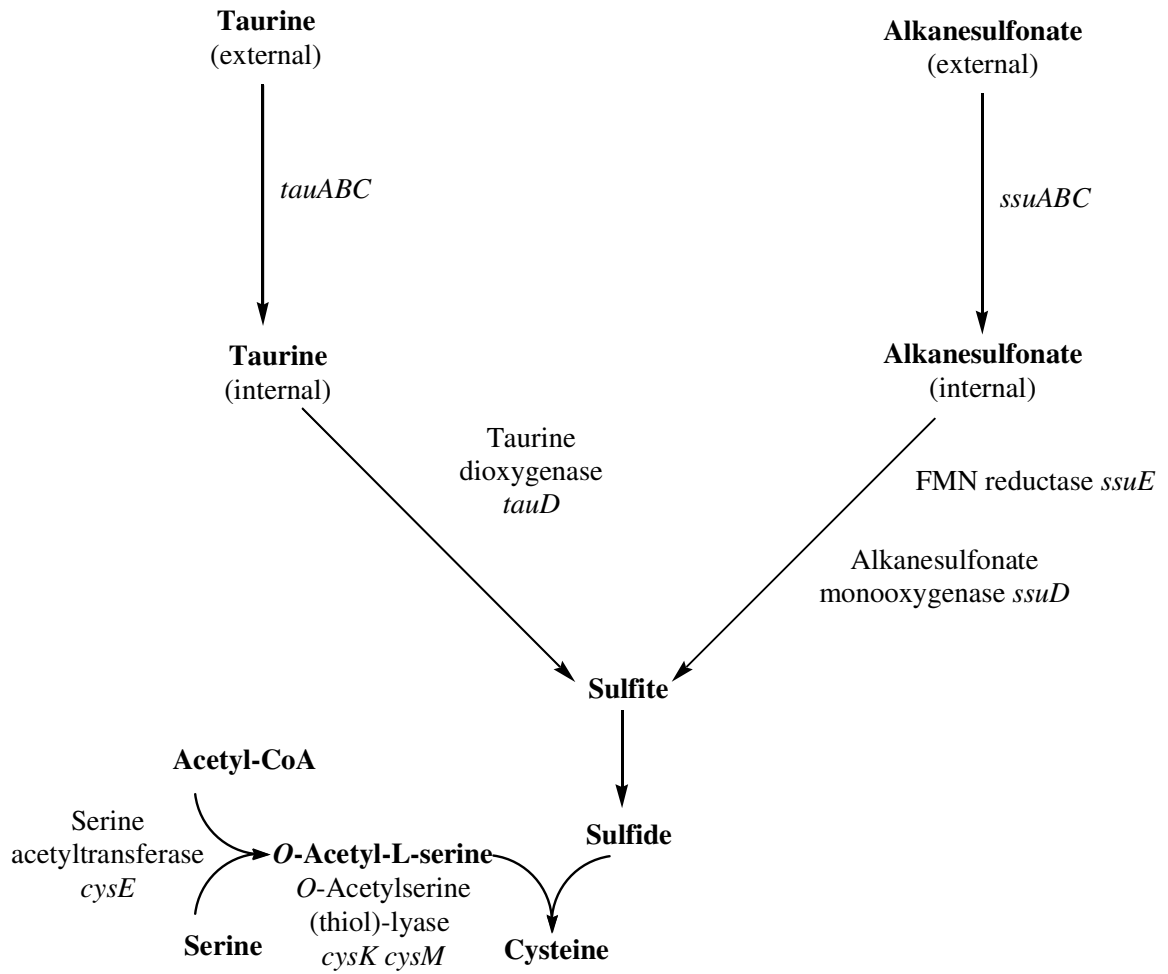


Figure 1.3. Assimilation of sulfur from different sources in normal environment condition and during sulfate-starvation in *E. coli* [37].

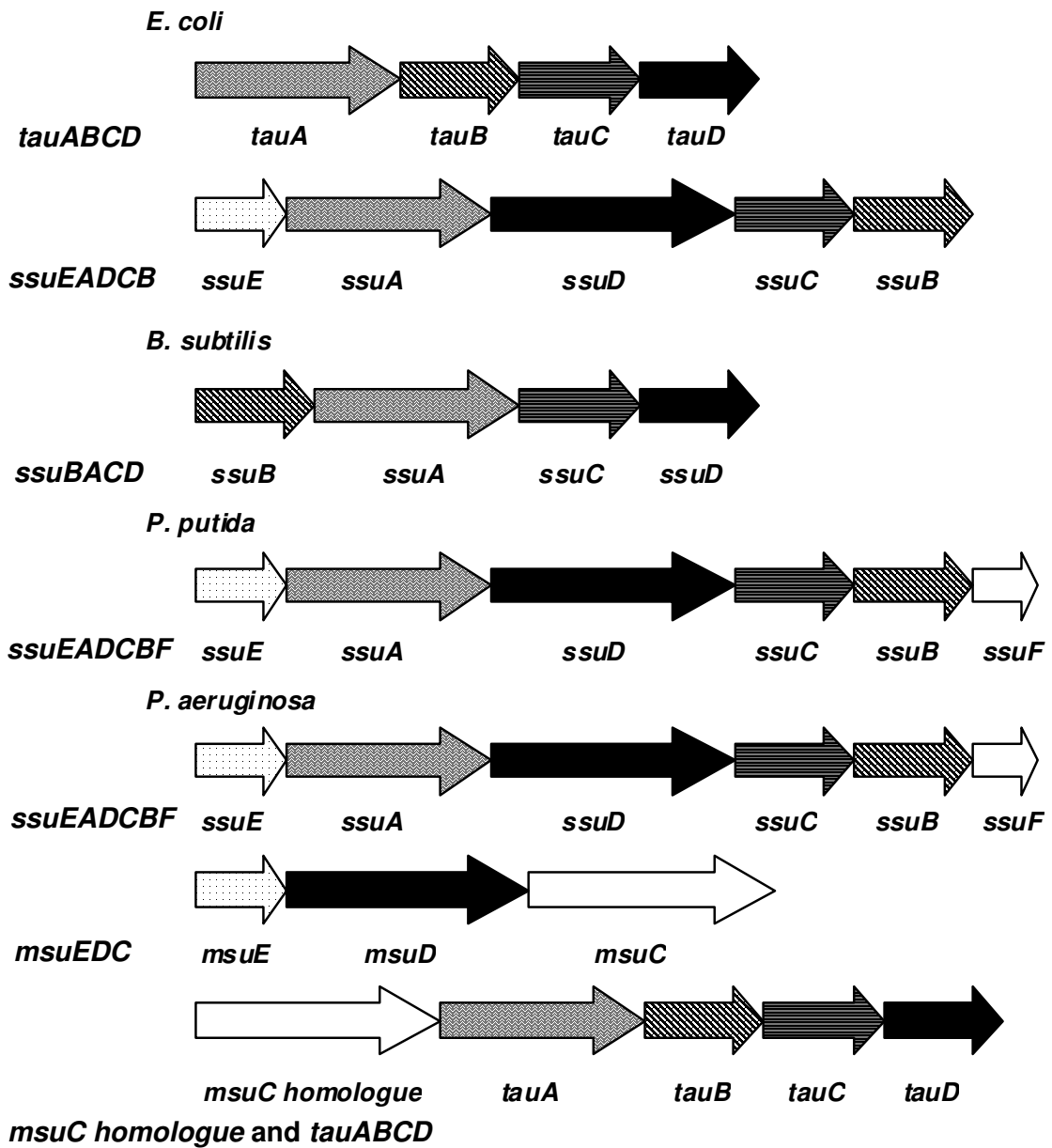


Figure 1.4. Gene clusters responsible for the synthesis of Ssi proteins in several bacterial species [1].

also found in *P. aeruginosa* [1]. In general, enzymes encoded in these operons are oxygenases and/or NAD(P)H-dependent FMN reductases. The *ssu* and *tau* operons also encode an ABC (ATP binding cassette)-type transporter, which includes periplasmic solute binding proteins, ATP binding proteins, and permease proteins. This type of transporter is one of the largest of all paralogous protein families. In *E. coli*, the genes encoding components of these transporters occupy almost 5% of the genome, and they are also commonly found in all species from microbes to human [50].

The *tauABCD* gene cluster in *E. coli* is responsible for the expression of the TauABC proteins, an ABC (ATP-binding cassette)-type transport system, and TauD, an α -ketoglutarate-dependent dioxygenase [51,52]. The *ssuEADCB* gene cluster in *E. coli* encodes SsuABC proteins, another ABC-type transport system, an FMN reductase (SsuE), and monooxygenase (SsuD) [53,54]. The *ssuF* gene that encodes a protein related to clostridial molybdopterin-binding proteins is uniquely found in *Pseudomonas* sp. The TauABC and SsuABC proteins appear to constitute an uptake system for their corresponding substrates (Figure 1.5). Taurine is exclusively transported into the cell by TauABC and desulfonated by TauD (solid line), while longer-chain aliphatic sulfonates (alkanesulfonates) are taken up by SsuABC and desulfonated by SsuED (large dashed line). Interestingly, in the SsuEADCB system, the SsuD-catalyzed reaction is dependent on SsuE. SsuE provides reduced flavin that serves as a cosubstrate for the SsuD-catalyzed desulfonation of substrates (Figure 1.5) [37]. Due to the type of substrates utilized by SsuD, this particular enzyme is referred to as alkanesulfonate monooxygenase. A wide range of substrates for both TauD and SsuD proteins from *E. coli* have been identified (Table 1.3). However, the mechanism on how different

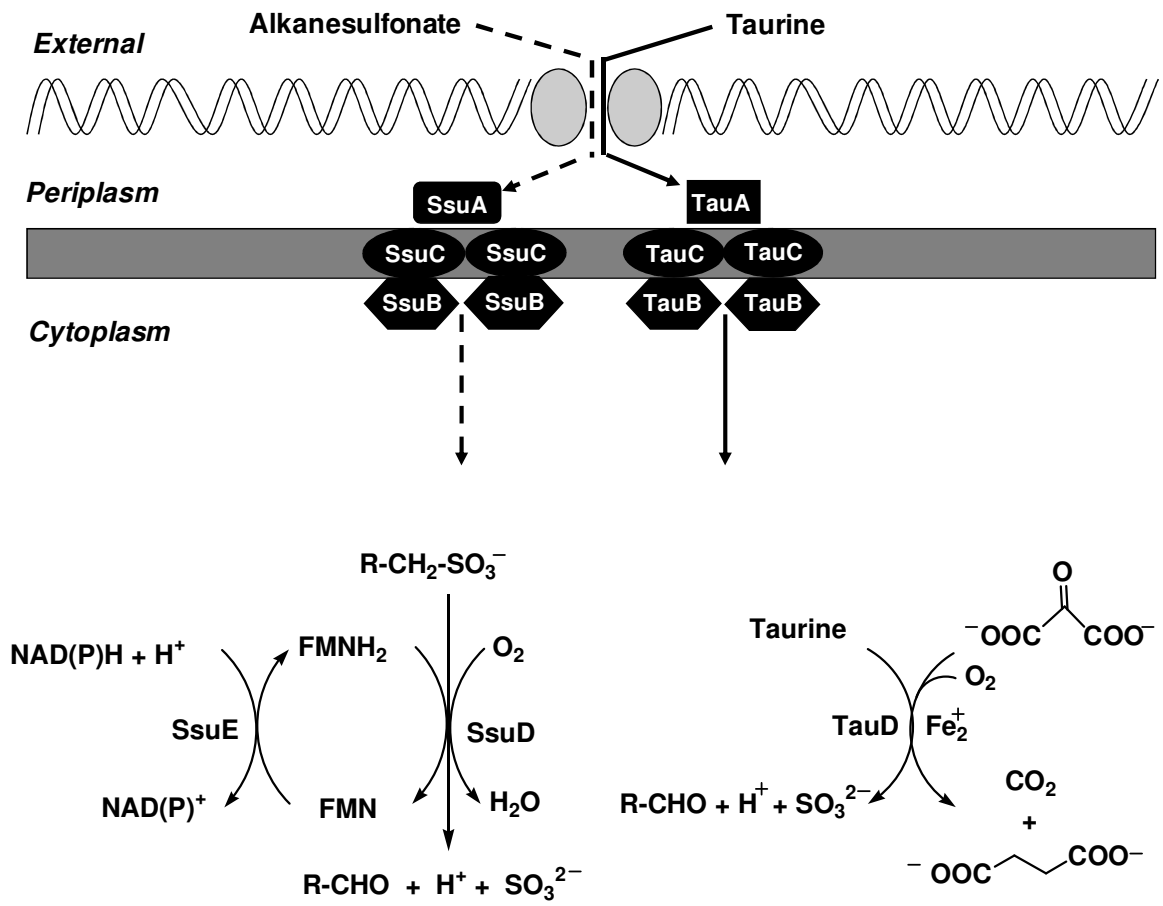


Figure 1.5. Substrate uptake from different sulfur sources by TauABC and SsuABC transporters in *E. coli* during sulfate starvation condition [37].

Table 1.3. Substrate for alkanesulfonate monooxygenase SsuD and α -KG-dependent taurine dioxygenase TauD [34].

Sulfonated substrate	Relative activity	
	SsuD	TauD
	%	
Taurine	0.0	100.0
<i>N</i> -Phenyltaurine	65.6	0.0
4-Phenyl-1-butanefulfonic acid	42.4	2.5
HEPES	10.6	5.0
MOPS	36.4	34.2
PIPES	29.2	3.1
2-(4-Pyridyl)ethanesulfonic acid	87.4	0.5
1,3-Dioxo-2-isoindolineethanesulfonic acid	100.0	30.1
Sulfoacetic acid	19.8	- ^a
L-Cysteic acid	0.0	0.0
Isethionic acid	14.3	1.2
Methanesulfonic acid	0.7	0.0
Ethanesulfonic acid	5.2	0.8
Propanesulfonic acid	14.0	2.3
Butanesulfonic acid	17.8	8.4
Pentanesulfonic acid	40.4	22.5
Hexanesulfonic acid	43.8	11.3
Octanesulfonic acid	46.3	-
Decanesulfonic acid	43.2	-
Dodecanesulfonic acid	20.1	3.3
Tetradecanesulfonic acid	2.9	-

^a -, not determined.

enzymes utilize a diverse range of substrates is not well characterized.

As previously mentioned there are three operons responsible for the expression of sulfur assimilation proteins under sulfate starvation conditions in *P. aeruginosa*, the *ssu*, *tau*, and *msu* operons. While the first two operons express Ssu and Tau proteins that are similar to the proteins expressed in *E. coli*, the *msu* operon is responsible for the expression of FMNH₂-dependent methanesulfonate sulfonase [1]. This enzyme catalyzes the desulfonation of alkanesulfonates, requiring oxygen and FMNH₂ for the reaction, and showed the highest activity with methanesulfonate [1].

1.6 Regulatory proteins of sulfur assimilation in E. coli

In *E. coli*, the expression of the *tau* and *ssu* genes requires a regulatory protein, Cbl [37,55]. CysB and Cbl proteins are classified as LysR-type transcriptional regulators, the largest family of prokaryotic transcription factors [56]. It was shown that the binding of both Cbl and CysB to the promoter region of the *tau* operon are required for expression [55]. In contrast to the *tau* operon system, the expression of the *ssu* operon is regulated only by the transcriptional activator Cbl [53]. Although the *ssu* promoter region contains binding sites for the CysB protein and for integration host factor, removal of these binding sites did not have a strong effect on expression from the *ssu* promoter [53]. However, the synthesis of Cbl itself is under control of the CysB protein [55]. It has been shown that CysB protein positively regulates the expression of the genes encoding the assimilatory sulfate reduction pathway [56]. CysB protein in the presence of the inducer N-acetylserine is a transcriptional activator and required for full

expression of the *cys* genes involved in cysteine biosynthesis [53,56]. The CysB protein may be regarded as the master regulator for sulfur assimilation in *E. coli*, while the Cbl protein functions as an accessory element specific for utilization of sulfur from organosulfur sources (Figure 1.6) [37].

Sequence alignment studies showed that Cbl has 45% sequence identity with CysB, and many of the residues in the binding pocket are conserved [57]. This suggests that the structure of the coinducer recognized by Cbl could be very similar to *o*-acetylserine, the coinducer for CysB [37]. However, in contrast to binding of CysB to the *cys* promoter regions, binding of Cbl to the *tau* and *ssu* promoter regions is not influenced by *o*-acetylserine, and the identity of the coinducer of Cbl is still unknown [37,52,53]. Despite the differences in how each operon is regulated, both operons are expressed under sulfur limitation conditions [1]. The presence of sulfur-containing molecules such as sulfate, sulfide, sulfite, L-cysteine, and L-cystine will significantly repress the expression, while their absence leads to induction of these enzymes [56,51].

1.7 The alkanesulfonate monooxygenase system from E. coli

As mentioned, the *E. coli ssu* operon is responsible for the synthesis of proteins involved in sulfur assimilation [53,54]. Two of the enzymes expressed from this operon are responsible for the desulfonation reaction of alkanesulfonates. For their role in sulfur acquisition and specificity for alkanesulfonates, they are known as a two-component alkanesulfonate monooxygenase system. The first enzyme is a NAD(P)H-dependent FMN reductase (SsuE) that catalyzes the reduction of FMN by NAD(P)H. The second is a monooxygenase (SsuD) that utilizes the reduced flavin (FMNH₂) provided by SsuE for

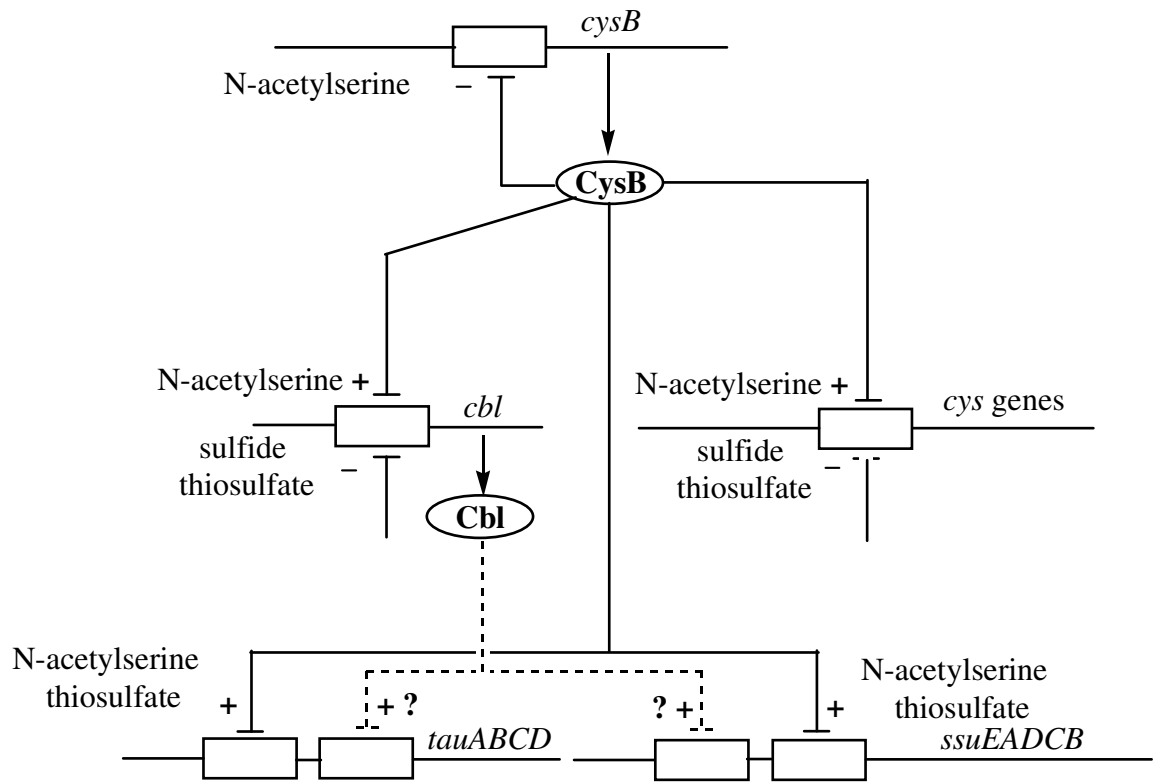


Figure 1.6. Model for the regulation of sulfur assimilation by CysB and Cbl in *E. coli* [37].

the desulfonation of alkanesulfonates to their corresponding aldehydes in the presence of dioxygen (Figure 1.7) [53]. Therefore, this enzyme system is also known as the flavin-dependent alkanesulfonate monooxygenase due to the absolute flavin requirement. Interestingly, in this enzyme system, flavin does not function as a cofactor, but serves as a cosubstrate [37,53,54].

The interesting features of flavins including a historical perspective, their physicochemical properties, the enzymes associated with the flavins, the reactions catalyzed, and their important roles in biological systems are the topics of the following section.

1.8 Flavins and flavoproteins

1.8.1 Flavins

First mention of the term lactochrome in the scientific literature dates back to 1879 when work on the composition of cow's milk resulted in the isolation of a bright yellow pigment [58]. This same pigment was then isolated from a range of sources and chemically characterized as a component of the vitamin B complex in the 1930s. Two different groups were able to determine the structure of this compound at nearly the same time in 1934 and it was renamed riboflavin, a name derived from the ribityl side chain and yellow color of the conjugate ring system [59,60]. Since then, flavin has been recognized as an agent that is capable of one- or two-electron transfer processes [61-63].

There are three common forms of flavins found in nature that are distinguished from one another by the functional group on the ribityl side chain; riboflavin, flavin

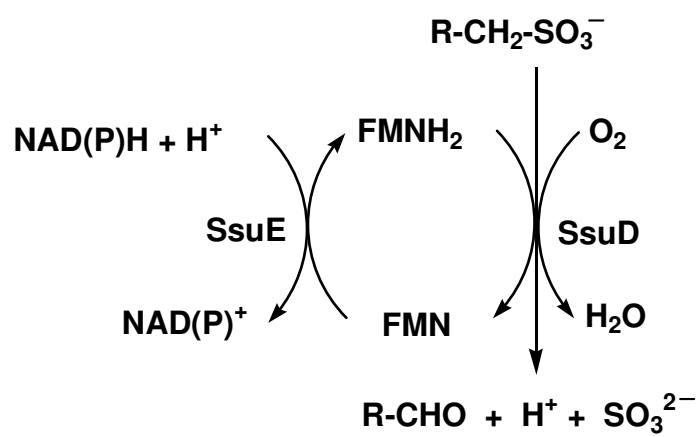


Figure 1.7. Overall reactions in the alkanesulfonate monooxygenase system from *E. coli* [53].

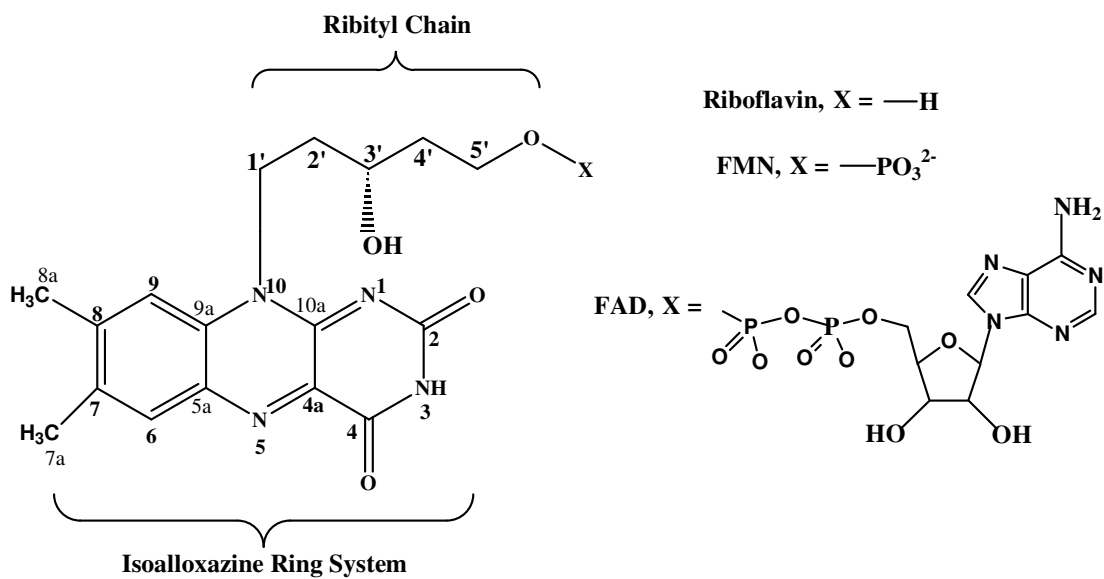


Figure 1.8. Structures of Riboflavin, FMN, and FAD.

mononucleotide (FMN), and flavin adenine dinucleotide (FAD) (Figure 1.8). They are usually found as prosthetic groups, which are either covalently or tightly bound to the enzymes. The three types of flavins have been found as cofactors in a wide range of enzymes and play essential roles in catalytic reactions. They play a critical role in aerobic metabolism by virtue of their ability to catalyze two-electron dehydrogenations of numerous substrates and to participate in one-electron transfer to various metal centers through their free radical states. In this regard, they are often found in multi-redox-center enzymes, such as in succinate and NADH dehydrogenase, xanthine oxidase or dehydrogenase, cytochrome P450 systems, and nitric oxide synthase and the electron transport system [63]. In addition to their roles as enzyme cofactors, flavins have recently been identified as substrates as opposed to strict prosthetic groups in some enzymes.

The versatility of flavins derives from their ability to exist in three different oxidation states, oxidized (yellow color), semiquinone ($1 e^-$ reduced) (light blue color or red color), and fully reduced states ($2e^-$ reduced) (colorless) (Figure 1.9) [64]. The structures of flavin in different oxidation states have been elucidated using both experimental and theoretical studies [63-65]. The structure of oxidized flavin is planar regardless of its protonation states or whether it participates in hydrogen bonding. The structures of flavin semiquinone radicals are planar or close to planar, but the reduced flavin is bent with a ring puckering angle of 27.3° along the N-5 and N-10 axis [65]. In free solution when the flavin is not bound to the protein, a mixture of oxidized flavin and reduced flavin rapidly sets up an equilibrium with a flavin radical (Eq. 1.1) [63]:

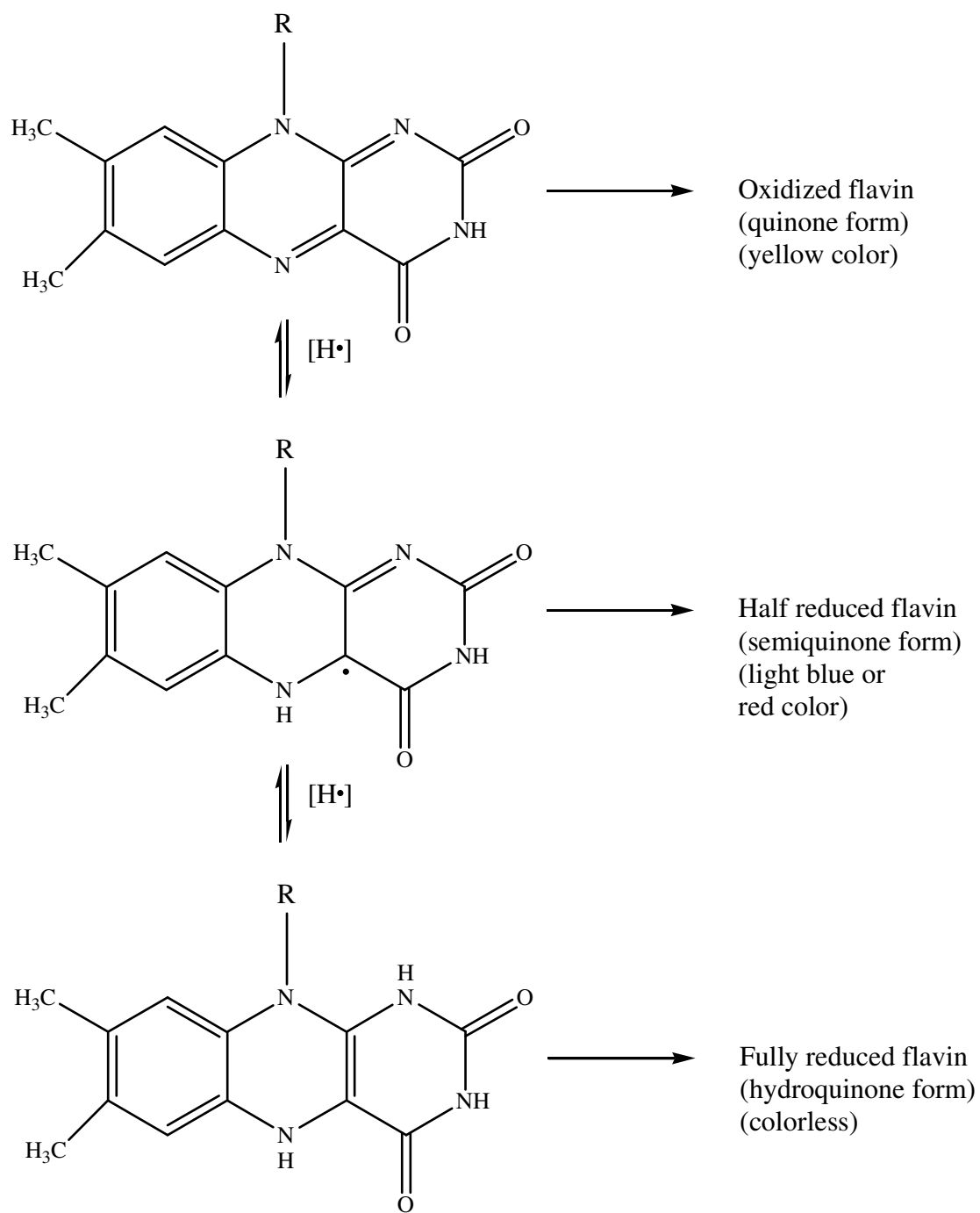


Figure 1.9. The structures of flavin in three different oxidation states.



where F refers to oxidized flavin, FH_2 refers to $2e^-$ -reduced flavin, and FH^\bullet refers to flavin semiquinone. At neutral pH, the equilibrium lies to the left, so that only about 5% of the radical is stabilized in an equimolar mixture of oxidized and reduced flavin. There are two forms of flavin semiquinone, neutral and anionic (Eq. 1.2).



The equilibrium for the semiquinone can shift significantly when the flavin is bound to a specific protein. Some enzymes almost completely destabilize the semiquinone, while others give nearly 100% stabilization. In some cases, the proteins may stabilize the neutral radical species over the range of pH values at which the enzyme is stable, that is the pK_a is shifted up from 8.5. In other cases, the enzyme stabilizes the semiquinone anion due to a decrease in the pK_a value from 8.5.

Different chemical characterizations of flavin structures have shown that the redox active center of the flavin coenzyme is the isoalloxazine ring system. The nitrogen atom in the 5 position (N-5) of the isoalloxazine ring is involved in determining some of the properties of the semiquinone radical form of the coenzyme [66]. Independent experiments have shown that the nitrogen atom at the 10 position (N-10) which is attached to the ribityl side chain, is typically involved in flavin-protein interactions [63]. In the oxidized form, flavin is yellow in color and has a strong absorbance at 450 nm (Figure 1.10). Upon a one electron reduction, the yellow color disappears to give a flavin semiquinone either neutral (light blue color) or anionic (red color). The neutral flavin semiquinone has a characteristic wide absorbance band at about 500-650 nm with a

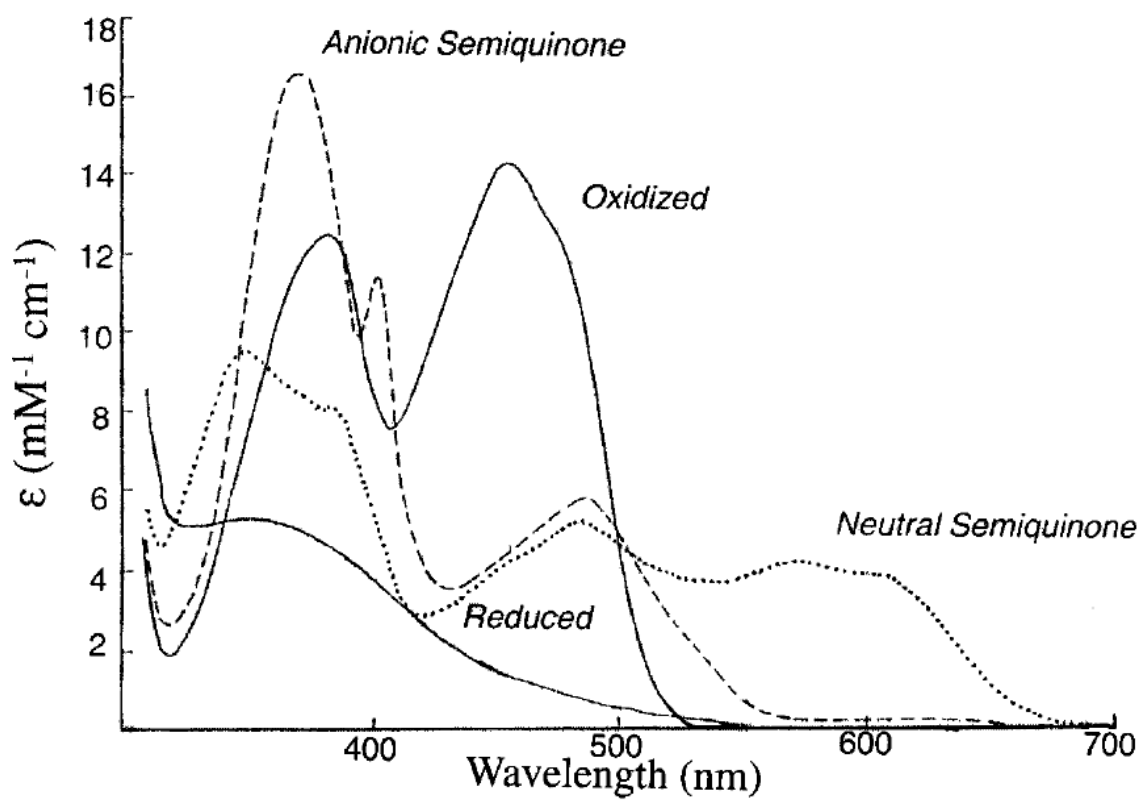


Figure 1.10. The spectra of flavin in different oxidation states [62,63].

Reprinted with permission from the American Chemical Society.

maximum at 580-600 nm. In contrast, the anionic semiquinone has very low absorbance above 550 nm, and a maximum at about 370 nm. Due to the color of their concentrated solutions, neutral and anionic semiquinones are also called blue and red, respectively [64] (Figure 1.10). Upon further electron reduction ($2e^-$), the semiquinone is converted to a colorless reduced flavin that correlates with disappearance in absorbance at 450 nm (Figure 1.10). The yellow color will resume when the flavin is reoxidized by dioxygen. The complete reduction process usually involves the addition of two hydrogen atoms in a 1,4 addition reaction [63]. The broad spectral differences of the flavin forms at different oxidation states (Figure 1.10), make this compound a perfect reporter agent to monitor the events occurring in catalysis [62,63].

1.8.2 Flavoproteins

Every protein that contains a nucleic acid derivative of riboflavin as a cofactor, flavin adenine dinucleotide (FAD) or flavin mononucleotide (FMN), is considered a flavoprotein [65]. However, it is not easy to classify this family of proteins due to a large difference in their biological functions. The classification of this enzyme family is a more dynamic process rather than a rigid conceptual matter. This is simply because flavoproteins are continually being identified with different properties.

Enzymologists have classified different types of flavoproteins based upon the type of chemical reactions catalyzed, the nature of the substrates, the physicochemical properties of the proteins, their structural motifs, and their electron acceptors [63,66]. For simplicity, this review is limited to the classification of flavoproteins closely related to the topic of this study. Two sub-families of flavin-dependent enzymes, the flavin

reductases and monooxygenases will be explained in more detail in the following sections. The nomenclature or classification of flavoproteins described in this section has been proposed by several groups.

1.8.3 Flavin reductases

Flavin reductases (FRs) or NAD(P)H-dependent flavin oxidoreductases are generally referred to as enzymes that are capable of catalyzing the reduction of oxidized flavin to generate reduced flavin in the presence of NAD(P)H (Eq. 1.3):



where F refers to flavin substrate (FMN or FAD) and FH₂ refers to the corresponding reduced flavin products.

A large number of flavin reductases from different organisms have been identified. However, the true physiological functions of reduced flavin has not been well established for many flavin reductases. This might be due to the nature of the reduced flavin species which is unstable and very reactive towards dioxygen. Therefore, the discussion of the role of reduced flavin in biological systems is often associated with the enzyme acceptor of this unstable intermediate. The first function of reduced flavin in biological systems is as an effective reducing agent or electron-transfer mediator [67]. This has been shown in the reduction of ferric complexes or iron proteins by flavin reductases via their reduced flavin product, as found in ribonucleotide reductase of microbial systems [68,69]. Another function of flavin reductases is to provide a reduced flavin as the substrate for monofunctional flavin-dependent oxygenases. Since they are only capable of catalyzing the oxidative-half reaction, their dependence on reduced flavin

must be provided by flavin reductases [53,65].

Flavin reductases are primarily found in bacterial enzymes, however, several have been identified in mammalian systems [65]. They are named based on the preferred substrate utilized by the enzymes [65]. The flavin reductases that prefer NADPH for their substrates are NADPH-preferring flavin reductases (FRP), and those that utilize NADH as their preferred substrates are NADH-preferring flavin reductases (FRD). The name FRG refers to flavin reductases that utilize both NADPH and NADH with similar efficiencies. Flavin reductases are further classified as flavoprotein (Class I) and non-flavoprotein (Class II) reductases [65,70,71]. Class I flavin reductases refer to enzymes that contain bound flavin as a cofactor, and Class II flavin reductases refer to those that use flavin as cosubstrate rather than a cofactor. Therefore, the classification for the flavin reductases is based on the preferred pyridine nucleotide and flavin content such as FRP-I (e.g. *Vibrio harveyi* flavin reductase), FRG-I (e.g. *V. fischeri* flavin reductase), and FRD-II (e.g. *Streptomyces coelicolor* flavin reductase) [65]. Many of the flavin reductases have not been fully characterized, and it is often unclear whether the flavin serves as a substrate or a prosthetic group [65]. For the flavin reductases that have not been characterized in regard to their pyridine nucleotide and flavin specificity, the general term “FR” is used [65].

1.8.4 Flavin monooxygenases

The flavoprotein monooxygenases are a class of flavin-dependent monooxygenases that typically contain a tightly bound flavin cofactor [72,63]. These enzymes are also referred to as bifunctional oxygenases due to the ability of this group of

enzymes to catalyze the reduction of the flavin cofactor by NAD(P)H in the reductive half-reaction and subsequently oxidize the reduced flavin to generate oxidized flavin and the product in the oxidative half-reaction [72,65]. Another group of monooxygenases, monofunctional flavin-dependent monooxygenases, do not contain a flavin cofactor and do not have the ability to reduce flavin by NAD(P)H [65,54,53]. The reduced flavin required for the oxygenation reaction is provided by a separate flavin reductase [54,53].

Flavin-dependent monooxygenases are involved in the activation of dioxygen through reduced flavin, forming several reactive intermediates (Figure 1.11) [63]. The initial reaction is a one-electron transfer reduction of a dioxygen molecule by the reduced flavin (I) to form a caged radical pair of neutral flavin radical and superoxide (II). This radical pair has several possible routes. It can either form a C4a peroxyflavin (IV), or a nucleophile, which on protonation becomes the electrophilic hydroperoxyflavin (V). Both peroxyflavin (IV) and hydroperoxyflavin (V) have the potential to eliminate hydrogen peroxide to yield oxidized flavin (VI), or there may be a second one-electron transfer from the radical pair to yield the same product. Alternatively, peroxyflavin species can be involved in the oxidative cleavage of a carbon-carbon bond adjacent to a carbonyl group (The Baeyer-Villiger oxidation reactions), while hydroperoxyflavin species are involved in hydroxylation reactions of aromatic compounds. The third alternative route is the uncoupled dissociation of the radical pair into its components, flavin radical and superoxide anion (upper right pathways). The superoxide can then react with peroxide to form hydroxyl radicals.

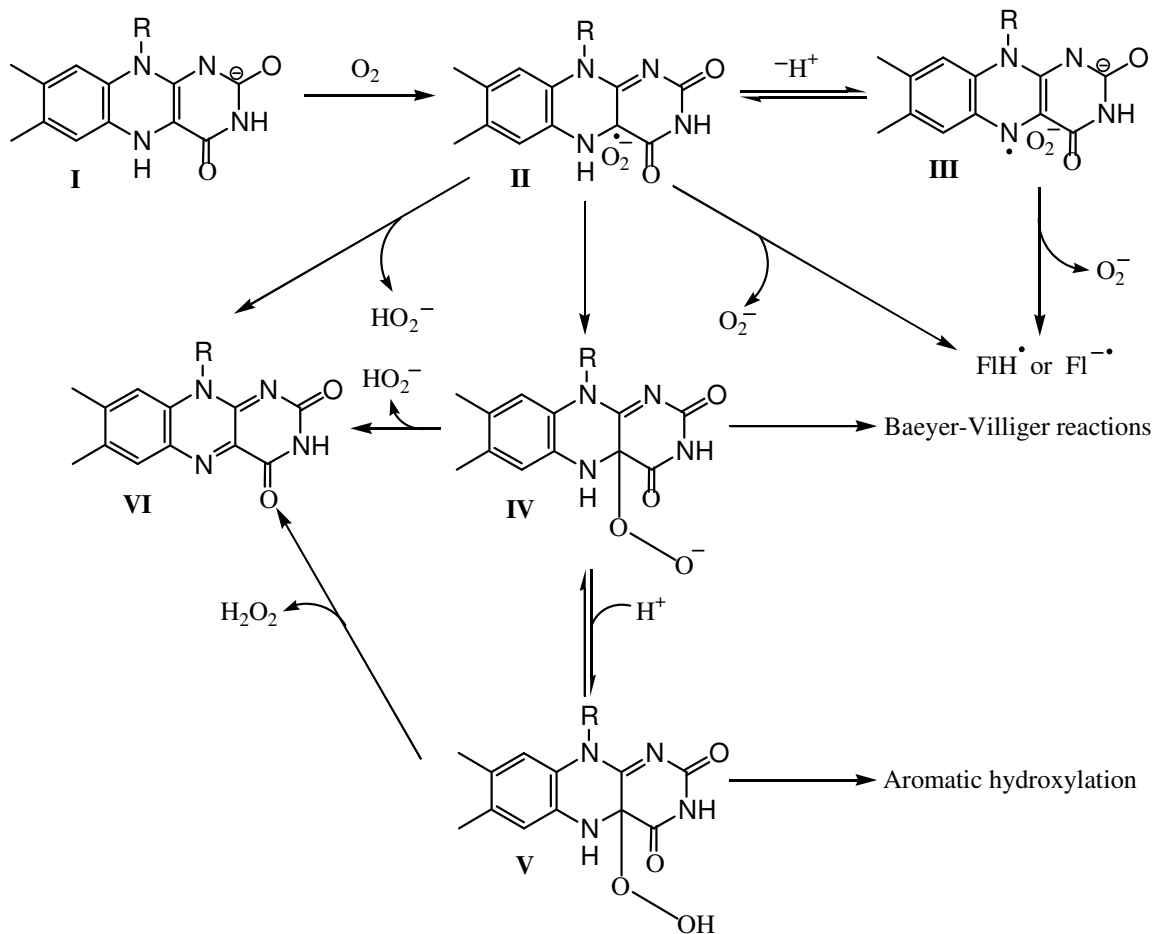


Figure 1.11. Reactive by products generated from reaction between reduced flavin and molecular oxygen [63].

1.8.5 Two component oxygenase systems

Oxygenases catalyze a variety of biological reactions, from the production of bioluminescence to the oxygenolytic reactions of a broad range of organic compounds [65]. Most oxygenases are single-component flavoenzymes capable of catalyzing reduction and oxidation reactions with tightly bound flavin as cofactor [65,73]. However, several oxygenases have also been identified as two component systems. In general, two-component oxygenases are composed of two distinct proteins with different activities, a flavin reductase and a monooxygenase [65]. An increasing number of FMNH₂-dependent oxygenases enzymes have been identified and characterized [53,54,65,72]. These enzymes are also referred to as two-component flavin-dependent monooxygenases due to their dependence on the flavin for catalytic activity [64].

During the last decade a large number of two-component flavin monooxygenases have been identified. They are involved in a variety of biological processes including biodegradation of organosulfurs and aromatic compounds in the environment, biosynthesis of antibiotics, and drug detoxification. These systems have been identified in a diverse range of bacterial organisms. In general, the two-component monooxygenase is composed of a flavin reductase that catalyzes the reductive half-reaction and a monooxygenase that catalyzes the oxidative half-reaction separately. Reduction of the flavin by flavin reductase is a critical control point for catalysis by flavin monooxygenases. Thus, this control prevents the wasteful use of NAD(P)H or the production of reduced flavin that would produce reactive oxygen species such as H₂O₂ [74]. In addition to the alkanesulfonate monooxygenase system, a two-component flavoenzyme, 4-hydroxyphenylacetate-3-monooxygenases, has been identified in *E. coli*,

P. aeruginosa, *P. putida*, and *Acinetobacter baumannii* [53,54,65,74-78]. This enzyme is involved in the hydroxylation reaction of all aromatic compounds. Two-component flavin-dependent monooxygenases from *S. coelicolor* and *S. pristinaespiralis* are involved in the biosynthesis of the natural occurring antibiotic actinorhodin and pristinamycin, respectively [75,76]. A two-component flavoenzyme monooxygenase from *V. harveyi* catalyzes the production of bioluminescence by the oxidation of reduced flavin and a long-chain aliphatic aldehyde [65]. A two-component enzyme, the NADH:flavin adenine dinucleotide oxidoreductase (TftC) and the chlorophenol 4-monooxygenase (TftD) of *Burkholderia cepacia* AC1100 are responsible for the degradation of the environmental pollutant 2,4,5-trichlorophenoxyacetic acid [77]. Interestingly, in these enzyme systems flavin does not function as a cofactor but serves as a cosubstrate for their catalytic activity. The unique features of the flavin-dependent two-component monooxygenase system from *E. coli*, including the nature of the enzymes, the substrates utilized, the reactions catalyzed, and applicational aspects of this enzyme system are the main subject of this literature study. The term alkanesulfonate monooxygenase system will be used to refer to this two-component system.

1.9 The Alkanesulfonate monooxygenase proteins

1.9.1 The flavin reductase (*SsuE*)

NAD(P)H-dependent FMN reductase *SsuE* (UniProtKB accession number P80644) catalyzes the reduction of FMN by NAD(P)H to generate FMNH₂ as the product [54]. *SsuE* is also capable of reducing FAD or riboflavin with lower catalytic efficiency [54,53]. Native *SsuE* was first characterized as a homodimeric protein with a monomeric

molecular weight of 25.4 kDa [54]. However, further investigation by analytical ultracentrifugation and electrospray mass spectroscopy analyses verified that the actual molecular weight for monomeric SsuE is 21.3 kDa in closer agreement with the calculated molecular weight [78]. Because SsuE does not possess a flavin cofactor, it cannot be classified as a flavoprotein reductase (Class I flavin reductases), instead it is classified as a non-flavoprotein reductase (Class II flavin reductases). SsuE is then named FRP-II based on its substrate specificity for NAD(P)H, although SsuE was able to oxidize NADH with much lower efficiency [54,78].

Interestingly, SsuE does not contain any sulfur-containing amino acid residues, except one initiation methionine residue. This indicates the efficiency of the bacteria in sulfur utilization when sulfur is limiting in the environment. Results from amino acid sequence alignment showed that SsuE has no significant amino acid homology with other flavin-dependent reductases [79,54]. However, several flavin reductases or flavoproteins from different bacterial species, such as NADH:FMN oxidoreductase from *P. aeruginosa* (MsuE_Pseae), iron-sulfur flavoprotein from *Methanosarcina thermophila* (ISF_Mette), and putative iron-sulfur flavoproteins from *Methanococcus janaschii* (ISF_Metja and ISF2_Metja), showed a small conserved motif at the N terminus with over 40% identity within a 45-amino acid internal region (Figure 1.12) [54]. Amino acid residues identical in all proteins are indicated with an asterisk. Amino acid residues identical in four or three proteins are indicated with a semicolon or a dot. Cysteine residues involved in the iron-sulfur cluster of flavoproteins are indicated in white on a black background. Despite the low amino acid sequence identity among the flavin reductases, they show a notable structural similarity. The crystal structure of *E. coli* flavin reductase, Fre, showed that the

```

ISF_Mette      MKITGISGSPRKGQNCEKIIGAALVAKERGFETDTVFI SNEEVAPCKAC 50
ISF2_Metja    MKVIGISGSPRPEGNTTLLVREALNAIAEEGIETEFISLADKELNPCIGC 50
ISF_Metja     MKVFGISGSPRLQG-THFAVNYALNYLKEKGAEVRYFSVSRKKINFCLHC 49
SsuE_Ecoli    MRVITLAGSPRFPSRSSSLLEYAREKLNGLDVEVYHWNLQNFAPEDLLYA 50
MsuE_Pseae    MLVVSIGGSPSTRSRSGVLLERSRQWLQDRGVEVVSFQVRDFPAEDLLHA 50
* : :.***          : : : . * . : .

ISF_Mette     GACRDQDF-CVIDDDMDEIYEKMRADGIIVAAPVYMGNYPAQLKALFDR 99
ISF2_Metja    NMCKEEGK-CPIIDDVDEILKKMKEADGIILGSPVYFGGVSAQLKMLMDR 99
ISF_Metja     DYCIKKKEGCIIHKDDMEEVYENLIWADGVIIIGTPVYQGNVTGQLKTLMDR 99
SsuE_Ecoli    RFD-----SPALKTFTEQLQQADGLIVATPVYKAAYSGALKTLLDL 91
MsuE_Pseae    RFD-----SPQVQHFQQLVAQADGLVVATPVYKASFAGALKTLLDL 91
                :. . : : ***:~::~*** . .. ** *:*

ISF_Mette     S-VLLRRKNFALKNKVGAALS VGGSRNGGQEKTIQSIHDWMHIHGMI VVG 148
ISF2_Metja    S-RPLR-IGFQLRNKVGAVAVGASRNGGQETTIQQIHNFFLIHSMIVVG 147
ISF_Metja     CRAILAKNPKVLRGRVGM AIVGGDRNGGQEI ALRTIHDFFIINEMIPVG 149
SsuE_Ecoli    LPERALQGKVVLP L ATGGTVAHLLAVDYALKPVLSALKAQEILHG VFADD 141
MsuE_Pseae    LPERALEHKIVLP IATGGSIAHMLAVDYALKPVLSALKAQETLQGI FADD 141
                * . * ::: :. : .: :: : : :

ISF_Mette     DN---SHFG--GITWNP-----AEEDTVGMQTVSETAKKLC DVLELIQK 187
ISF2_Metja    DNDPTAHYGGTGVGKAPGD----CKNDDIGLETARNLGKKVAEVVKLIKK 193
ISF_Metja     GGSFGANLGATFWSKDRGKK--GVEEDEEGLRVL RKT LNRFYEV LKEKRG 197
SsuE_Ecoli    SQVIDYH--HRPQFTPNLQTRLDTALETFWQALHRR-DVQVPDLLSLRGN 188
MsuE_Pseae    SQIAYGEGAKPAQLAPALEERLHDSLETFHVALARRPRPVAPGVLNER-- 189
                . . : : :

ISF_Mette     NRDK----- 191
ISF2_Metja    -----
ISF_Metja     L----- 198
SsuE_Ecoli    AHAENTERRPASTE 202
MsuE_Pseae    ---LISARWSI--- 197

```

Figure 1.12. Sequence alignment of *E. coli* SsuE (SsuE_Ecoli) [54].

enzyme structure is similar to the structures of the ferredoxin reductase family [79]. Ferredoxin-NADP⁺ reductase (FNR) catalyzes the two-electron reduction of NADP⁺ by pairing electrons coming through ferredoxin (a one-electron carrier) in the photosynthetic electron transport chain of chloroplasts [80]. Although SsuE shows a low amino acid sequence identity with other flavin reductases, a conserved RXXS motif found in Fre and FNR, which is believed to be involved in flavin binding, is also found in SsuE [79].

1.9.2 The alkanesulfonate monooxygenase (SsuD)

The flavin-dependent alkanesulfonate monooxygenase SsuD (UniProtKB accession number P80645) catalyzes the oxygenolytic of C-S bond cleavage of alkanesulfonates in the presence of FMNH₂ and dioxygen [81,54]. The monomeric molecular weight for SsuD was 45.3 kDa by gel filtration chromatography [54,81]. However, the corrected monomeric molecular weight for SsuD protein was later determined to be 41.6 kDa by analytical ultracentrifugation and electrospray mass spectroscopy [78]. The homotetrameric structure of SsuD is uncommon among flavin-dependent monooxygenase where most exist as heterodimeric or homodimeric proteins. For instance, all known bacterial luciferases are $\alpha\beta$ dimers with the active site located in the α subunit [65,82]. The monooxygenase component of pristinamycin II_A synthase (SnaA) was also shown to be an $\alpha\beta$ heterodimer, whereas component A of the nitrilotriacetate monooxygenase (NtaA) was a homodimeric enzyme [82,83]. Functionally, SsuD is categorized as a monofunctional monooxygenase that can only catalyze the oxidative half-reaction and does not contain any bound flavin cofactor. The term flavin-dependent for this enzyme is due to the absolute requirement for the reduced

flavin substrate provided by the SsuE-catalyzed reaction.

The three-dimensional structure of SsuD in the absence of substrates has been solved to 2.3 Å resolution (PDB accession file 1M41) [81]. The monomeric structure of SsuD is shown in ribbon diagrams (Figure 1.13). Secondary structural elements are colored in red for α -helices, green for β -strands, and white for loops. It has dimensions of 60 Å x 50 Å x 40 Å and consists of a single domain. Each subunit of the homotetrameric enzyme is composed of an eight-stranded β/α (TIM)-barrel motif enlarged by four insertion regions that contribute to intersubunit interactions. The TIM barrel fold motif is commonly found in enzymes that contain a flavin binding pocket [84].

Sequence alignment studies have shown that there are conserved residues among flavin-dependent monooxygenases. The Cys54, Phe7, His11, His333, Tyr331, His228, Arg297 and Arg226 amino acid residues are believed to form the putative binding pocket and catalytic center of SsuD as shown in the diagram (Figure 1.14A). The space filling model shows the cavity of SsuD with Arg297 (green color) protruding on the surface of the structure. The Arg297 residue may function as gate for reduced flavin transfer or substrate binding during catalysis (Figure 1.14B) [81,84]. A random mutation of the Arg residue to Cys in the initial cloning of SsuD showed that the enzyme activity had been disrupted completely [54]. Several other amino acids residues such as His228, Tyr331, His11, His333, and R226 along with Cys54 form an enzyme cavity at the C-terminal end of the TIM barrel (Figure 1.14B). Further analysis has shown that many of the conserved residues that were shown to be directly involved in catalysis in bacterial luciferase are also found in the putative active site of SsuD. Amino acids Cys54, His 228, and Tyr331 of SsuD are found in a similar location and spacially resemble the Cys106, His44, and

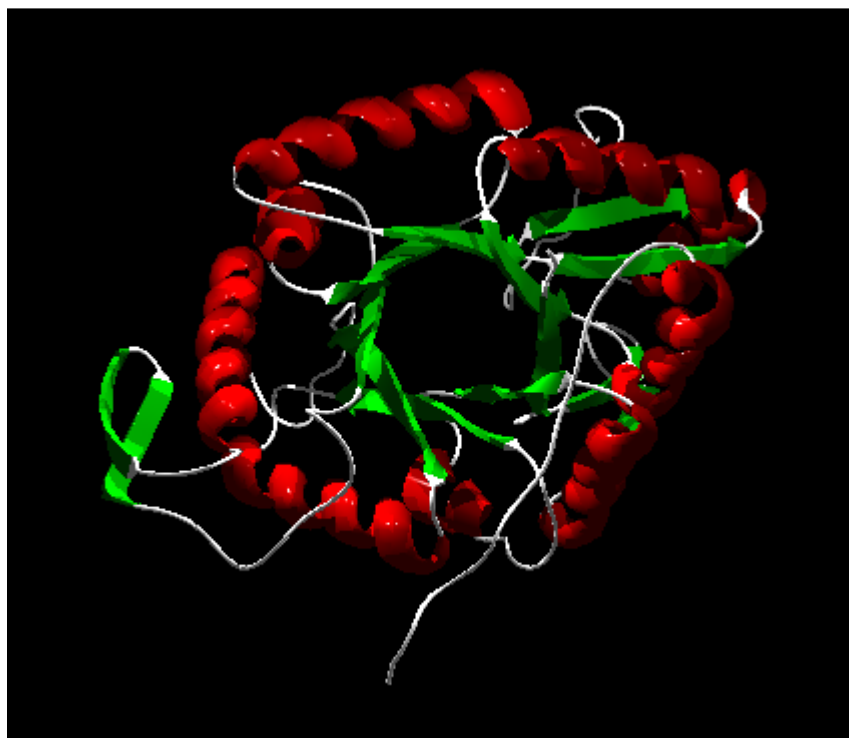


Figure 1.13. Three dimensional structure of the alkanesulfonate monooxygenase monomer [81].

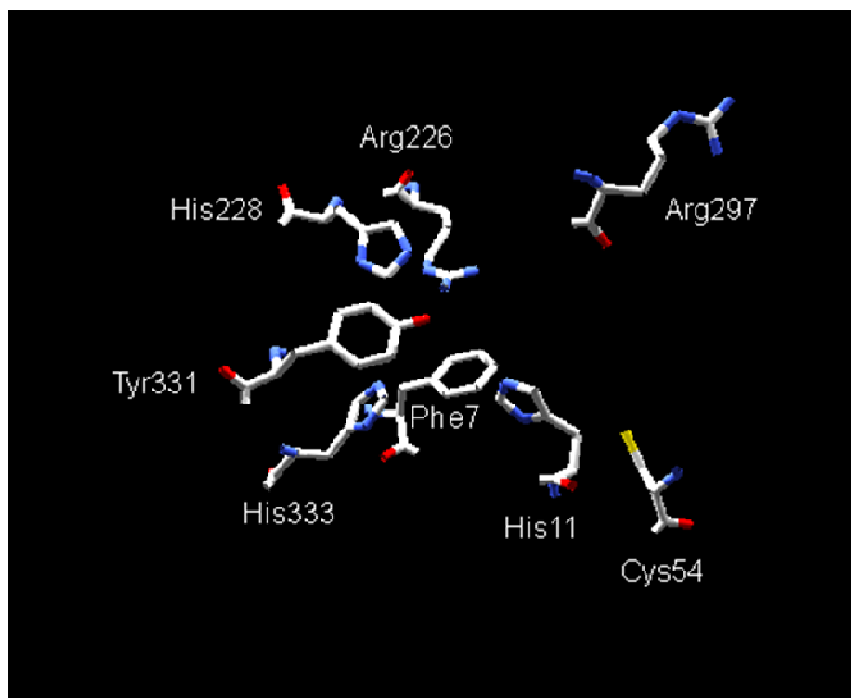
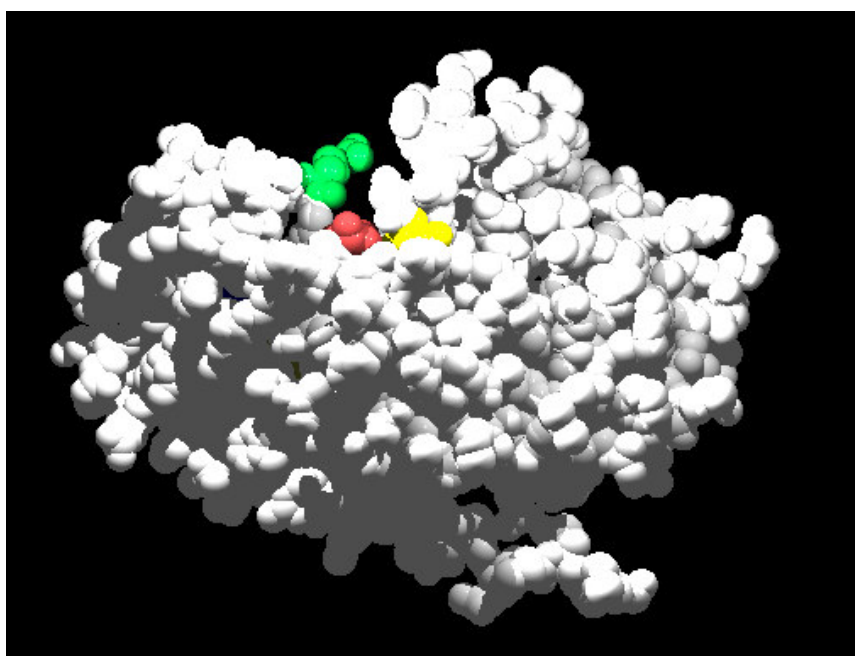
A**B**

Figure 1.14. The active-site pocket of alkanesulfonate monooxygenase in stick and space-filling model [81].

Tyr110 residues in LuxA bacterial luciferase [85,81]. The Cys54 amino acid was also suspected to be involved in enzyme activity, since cysteine-labeling with methylmercury destroyed SsuD activity [81].

Several SsuD homologs that are present in *Bacillus* sp., *Pseudomonas* sp., *Yersinia* sp., *Klebsiella* sp., and *Mycobacterium* sp. share over 50% amino acid sequence identity with *E. coli* SsuD and are suspected to be involved in sulfur assimilation in these organisms [37]. Amino acid sequence alignments between SsuD and related FMNH₂-dependent monooxygenases shows that Arg297, Cys54, His 228, Tyr331 are conserved in SsuD homologs as well as in the monooxygenase component of pristinamycin II_A synthase (SnaA), component A of the nitrilotriacetate monooxygenase (NtaA), and component A of thiosulfate-oxidizing periplasmic multienzyme system (SoxA) (Figure 1.15) [37,81]. Residues conserved in all five proteins are indicated with an asterisk. Residues conserved in at least three proteins are indicated with a semicolon or a dot. Dotted lines indicate the missing regions of the SsuD structure.

Results from amino acid sequence analyses showed that SsuD contains only one cysteine and four methionine residues including the methionine at the initiation sequence. This again indicates the efficiency of the bacteria in sulfur utilization, and is consistent with the low sulfur amino acid content observed in SsuE. The low content of sulfur-containing amino acids in both enzymes provides direct evidence on how the bacterial species survives by limiting the use of sulfur in the production of proteins needed for sulfur assimilation.

The SsuD enzyme utilizes a wide range of substrates from C-2 to C-10 alkanesulfonates, as well as N-phenyltaurine, 4-phenyl-1-butanefulfonic acid [54].

```

NTAA_CHEH      MGAN-KQMNLFQISGV--HYGGWRYPSAQPHRATDIQYYAEIVRTAE 47
SNA_A_STRP     MTAPRRRITLAGI IDGPGG--HVAAWRHPATKADAQLDFEFHRDNARTLE 48
SOXA_RHOS      MTQQ-RQMLLAGFFSAGNVTHAHGAWRHTDASNDFLSG-KYYQHIARTLE 48
SSUD_BACS      -----MEILWFIP THGD-----ARYLGSSESDGRTADHLYFKQVAQAAD 38
SSUD_ECOL      -----MSLNMFWFLP THGD-----GHYLTGTEEGSRPVHDGYLQQAQAAD 40
               : : : : . . . . : : : :
NTAA_CHEH      RGKLDFCFLADSI AAYEGSADQQDRSKDALMAAEPKRLLPEPTLLAALAM 97
SNA_A_STRP     RGLFDVAVFIADIVAVWG-----TRLDSL CRTSRTEHFEP LTLAAYAA 91
SOXA_RHOS      RGKFDLLFLPDGLAVEDSYGDNLD TGVG--LGGQGA VALEPASVVATMAA 96
SSUD_BACS      RLGYTGVLLP-----TGRSCEDPWLTA SALAG 65
SSUD_ECOL      RLGYTGVLLP-----TGRSCEDAWLVAAS MIP 67
               * : : : . . . . : : : :
NTAA_CHEH      VTEHIGLVTTATTTYN EPTYMARLFASLDHITN GRAGWNVVTSANLAEAH 147
SNA_A_STRP     VTEHIGLCATATTTYN EPHAIAARFASLDHLSGGRAGWNVVTSAPWESA 141
SOXA_RHOS      VTEHLGLGATISATY YPPYHVARVFATLDQLSGGRVSWNVVTSLNDAEAR 146
SSUD_BACS      ETKDLKFLVAVRPGLMQPSLAARMTSLDRISDGRLLIN VVAGDYPYELA 115
SSUD_ECOL      VTQRLKFLVALRPSVTSPTVAARQAATLDRLSNGRALFN LVTGSDPQELA 117
               * : : : . . . . * * * : : : * * * : : :
NTAA_CHEH      NFGRDGHVEHGD RYARAEEF INVVFKLWDSIEDGAYLRDKLAGRYLSEK 197
SNA_A_STRP     NFGFPHEHLEHGKRYERAEEF IDVVKKLWDS-----DGRP----- 175
SOXA_RHOS      NFGINQHLEHDARYDRADEFLEAVKKLWNSWDEDALVLDKAAGVFADPAK 196
SSUD_BACS      GDG--LFI SHDERYEATDEFLT VWRLLQG----- 143
SSUD_ECOL      GDG--VFLDHSERYEASAEFTQVWRLLQR----- 145
               . * : : * . * * : * * . : * :
NTAA_CHEH      IHFINHIGEHFKV RGPLNVPRPPQGHPIVQAGSSHPGKELAAARTAEVV 246
SNA_A_STRP     ---VDRHGRTHFEAPG-PLGIARPPQGRPVI IQAGSSPVGREFAARHAEVI 221
SOXA_RHOS      VHYVDHHEGLNVRG-PLQVPRSPQGEPIVLLQAGLSPRGRRFAGKWA EAV 245
SSUD_BACS      -ETVSYEGKH I KVENSNLLFPPQEPHPPIYFGSSSQAGIEAAAKHTDVY 192
SSUD_ECOL      -ETVDFNGKH I HVGAKLLFPAIQQPYPPLYFGSSDVAQELAAEQVDLY 194
               :.. * :.. . * .. : * : . * * . . * . . :
NTAA_CHEH      FTAQQTLADGKAFYSDVKGRMAKYGRSSEN LKVLPGVVVVAETESEAKA 296
SNA_A_STRP     FTRHNRLSDAQDFYGD LKARVARHGRDPEKVLVWPTLAPIVAATDTEAKQ 271
SOXA_RHOS      FSLAPNLEVMQATYQG IKAEVDAAGRDPDQTKIFTAVMPVLGESQAVAQE 295
SSUD_BACS      LTWGEPPQVQKEK IERVKKQAAKEGR---SVRFGIRLHV IARETEQEAW 239
SSUD_ECOL      LTWGEPELVKEK I EQVRAKAAAHGR---KIRFGIRLHV I VRETND EAWQ 241
               : : : : : : * * . . : : *
NTAA_CHEH      KYETVSNLVPDFGLFMLS DLLGEIDLKQFIDG PLPEDLPEAKGS--QS 344
SNA_A_STRP     RLQELQDLTHDHALR TLQDHLGDVDSLAYSIPIDGPVP-DIPYTNQS--QS 318
SOXA_RHOS      RLEYLNSLVHPEVGLS TLSSHTG-INLAAYPLDTP I KDILRDLQDRNVPT 344
SSUD_BACS      AAERLISHLDDDT-----I AQAALSRYDSSGQQRMAVLHQGDR---T 280
SSUD_ECOL      AAERLISHLDD E-----I AQAAAFARTDSVGQQRMAALHNGKR---D 282
               : : . . . . :
NTAA_CHEH      RREVIINLARRENLTIRQLYQRVSGASGHR-SIWGTPKQIADQFEQWVYE 393
SNA_A_STRP     TTERLIGLARRENLS IRELALRLMGD----IVVGTPEQLADHMESWFTG 363
SOXA_RHOS      QLHMFAAATHSEELT LAEMGRRYGTNVGFVPQWAGTGEQIAD ELIRHFEG 394
SSUD_BACS      KLEISPNLWAG IGLVRGGAGT-----ALVGDPTIADR IAEYQAL 320
SSUD_ECOL      NLEISPNLWAGVGLVRGGAGT-----ALVGDGPTVAARINEYAAL 322
               . . * . . * * : * * :
NTAA_CHEH      EAADGFNILPPYLPESMND FVNFVVPPELQRRGIFRTEYEG-STLRDHLGL 442
SNA_A_STRP     RGADGFNIDFPYLPGSADDFVDHVVPPELQRRGLYRSGYEG-TTLRANLGI 412
SOXA_RHOS      GAADGFIISP AFLPGSYDEFVDQVVPVLQDRGYFRTEYQG-NLIRDHLGL 443
SSUD_BACS      GIESFIFSGYPHLEEAY-YFAELVFP LLPFENDRTRK LQ--NKRGEAVGN 367
SSUD_ECOL      GIDSFVLSGYPHLEEAY-RV GELLFPLLDVAIPEIPQPQLNPQGEAVAN 371
               . . . * : . : : * * : . . :
NTAA_CHEH      ARPKNSVAKPS 453
SNA_A_STRP     DAPRKAGAAA- 422
SOXA_RHOS      RVPQLQGQPS- 453
SSUD_BACS      TYFVKEKNA-- 376
SSUD_ECOL      DFIPRKVAQS- 381

```

Figure 1.15. Sequence alignment of SsuD from *E. coli* with its *Bacillus subtilis* homologue SsuD_Bs, *C. heintzii* nitrilotriacetate monooxygenase NtaA, *S. ristinaespiralis* pristinamycin synthase subunit A SnaA, *Rhodococcus sp.* IGTS8 dibenzothiophene desulfurization enzyme SoxA [81].

Among the substrates that have been tested, decanesulfonic acid (C-10), octanesulfonic acid (C-8), and 1,3-dioxo-2-isoindolineethanesulfonic acid were the best substrates based on catalytic efficiencies (Table 1.4) [34]. There was no activity observed when taurine, methanesulfonic acid, L-cysteine, L-cysteic acid, ethanedisulfonic acid, and aromatic sulfonates were tested as the substrates for SsuD (refer to Table 1.3). The ability of SsuD to cleave the C-S bond of alkanesulfonates is not a commonly observed enzymatic mechanism. The enzymatic mechanism involving C-S bond cleavage in bacterial systems is found for the utilization of carbon as energy sources instead of sulfur acquisition [37,87]. However, a different set of enzymes and metabolic pathways from SsuD are used to obtain carbon. Therefore, the enzymatic mechanism of C-S bond cleavage for sulfur utilization by SsuD may be distinct from the enzymatic mechanism of C-S bond cleavage for utilization of carbon as energy sources. This assumption is based on the observation that the alkanesulfonate monooxygenase system does not play a role in carbon metabolism, and its synthesis is under the regulation of sulfur availability [88].

1.10 Reduced flavin and reduced flavin transfer in biological systems

1.10.1 Reduced flavin

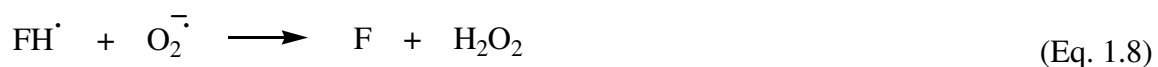
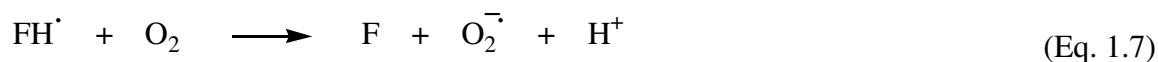
Reduced flavin refers to the product from the reduction of FMN or FAD catalyzed by NAD(P)H-flavin reductases. Free reduced flavin is a very unstable species, and its function in biological systems has not been fully characterized. Recent findings suggest that reduced flavin, as an intermediate product, is required as a substrate for certain enzymes that are not part of a strict two-component complex. The flavin in its fully reduced form is an effective reducing agent or electron-transfer carrier. For example,

Table 1.4. Kinetic parameters of alkanesulfonate monooxygenase with various substrates [34].

Sulfonated substrate	K_m	V_{max}	k_{cat}/K_m
	<i>units/m</i>		
	μM	<i>g</i>	$min^{-1} \mu M^{-1}$
Decanesulfonic acid (25-500 μM)	35	1.4	6.7
Octanesulfonic acid (33-666 μM)	44	1.6	6.1
1,3-Dioxo-2-isoindolineethanesulfonic acid (33-500 μM)	114	4.1	6.0
2-(4-Pyridyl)ethanesulfonic acid (33-500 μM)	139	3.8	4.6
Hexanesulfonic acid (50-500 μM)	95	2.3	4.0
<i>N</i> -Phenyltaurine (50-500 μM)	237	4.6	3.2
4-Phenyl-1-butanesulfonic acid (70-500 μM)	110	1.8	2.7
Pentanesulfonic acid (70-500 μM)	189	2.0	1.8
MOPS (70-1000 μM)	617	4.1	1.1
Butanesulfonic acid (250-1000 μM)	870	3.3	0.6
PIPES (333-3000 μM)	1110	2.4	0.4

ferric complexes or iron proteins can be reduced by the reduced flavin product of flavin reductases [67,89]. Flavin reductases from *E. coli* have been shown to stimulate the production of superoxide radicals by supplying reduced flavin for reactivation of ribonucleotide reductase [90]. Several other studies have shown that microbial systems also effectively utilize reduced flavin in reducing the iron center of ribonucleotide reductase [65,91,92,93]. The absolute requirement of flavin reductases for the activation of these processes suggests that the reduced flavin is essential in biological functions.

The majority of flavoprotein-reducing substrates are dehydrogenated in a two-electron reduction step generating reduced flavin, and reduced flavin is then re-oxidized by its oxidizing substrate. In many flavoenzymes, dioxygen is the oxidizing physiological substrate, therefore when reduced flavin is uncoupled from a catalytic reaction it leads to deleterious effects to the system. Oxidation of reduced flavin can occur either in a two-electron step, or in single one-electron steps, in which the flavin semiquinone would be observed as an intermediate [63,94]. It has been fully established that reduced flavin is a highly reactive intermediate and is easily oxidized in the presence of dioxygen generating various toxic species (Eq. 1.5-1.8) [95]. In air-saturated solution, the FMNH₂ for example, has a half-life of only ~25 ms [65].



Autoxidation of biomolecules would generate reactive by-products, such as hydrogen peroxide (H_2O_2), superoxide anion radical (O_2^-), and the highly reactive hydroxyl radicals ($\cdot\text{OH}$) [96]. The autoxidation of reduced flavin by molecular oxygen typically yields a mixture of hydrogen peroxide (H_2O_2) and superoxide anion radical (O_2^-) [73,97]. Electron transfer to dioxygen only occurs in two one-electron steps in which initial electron transfer generates O_2^- and flavosemiquinone (FH^\bullet) (Figure 1.16) [94]. The flavosemiquinone can react with another dioxygen molecule to generate O_2^- (Figure 1.16, left pathway). Typically either the generated O_2^- or the semiquinone species undergoes a spin inversion before the O_2^- can depart, permitting orbital overlap and the formation of a peroxy adduct at position C4a on the isoalloxazine ring. The hydroperoxyflavin (FIOOH) intermediate will be generated, and the reaction of this intermediate with a proton (H^+) will release H_2O_2 (Figure 1.16, right pathway).

The rate of the reaction between enzyme-bound reduced flavin and dioxygen vary over several magnitudes depending on the protein [94,98,99]. Part of the variation may be due to differences in the extent at which the isoalloxazine ring is exposed to solvent [94]. Considering the reactivity of reduced flavin towards dioxygen, the fate of reduced flavin will be critically dependent on the mechanism of the transfer of this unstable intermediate in biological systems.

1.10.2 Reduced flavin transfer in biological systems

Because reduced flavin can be rapidly oxidized generating oxygen radicals, the mechanism involving direct transfer of the reduced flavin would likely be more favorable in a cellular system. Therefore, in the alkanesulfonate monooxygenase system the

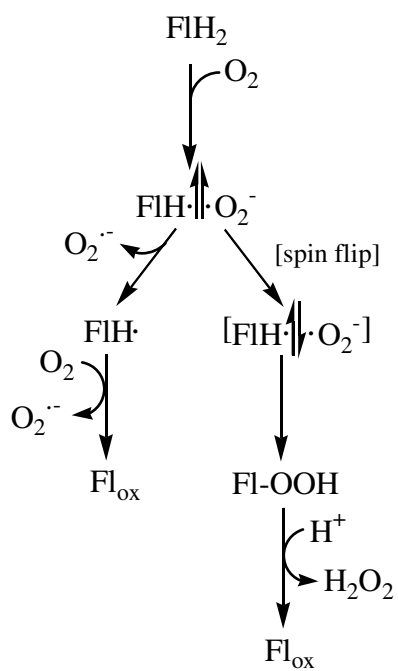


Figure 1.16. Autoxidation reaction of reduced flavin with molecular oxygen [86].

transfer of FMNH₂ may be tightly controlled through protein interactions and specific channeling between SsuE and SsuD. Alternative results describing the transfer of reduced flavin have been reported depending on the system being studied. From the enzyme systems that have been studied, the mechanism of reduced flavin transfer fall into three categories: a) free diffusion; b) direct channeling; and c) mixed flavin transfer.

1.10.2.1 Reduced flavin transfer by free diffusion

In the free diffusion mechanism, the reduced flavin product diffuses between two proteins without any interactions between the reduced flavin donor and acceptor proteins (Figure 1.17). This type of mechanism has been reported in the NAD(P)H-flavin oxidoreductase (HpaC) and 4-hydroxyphenylacetate 3-hydroxylase (HpaB) coupled assay from *E. coli*. Using *in vitro* kinetic and fluorescence analyses, there was no substantial change in the apparent K_m value for FAD in the coupled-enzyme reaction. These results suggest that protein-protein interactions between HpaC and HpaB do not play a role in the coordinated production and utilization of FADH₂ in *E. coli* [100]. Similar results were observed in the two-component flavin-dependent *p*-hydroxyphenylacetate hydroxylase (HPAH) from *P. aeruginosa* [75,101]. The mechanism of reduced flavin transfer by free diffusion has also been reported in a two-component flavin-dependent monooxygenase (ActVB flavin reductase and ActVA-ORF5 monooxygenase) involved in actinorhodin biosynthesis in *Streptomyces coelicolor* [102]. Affinity chromatography and fluorescence spectroscopic studies showed no protein-protein interactions between the ActVB and ActVA are necessary for efficient transfer of reduced flavin. In this enzyme system, reduced flavin transfer occurs by a rapid-diffusion process. The reduced

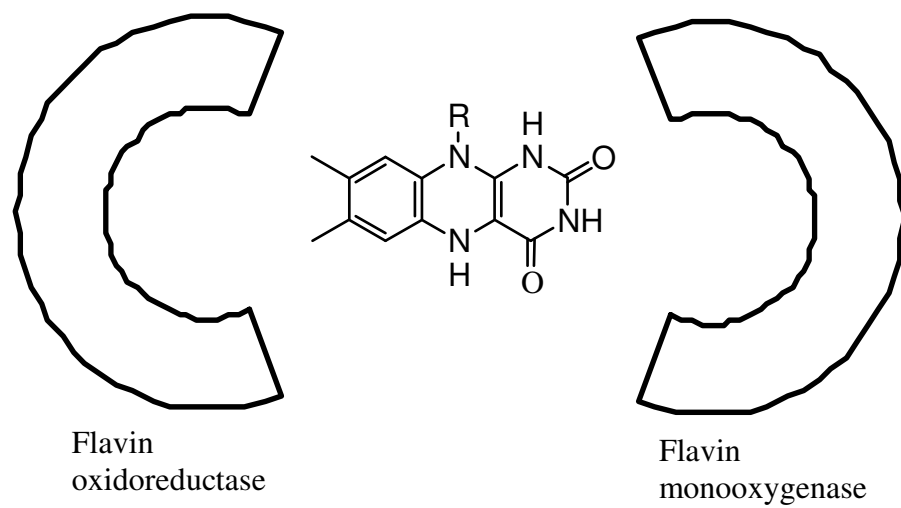


Figure 1.17. Mechanism of reduced flavin transfer through free diffusion between flavin oxidoreductase and flavin monooxygenase.

flavin then reacts with dioxygen to generate a flavin-peroxide intermediate. Although the mechanism of reduced flavin transfer by free diffusion is found in several enzyme systems, this mechanism is inefficient considering reduced flavin is highly reactive with dioxygen generating reactive oxygen intermediates. Moreover, under certain conditions such as physiological stress, the deleterious effects from the reaction of free reduced flavin with dioxygen may severely impact the cell.

1.10.2.2 Direct reduced flavin transfer

Because of the lability of reduced flavin, the protection of this intermediate from solvent contact or from side reactions is required during transfer. This can be achieved through the formation of a protein complex or molecular channel between the flavin reductase and the monooxygenase (Figure 1.18). Molecular channels will protect the reduced flavin from autoxidation by dioxygen. This reduced flavin transfer mechanism has been identified in several enzyme systems and they all showed similar kinetic properties. An altered kinetic mechanism for SsuE has been observed in the presence and absence of SsuD and the alkanesulfonate substrate [78]. In single-enzyme kinetic assays, SsuE follows an ordered sequential mechanism, with NADPH as the first substrate to bind and NADP⁺ as the last product to dissociate. However, in the presence of SsuD and octanesulfonate the kinetic mechanism of SsuE is altered to a rapid equilibrium ordered mechanism. Studies described herein have shown that SsuE and SsuD proteins are able to form stable protein-protein interactions in a 1:1 molar ratio [103]. Direct transfer of reduced flavin has been demonstrated through kinetic analyses between NADPH-dependent flavin reductase (FRP) and bacterial luciferase. The mechanism of FRP is

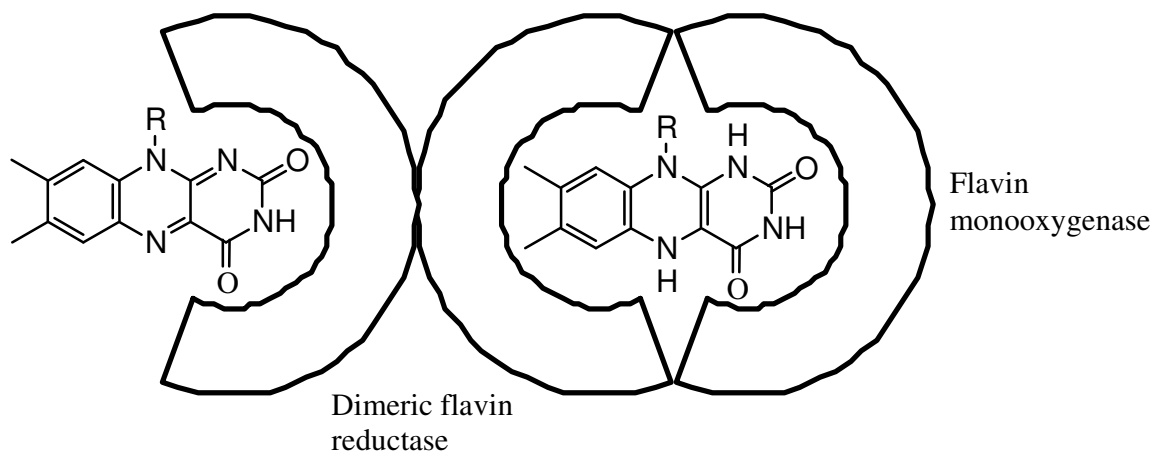


Figure 1.18. Direct reduced flavin transfer through protein-protein interactions between a flavin reductase and flavin monooxygenase.

altered from a ping-pong to a sequential kinetic mechanism in the luciferase-coupled assay providing strong support for complex formation as shown by fluorescent spectroscopy studies. These experimental results are further maintained by the observed decrease in the K_m values for both FMN and NAD(P)H in the luciferase-coupled assay when compared to the single FRP assay [104,105,106].

The mechanism involving direct transfer of the reduced flavin would likely be more favorable in a cellular system due to the instability of reduced flavin. In this case, and in similar enzyme systems, the transfer of reduced flavin may be tightly controlled through protein-protein interactions and specific channeling between SsuE and SsuD to avoid deleterious effects of toxic products generated by autoxidation of reduced flavin.

1.10.2.3 Mixed mechanism of reduced flavin transfer

Numerical simulations from steady-state kinetic studies of styrene monooxygenase (SMO) from *Pseudomonas putida* S12 supports an alternative mechanism for flavin transfer (Figure 1.19). The observed coupling of NADH to styrene oxidation can be best explained by a model that includes both the direct transfer and passive diffusion of reduced FAD from the NADH-specific flavin reductase (SMOB) to the FAD-specific styrene epoxidase (SMOA). The mechanism involves the formation of a transient protein complex with both the reductase and monooxygenase enzyme associated with the flavin [107]. In this enzyme system, the isoalloxazine ring of the oxidized FAD may be sufficiently accessible such that the NADH can provide electrons in the SMOB-catalyzed reductive half-reaction while the AMP portion of FAD is still associated with SMOA. The AMP moiety of FAD may remain accessible to SMOA

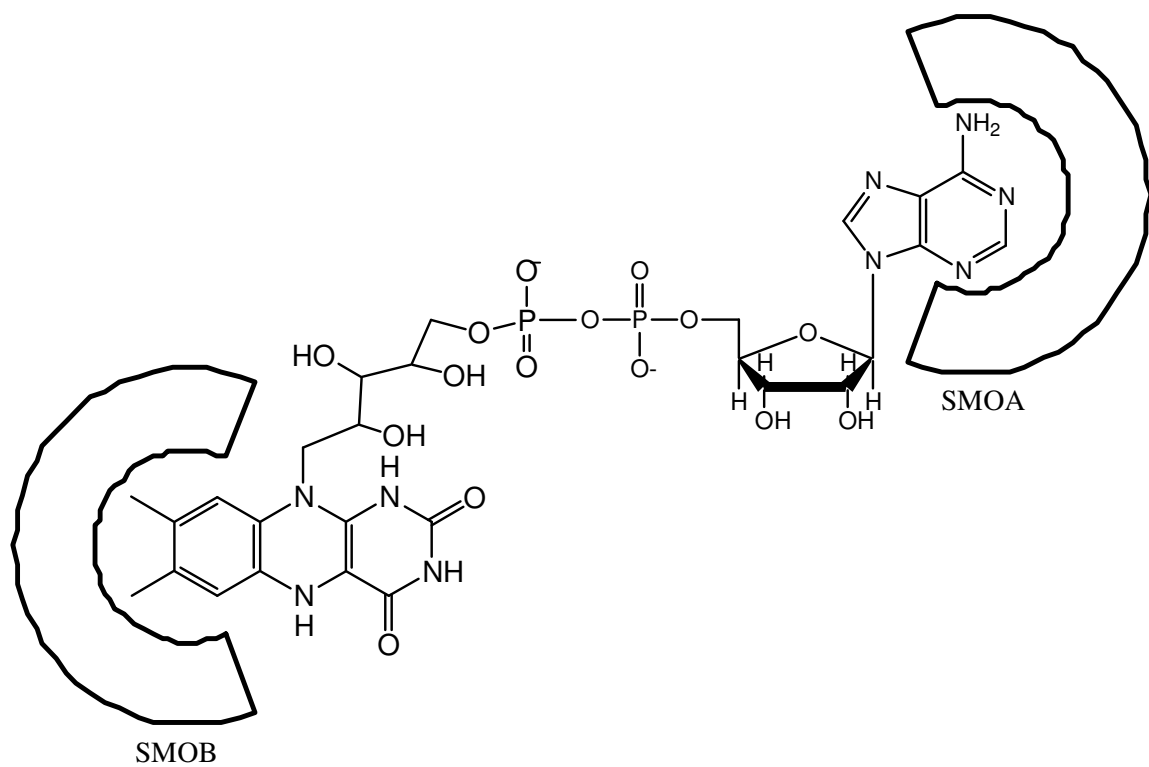


Figure 1.19. Mixed mechanism of reduced flavin transfer between NADH-specific flavin reductase (SMOB) to the FAD-specific styrene epoxidase (SMOA) from *Pseudomonas putida* S12 [107].

during binding and reduction of the isoalloxazine ring of free FAD by SMOB.

1.11 Basic principles of protein-protein interactions

Protein-protein interactions are essential in many biological processes. Any major biochemical process such as DNA replication, transcription, and translation, vesicle transport, and signal transduction rely on protein-protein associations [108-111]. The vast majority of proteins bind to other proteins at some time in their existence in order to perform various functions [110-115]. While numerous studies have addressed protein-protein interactions, the principles governing such interactions are not fully understood. From a structural point of view, there is no general pattern observed in the motif of binding sites. One of the reasons is because similar proteins structures can associate in different ways, or conversely proteins with globally different structures can associate in similar ways [116].

Contacting residues are those responsible for the interactions across interfaces. Two residues are defined to be contacting if the distance between any two atoms from different chains is less than the sum of their corresponding van der Waals radii plus 0.5 Å [117,118]. Residues are defined as nearby if the distance between its C_α atom and a C_α atom of any contacting residue is less than 6 Å [116]. Protein-protein interactions may be mediated by a small region of one protein fitting into a cleft in another protein or by two surfaces interacting over a large area [109]. Most interfaces are composed of two protein surfaces with both shape and electrostatic complementary [119,108]. Almost of all these interfaces bury more than 600 Å² of total surface area and it is often assumed that the energy protein-protein binding is directly related to the buried hydrophobic surface

area [108,120-122].

1.11.1 Hot spots of protein-protein interfaces

Alanine-scanning mutagenesis has shown that there is little correlation between buried surface area and free energy binding. A highly uneven distribution of energetic contributions of individual residues is found across each interface with certain residues responsible for the bulk of the binding energy [123,124]. These critical residues are called hot spots and are defined as a residue that when mutated to alanine, gives rise to a distinct increase in the absolute binding energy ($\Delta\Delta G$) of more than 2 kcal/mol. These hot spots are enriched in tryptophan, tyrosine, and arginine with the percentage of appearance at more than 10% [110,123,124].

It is well established that most hydrophobic residues are found in the interior of proteins, while polar and charged residues are found on the surfaces. Interestingly, tryptophan is found in interiors and on surfaces with nearly identical frequencies, the only hydrophobic residues for which this is true [125]. A data set of as many as 2325 alanine mutants of 25 monomer and dimer structures have been analyzed by using this experimental approach for which the change in free energy of binding upon mutation to alanine was measured [110]. These hot spots are surrounded by energetically less important residues that most likely serve to exclude bulk solvent from the hot spot by forming hydrogen bonds between residues. Exclusion of solvent is found to be essential for highly energetic interactions [116,110]. To a lesser extent, conservation of phenylalanine and methionine also signify a potential binding site. There is a positive correlation between energy hot spots and structurally conserved residues [126].

Computational analysis on hot spot residues indicate that hot spots are not randomly spread along the protein-protein interfaces, but tend to be clustered and are located within dense regions. Within an assembly, the tightly packed hot spots form networks of interactions. These assembly areas are called hot regions, and an interface may contain a single, or a few hot regions. The regions contain residues that are moderately conserved and further demonstrate the crucial role of the conserved interactions in the local densely packed environment [116].

1.11.2 Parameters in measuring protein-protein interfaces

Protein-protein interfaces are defined based on the change in their solvent accessible surface area (Δ ASA) when going from a monomeric to a dimeric state [108]. The interface residues (atoms) are defined as those having ASAs that decrease by $>1 \text{ \AA}^2$ on complexation [127,128,108]. There are several fundamental properties that characterize a protein-protein interface, which can be calculated from the coordinates of the complex [108].

1.11.2.1 Size and shape

The size and shape of protein interfaces can be measured simply in absolute dimensions (\AA) or in terms of the Δ ASA on complexation. The Δ ASA is often used, since there is a correlation between the hydrophobicity free energy of transfer from a polar to a hydrophobic environment and the solvent ASA [129]. Calculating Δ ASA may provide a measure of the binding strength. The shape of the interfaces can also be analyzed and is relevant in designing molecular mimics. Two protein subunits may

interact and form a protein-protein interface with relatively flat surfaces or form a twisted interface. A term “planarity”, which is a measure of how far the interface residues deviate from a plane, is commonly used to assess how flat or how twisted the protein-protein interfaces are. A term “circularity” is often used to provide a rough guide to the shape of the interface. An interface with a circularity ratio of 1.0 indicates an approximately circular interface.

1.11.2.2 Electrostatic and shape complementary

Electrostatic and shape complementary between surfaces of the interacting proteins have been used for characterization of protein-protein interfaces. Different methods have been used to evaluate the electrostatic and shape complementary of the interacting surfaces including the evaluation of gap indices in protein-protein interactions [130,131]. Gap index is measured according to the following equation (Eq. 1.9):

$$\mathring{A} = \mathring{A}^3 / \mathring{A}^2 \mathring{A} = \frac{\mathring{A}^3}{\mathring{A}^2} \quad (\text{Eq. 1.9})$$

where \mathring{A} is gap index, \mathring{A}^3 is gap volume between molecules, and \mathring{A}^2 is interface ASA (per complex). Based on gap index values from different types of protein complexes, the interacting surfaces of homodimers, enzyme-inhibitor complexes, and permanent heterocomplexes are the most complementary, whereas the antibody-antigen complexes and other nonobligatory heterocomplexes are the least complementary [108].

1.11.2.3 Residue interface propensities

The relative importance of different amino acids residues in the interfaces of complexes can give a general indication of the hydrophobicity, that can only be interpreted if the distribution of residues occurring in the interface are compared with the distribution of residues occurring on the protein surface as a whole. Residue interface propensities for each amino acid is defined as the fraction of ASA that an individual amino acid contributes to the interface compared with the fraction of ASA that an individual amino acid contributes to the whole surface (exterior residues plus interface residues) [108]. A propensity of >1 denotes that a residue occurs more frequently in the interface than on the protein surface. The propensities for hydrophobic residues, with the exception of methionine, show a greater preference for the interfaces of homodimers than for those of heterocomplexes. The lower propensities for hydrophobic residues in the heterocomplex interface is balanced by an increase propensity for polar residues.

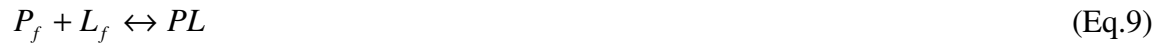
1.11.2.4 Hydrophobicity and hydrogen bonding

The mean hydrophobicity value of residues involved in protein-protein complexes will vary depending on the subunit composition of the protein complexes [132]. Studies have indicated that when the hydrophobicity values of the interface are compared between the homodimers and the heterocomplexes, the interfaces of the heterocomplexes are less hydrophobic than those of homodimers and are positively correlated with the residue propensities [108]. Major polar interactions between the components in the complexes can be predicted from the mean number of hydrogen bonds per 100 Å² of ΔASA. Studies have shown that the heterocomplexes that exist as both monomers and

complexes have more intermolecular hydrogen bonds per Δ ASA. This is positively correlated with the residue propensities in which the transient complexes (those with components that occur as both monomers and complexes) contained more hydrophilic residues in their interfaces than the permanent complexes [108].

1.11.2.5 Binding constants

The strength of protein-protein interactions can be measured through binding constant values that can be expressed in three different ways [109]. 1). Dissociation constant (K_d), the most commonly used binding constant is defined by the following equations (Eq. 9-10):



$$K_d = \frac{[P_f][L_f]}{[PL]} \quad (\text{Eq.10})$$

with the bound protein P, the bound ligand L, and the protein-ligand complex PL, while $[P_f]$ and $[L_f]$ refer to the concentration of unbound P and L, respectively. A smaller K_d value represents stronger binding. 2). Affinity constant (K_a), with $K_a = 1/ K_d$. 3). A ratio of two rate constants, that is between the rate of formation of PL and the rate of breakdown of PL. The rate of formation of PL is $k_a [P_f] [L_f]$, where k_a is the association rate constant. The rate of breakdown of PL is $k_d [PL]$, where k_d is the dissociation rate constant. At equilibrium, the rate of formation of PL equals the rate of breakdown of PL, and $K_d = k_d/k_a$.

The order of magnitude of K_d values for protein-protein interactions varies between 10^{-3} M to 10^{-16} M [109]. A K_d value for protein-protein interactions in the

nanomolar to micromolar range is considered a relatively strong interaction, and the protein-protein interactions are considered too strong when the K_d value is less than 10^{-12} M [109]. Protein-protein interactions that are too strong are usually generated from the association of multisubunit proteins. Any protein composed of three or more subunits can have significant interactions among individual pairs of the component protein. Thus, complicated structures might effectively lock the proteins together in undissociable units [109]. Examples of very strong protein-protein interactions have been found between human placental RNase inhibitor (PRI) with both angiogenin ($K_d = 7 \times 10^{-16}$ M) and human placental RNase ($K_d = 9 \times 10^{-16}$ M) [133-135].

1.11.3 The role of protein-protein interactions in metabolic processes

Protein-protein interactions play important roles in various biological processes. Such interactions may or may not lead to physicochemical changes of the interacting proteins. Nevertheless, any protein association has its unique function in cellular systems. Due to the diverse involvement of protein-protein interactions in living systems, the discussion of their roles will be limited to the formation of molecular channels and allosteric communication in enzymatic reactions.

Substrate channeling (or tunneling) is an important mechanistic process for the direct delivery of an intermediate from one active site of an enzyme to the active site of a second enzyme or within an enzyme with multiactive sites [136-138]. Substrate channeling has many advantages over free diffusion of reaction products within the bulk solvent. First, the transit time for the movement of reaction products from one active site to the next is reduced [139,140]. Second, chemically labile intermediates can be

protected from decomposition by the aqueous external environment [141]. Third, unfavorable equilibria can be circumvented and reaction intermediates can be segregated from competing enzymatic transformations [142,143].

Examples of substrate channeling have been found in different enzyme systems from various organisms, such as in multisubunit carbamoyl phosphate synthetase from *E. coli* [144]. Site-directed mutagenesis and structural analyses studies on this enzyme have shown the existence of a molecular channel as an escape route for the ammonia intermediate. The formation of molecular channels have been reported not only in multifunctional or multisubunits enzymes, but also in protein complexes between two separate proteins such as thymidylate synthase (TS) and dihydrofolate reductase (DHFR) [144]. These enzymes catalyze sequential reactions of thymidine 5'-monophosphate (dTMP) and 7,8-dihydrofolate (DHF) biosynthesis and in bacteriophage, bacteria, fungi, and mammals [144]. The kinetic evidence for substrate channeling of DHF between TS and DHFR has been reported for the TS-DHFR complex from *E. coli* and *Leishmania casei* (*L. casei*) [144,145]. In these enzyme systems, the production of NADP⁺ displayed a lag when TS was limiting and the overall time course closely matched the one predicted theoretically in a coupled system of two noninteracting enzymes [144].

The formation of a molecular channel may alter the physical and chemical properties of the interacting proteins. Depending on the nature of the proteins and the experimental approaches used, these alterations can be used to support the existence and importance of a channeling mechanism in certain enzymatic reactions. The reaction at one active site is affected by the reaction or substrate-enzyme interactions at another active site of the multisubunit enzyme or multienzyme complexes through a process

known as allosteric communication. The existence of allosteric communication between active sites is usually indicated by the alteration of kinetic properties of the enzymes [146,147]. For example, in tryptophan synthase from *Salmonella typhimurium* a reactive indole intermediate is channeled from the α subunit to the β subunit through a 25 Å long channel [146]. The α -subunit catalyzes the cleavage of indole 3-glycerol phosphate to produce indole and D-glyceraldehyde 3-phosphate. The β -subunit is involved in the formation of L-tryptophan from L-serine and indole intermediate. In the process, the formation of indole intermediate at the α -site is increased more than 30-fold by the formation of the α -aminoacrylate aldimine at the β -site [147].

Evidence of allosteric communication between the active sites of multisubunits enzyme has also been shown by the three catalytic sites of carbamoyl phosphate synthetase. Rapid-quench experiments indicated that during the assembly of carbamoyl phosphate, the formation of carboxy phosphate triggers a conformational change that is transmitted to the small subunit where the hydrolysis of glutamine is stimulated [144,148]. The observed enhanced ATPase rate in the presence of glutamine reflects the faster rate of attack on the carboxyl phosphate by the ammonia intermediate relative to water. Here, ammonia is not released until carboxy phosphate is ready to form carbamate [148].

1.12 Research objectives

Reduced flavins play important roles in biological systems. Due to its reactive properties, especially under aerobic conditions, the concentration level of free reduced flavin should be tightly controlled to avoid the generation of toxic molecules to living

cells. The mechanism of reduced flavin transfer in biological systems is still poorly understood. Therefore, studies of reduced flavin transfer become critical to fully understand the fate and function of this important intermediate. Varied results in the mechanism of reduced flavin transfer have been reported depending on the system being studied. In this study, the mechanism of reduced flavin transfer in the alkanesulfonate monooxygenase system, a two-component enzyme from *E. coli* is investigated. In this enzyme system, the NAD(P)H-dependent FMN reductase (SsuE) generates reduced flavin (FMNH₂) and the SsuD monooxygenase utilizes the reduced flavin for desulfonation of aliphatic sulfonates to sulfite and their corresponding aldehydes in the presence of molecular oxygen [37,54].

Due to the reactivity of reduced flavin with oxygen, direct reduced flavin transfer through a channeling mechanism is favored. A channeling mechanism would protect the reduced flavin from futile oxidation before catalysis can occur. The focus of these studies was to determine if protein-protein interactions occur between the alkanesulfonate monooxygenase proteins. The effect of these interactions on the mechanism of FMN reduction by SsuE and the amino acid residues involved in protein-protein interactions were also studied. Determination of amino acid residues involved in protein-protein interactions is very important to fully understand the mechanism of reduced flavin transfer. Two-component systems involving reduced flavin transfer have been identified from a large number of bacterial species. Therefore, the results from these studies will contribute to the establishment of the reduced flavin transfer mechanism in two-component bacterial systems.

CHAPTER TWO

MATERIALS AND METHODS

2.1 Bacterial strains and plasmid vectors

Various *E. coli* strains including XL-1, BL21(DE3), BL21(DE3)pLysS, Origami, Tuner, and Tuner pLysS were purchased from Stratagene (La Jolla, CA) (Table 2.1). Plasmid vectors pETDuet-1 and pET21a were obtained from Novagen (Madison, WI).

2.2 Biochemical and chemical reagents

Ampicillin, dithiothreitol (DTT), FMN, glucose, glucose oxidase, glycine, lysozyme, 2-morpholinoethanesulfonic acid (MES), β -mercaptoethanol, NADPH, potassium phosphate (dibasic anhydrous and monobasic anhydrous), silver nitrate, sodium chloride, sodium thiosulfate, streptomycin sulfate, trifluoroacetic acid, trypsin, and Tris base were purchased from Sigma-Aldrich (St. Louis, MO). The chemical cross-linking reagents ProFound Label Transfer Sulfo-SBED Protein:Protein Interaction Agent, 1-ethyl-3-(3-dimethylaminopropyl) carbodiimide hydrochloride (EDC), *N*-hydroxysulfosuccinimide (sulfo-NHS), bis(sulfosuccinimidyl) suberate (BS³), ethylene glycol bis(succinimidylsuccinate) (EGS), and mass spectroscopy matrices were from Pierce (Rockford, IL). Absolute ethanol, acetonitrile, agarose, ammonium bicarbonate,

Table 2.1. Bacterial *E. coli* strains used for protein expression.

Bacterial Strain	Description	Source
XL-1	XL1-Blue cells are endonuclease (<i>endA</i>) deficient, which greatly improves the quality of miniprep DNA, and are recombination (<i>recA</i>) deficient, improving insert stability. The <i>hsdR</i> mutation prevents the cleavage of cloned DNA by the <i>EcoK</i> endonuclease system. The <i>lacIqΔMI5</i> gene on the F' episome allows blue-white color screening.	Stratagene
BL21(DE3)	DE3 lysogen contains T7 polymerase upon IPTG induction. This strain is deficient of lon and omp-t proteases and is therefore suitable for expression of non-toxic genes.	Novagen
BL21(DE3)pLys	DE3 lysogen expresses T7 polymerase upon IPTG induction. The pLysS plasmid produces T7 lysozyme to reduce basal level expression of the gene of interest. Thus it is suitable for expression of toxic genes [pLysS contains the p15A origin. This origin allows pLysS to be compatible with plasmids containing the ColE1 or pMB1 origin (i.e. pUC- or pBR322- derived plasmids)]. Requires chloramphenicol for growth.	Novagen
Origami	Origami host strains are K-12 derivatives that have mutations in both the thioredoxin reductase (<i>trxB</i>) and glutathione reductase (<i>gor</i>) genes, which greatly enhances disulfide bond formation in the cytoplasm. Requires kanamycin and tetracyclin for growth.	Novagen
Tuner	Contains a mutation in the lac permease (<i>lacZY</i>) gene. This enables adjustable levels of protein expression throughout all cells in a culture. The lac permease (<i>lacY</i>) mutation allows uniform entry of IPTG into all cells in the population, which produces a concentration-dependent, homogeneous level of induction. By adjusting the concentration of IPTG, expression can be regulated from very low levels up to the robust, fully induced levels commonly associated with pET vectors. Lower level expression may enhance the solubility and activity of difficult target proteins.	Novagen
Tuner pLysS	Contains the pLysS plasmid (tighter control over expression) in addition to the lac permease mutation. Requires chloramphenicol for growth.	Novagen

ammonium sulfate, ethidium bromide, formaldehyde, glacial acetic acid, isopropyl- β -D-thiogalactoside (IPTG), 2-propanol, glycerol, sodium carbonate, and sodium phosphate were purchased from Fisher Biotech (Pittsburgh, PA). Octanesulfonate was from Fluka (Milwaukee, WI). LB-agar and LB-medium were from BIO 101 Systems (Carlsbad, CA). Streptavidin agarose column matrix was obtained from Invitrogen (Carlsbad, CA). Phenyl Sepharose column matrix was from Amersham Biosciences (Piscataway, NJ). Acrylamide/Bis solution, sodium dodecyl sulfate (SDS), and Macro-prep High Q Support were from Bio-Rad (Hercules, CA). All buffers and media solution were prepared using water purified at a resistance of 18.2 M Ω /cm through a Millipore system (MilliQ, QPAK II). Standard buffer solution contained 25 mM potassium phosphate (pH 7.5) and 10% glycerol unless otherwise noted.

2.3 Construction and expression of double cloning expression system

The T7 RNA polymerase-dependent expression vector pETDuet-1 containing two multiple cloning sites (MCS1 and MCS2) (Figure 2.1) was utilized for sub-cloning His-tagged *ssuE* (0.6 kb) and *ssuD* (1.1 kb) genes. The pETDuet-1 vector was PCR amplified using the primers 5' TGA CGT CTC TTC CCT CGA GTC TGG TAA AGA AAC C 3' and 5' AAT TGA CTC TTC CCA TAT GTA TAT CTC CTT CTT ATA C 3'. The *ssuD* gene carried by pET21a vector was PCR amplified using the primers 5' AAG GAA CTC TTC TAT GAG TCT GAA TAT GTT CTG G 3' and 5' GCC ATT CTC TTC TGA GTT AGC TTT GCG CGA C 3'. The *ssuD* gene was subcloned into pETDuet-1 vector at MCS2 utilizing the SeamLess[®] Cloning Kit (Stratagene, La Jolla, CA). The plasmid construct containing the *ssuD* gene was PCR amplified using primers 5' AAG GAG CTC

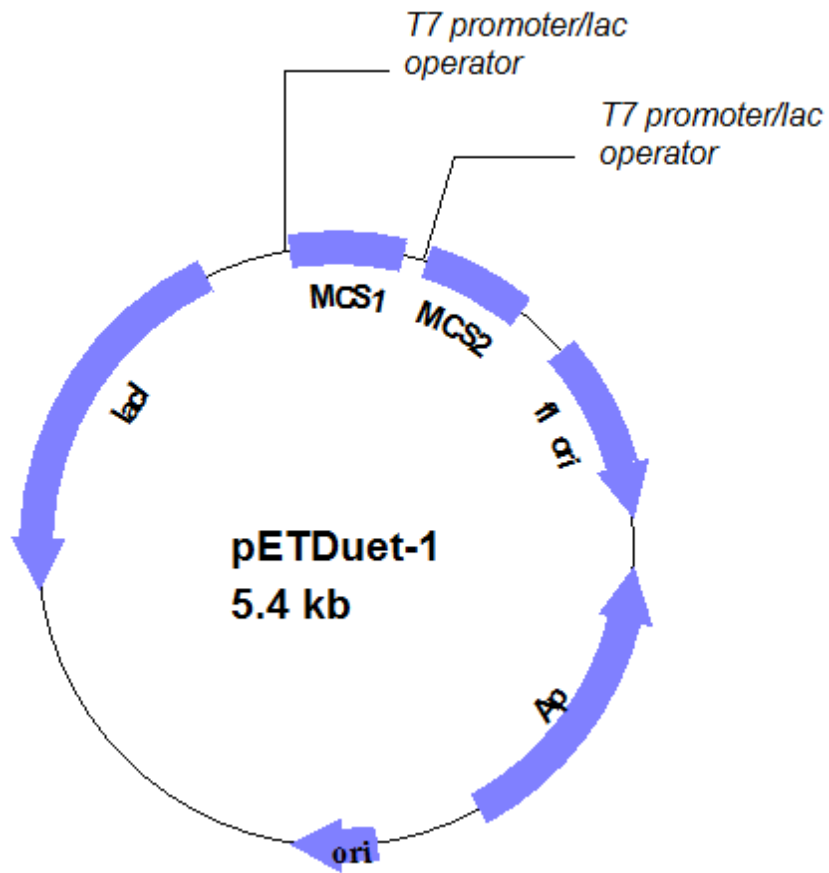


Figure 2.1. The pETDuet-1 vector expression system containing two multiple cloning sites (MCS1 and MCS2).

TTC CAT GGG CAG CAG CAG CCA TCA CCA TCA TC 3' and 5' TGG CTG CTC TTC ATG GTA TAT CTC CTT CTT AAA G 3'. The pET21a vector containing the C-terminally His-tagged *ssuE* gene was constructed by mutation of the native *ssuE* stop codon using primers 5' TTA TAA CTC TTC ACC ATG CGT GTC ATC ACC CTG 3' and 5' CAG TTT CTC TTC GCA TCG CAT GGG CAT TAC CTC G 3' with the QuickChange site-directed mutagenesis kit (Stratagene, La Jolla, CA). The His-tagged *ssuE* construct was then PCR amplified using primers 5' ATA AGG CTC TTC TAT GCG TGT CAT CAC CTG 3' and 5' CAG TTT CTC TTC CGA GTT ACG CTG GGC ATT 3'. The His-tagged *ssuE* gene was subcloned into pETDuet-1/*ssuD* at MCS1 vector gene utilizing the SeamLess[®] Cloning Kit (Stratagene, La Jolla, CA). All generated constructs were verified by sequence analysis at Davis Sequencing (University of California, Davis).

The plasmid construct was transformed and expressed in *E. coli* strains BL21(DE3), BL21(DE3)-pLysS, Origami, Tuner, and Tuner pLysS. The plasmid construct was also transformed into XL-1 strains for bacterial culture storage at -80 °C. Each cell culture was grown separately on LB medium containing the appropriate antibiotic (Table 2.1) in addition to ampicillin to select for the pET-Duet-1 or pET21a plasmid constructs. The concentrations of ampicillin, chloramphenicol, kanamycin, and tetracycline used in the growth media were 100, 50, 50, and 50 mg/mL, respectively. A single colony containing the plasmid construct was used to inoculate 5 mL LB-Amp medium, and incubated overnight at 37 °C. A 1% inoculum of the 5 mL cell culture was used to inoculate 100 mL LB-Amp, and the culture was incubated at 37 °C until the A_{600} reached 0.4. The flask was then transferred from 37 °C to 18 °C, and the proteins were

expressed by the addition of IPTG to a final concentration of 400 μM . The incubation was continued for 6 h, and cells were harvested by centrifugation at 5,000 rpm for 15 min at 4°C and stored at -80°C. Each protein was purified according to a previously published protocol [78].

2.4 Construction and expression of recombinant proteins

The T7 RNA polymerase-dependent expression vector pET21a carrying either the native *ssuE* or *ssuD* gene was utilized for protein expression and purification as previously described [78]. The concentrations of SsuE or SsuD proteins in solution was calculated using the molar extinction coefficients of the two proteins (20.3 $\text{mM}^{-1} \text{cm}^{-1}$ and 46.9 $\text{mM}^{-1} \text{cm}^{-1}$ at 280 nm, respectively) or the previously determined molecular masses of SsuE and SsuD proteins (21.3 kDa and 41.6 kDa, respectively) [54, 78].

The pET21a vector containing the C-terminally His-tagged *ssuD* gene was constructed by mutation of the native *ssuD* stop codon with the QuickChange site-directed mutagenesis kit (Stratagene, La Jolla, CA). The native construct was PCR amplified using the primers 5' CGT AAA GTC GCG CAA AGC GCG CTC GAG CAC CAC CAC 3' and 5' GTG GTG GTG CTC GAG CGC GCT TTG CGC GAC TTT ACG 3'. The generated mutation was verified by sequence analysis at Davis Sequencing (University of California, Davis).

The His-tagged SsuD protein was expressed in *E. coli* BL21(DE3). A single colony of *E. coli* BL21(DE3) containing the His-tagged *ssuD* gene was used to inoculate 5 mL LB medium containing 100 mg/mL ampicillin (LB-Amp) with incubation overnight at 37 °C. A 1% inoculum of the 5 mL cell culture was used to inoculate 100

mL LB-Amp, and the culture was incubated at 37 °C until the A_{600} reached 0.4. The flask was then transferred from 37 °C to 18 °C, and the protein was expressed by the addition of IPTG to a final concentration of 400 μ M. The incubation was continued for 6 h, and cells were harvested by centrifugation at 5,000 rpm for 15 min at 4 °C and stored at -80 °C. Cells from the 100 mL growth were resuspended in 50 mL standard buffer containing 4 μ g/mL lysozyme. Cell lysis was performed by sonication, followed by the addition of 1.5% streptomycin sulfate to precipitate nucleic acids.

2.5 Affinity chromatography binding assay

A 50 mL cell lysate containing the expressed His-tagged SsuD protein was loaded onto a column containing Ni-nitrilotriacetic acid (NTA) Superflow resin (QIAGEN, Valencia, CA), and the column was washed with 100 mL standard buffer to remove unbound protein prior to loading the cell lysate containing native SsuE. The column was then washed again with 100 mL standard buffer after loading the native SsuE protein. The unbound protein was eluted from the column with 100 mL standard buffer containing 125 mM imidazole, followed by elution of the His-tagged SsuD protein with 100 mL standard buffer containing 300 mM imidazole. The eluted proteins from both buffer concentrations were collected and analyzed by SDS-PAGE. Two sets of control experiments were performed to ensure that complex formation between SsuE and His-tagged SsuD protein in the Ni-NTA column was not due to nonspecific binding or protein aggregation. The first control experiment was performed by loading the cell lysate containing native SsuE protein onto a Ni-NTA column in the absence of the His-tagged SsuD protein. The second control experiment was performed by loading a protein

available in our laboratory, the rat cysteine dioxygenase protein, onto a Ni-NTA column in the presence of His-tagged SsuD protein. For each control, the column was washed with 100 mL standard buffer, followed by a second wash with 100 mL standard buffer containing 125 mM of imidazole. A final wash with 100 mL standard buffer containing 300 mM of imidazole was performed and the protein fractions collected and analyzed by SDS-PAGE.

2.6 Far-UV circular dichroism

The spectrum of SsuE was obtained with 2.4 μ M SsuE in 25 mM potassium phosphate buffer (pH 7.5), 10% glycerol, and 100 mM NaCl at 25 °C (400 μ L total volume). The SsuD spectrum was obtained with 1.2 μ M SsuD in 25 mM phosphate buffer (pH 7.5), 10% glycerol, and 100 mM NaCl at 25 °C (400 μ L total volume). The SsuE/SsuD spectrum was obtained with 2.4 μ M SsuE and 1.2 μ M SsuD in 25 mM phosphate buffer (400 μ L total volume), 10% glycerol, and 100 mM NaCl at 25 °C. Spectra were recorded on a Jasco J-810 Spectropolarimeter (Easton, MD). Measurements were taken in 0.1-nm increments from 300 to 185 nm in a 0.1-cm path length cuvette with a bandwidth of 1 nm and a scanning speed of 50 nm/min. Each spectrum is the average of four scans; smoothing of the data was performed using the default parameters within the Jasco J-720 software.

2.7 Visible circular dichroism

The spectrum of FMN was obtained with 20 μ M FMN in 25 mM potassium phosphate buffer (pH 7.5), 10% glycerol, and 100 mM NaCl at 25 °C (2.0 mL total

volume). The FMN/SsuE spectrum was obtained with 20 μM of SsuE and FMN in 25 mM potassium phosphate buffer (pH 7.5), 10% glycerol, and 100 mM NaCl at 25 $^{\circ}\text{C}$ (2.0 mL total volume). The FMN/SsuE/SsuD spectrum was obtained with a 1:1 stoichiometric addition of 20 μM SsuD to 20 μM FMN-bound SsuE in 25 mM potassium phosphate buffer (pH 7.5), 10% glycerol, and 100 mM NaCl at 25 $^{\circ}\text{C}$ (2.0 mL total volume). Spectra were recorded on a Jasco J-810 spectropolarimeter (Easton, MD). Measurements were taken in 0.2-nm increments from 550 to 300 nm in a 1-cm path length cuvette with a bandwidth of 1 nm and a scanning speed of 50 nm/min. Each spectrum is the average of eight scans; smoothing of the data was performed using the default parameters within the Jasco J-720 software. The concentration of FMN was calculated using a molar extinction coefficient of $12.2 \text{ mM}^{-1} \text{ cm}^{-1}$ at 450 nm.

2.8 Fluorescence spectroscopy

Binding of FMN to SsuE was determined by spectrofluorometric titrations, monitoring the decrease in the relative intensity of the FMN spectra due to fluorescence quenching of the flavin upon binding SsuE. SsuD interactions with FMN-bound SsuE were monitored by spectrofluorometric titration, monitoring the increase in the relative intensity of the FMN spectra due to interactions between the two proteins. Spectra were recorded on a Perkin- Elmer LS 55 luminescence spectrometer (Palo Alto, CA) with both excitation and emission slit widths set at 10 nm.

2.8.1 Fluorometric titration of FMN with SsuE

A 0.04 μM FMN solution in 25 mM potassium phosphate buffer (pH 7.5) (1.0 mL total volume) was titrated with 1 μL aliquots of SsuE for a total of 10 to 15 titrations (0.04 - 0.40 μM). Emission intensity measurements from 470 to 650 nm were made using an excitation wavelength of 450 nm.

2.8.2 Fluorometric titration of FMN-bound SsuE with SsuD

A 0.40 μM FMN-bound SsuE sample in 25 mM potassium phosphate buffer (pH 7.5) (1.0 mL total volume) was titrated with 1 μL aliquots of SsuD for a total of 25 to 30 titrations (0.02 - 0.95 μM). Emission wavelengths from 470 to 650 nm were measured using an excitation wavelength of 450 nm. The concentration of SsuD bound to SsuE was determined by applying the following equation (Eq. 2.1) [100]:

$$[\text{SsuD}]_{\text{bound}} = [\text{SsuE}][(I_c - I_0)/(I_f - I_0)] \quad (\text{Eq. 2.1})$$

where $[\text{SsuE}]$ represents the initial concentration of enzyme, I_0 is the initial fluorescence intensity of FMN prior to addition of SsuD, I_c is the fluorescence intensity of FMN following each addition of SsuD, and I_f is the final fluorescence intensity. The concentration of SsuD bound ($[\text{SsuD}]_{\text{bound}}$, y) was plotted against the total SsuD ($[\text{SsuD}]_{\text{total}}$, x) to obtain the dissociation constant (K_d) for the binding between SsuE and SsuD according to equation below (Eq. 2.2), where n is the binding capacity of SsuE [100]:

$$y = \frac{(K_d + x + n) - \sqrt{(K_d + x + n)^2 - 4xn}}{2} \quad (\text{Eq. 2.2})$$

2.9 UV-visible spectroscopy of filtration of FMN-bound SsuE

The flavin spectra were obtained at 450 nm before and after filtration with 20 μ M FMN in 25 mM potassium phosphate (pH 7.5), 10% glycerol, and 100 mM NaCl at 25 °C in the presence of 20 μ M of SsuE and SsuD proteins in a 2.0 mL total volume. The filtration was performed by centrifugation at 3,000 rpm for 15 min, utilizing a 10,000-molecular-weight-cutoff Amicon Ultra-4 centrifugation filter from Millipore (Bedford, MA). Control experiments with only FMN were performed by monitoring the spectra at 450 nm before and after filtration.

2.10 Isothermal titration calorimetry

Isothermal titration calorimetry (ITC) experiments were performed utilizing a VP-ITC MicroCalorimeter instrument (MicroCal, LLC, Northampton, MA). ITC data were obtained by titrating 1 μ M of SsuE in the sample cell with 5 μ L aliquots of 50 μ M SsuD as the titrant at 30 °C. The data obtained were fitted using Origin® software. The final results were corrected for the heat released when titrating with SsuD into buffer only (25 mM potassium buffer pH 7.5, and 100 mM NaCl).

2.11 Chemical cross-linking

Chemical cross-linking experiments were conducted for two purposes: 1) to investigate the ability of SsuE and SsuD proteins to form a complex utilizing a trifunctional cross-linking reagent; 2) to determine the amino acid residues involved in protein-protein interactions employing various bifunctional cross-linking reagents.

2.11.1 Interactions between SsuE and SsuD proteins

Chemical cross-linking experiments to investigate complex formation between SsuE and SsuD were performed using the ProFound Label Transfer Sulfo-SBED (sulfosuccinimidyl [2,6-(biotinamido)-2-(*p*-azidobenzamido)-hexanoamido]-ethyl-1,3'-dithiopropionate) Protein:Protein Interaction Agent (Figure 2.2) (Pierce, Rockford, IL). The cross-linking reagent has three functional groups, the sulfo-NHS, the photo-reactive aryl-azide, and the biotin label. A 10 μ M sample of the SsuE protein was incubated in the dark at room temperature for 30 min with 1 mM of cross-linking reagent in a total volume of 500 μ L. The amino group of SsuE reacted with the reagent via its sulfo-NHS reactive group. The unreacted reagent was removed by washing the sample twice with 25 mM potassium phosphate buffer (pH 7.5) and 100 mM NaCl by centrifugation at 3,000 rpm for 15 min, utilizing a 10,000-molecular-weight-cutoff Amicon Ultra-4 centrifugation filter from Millipore (Bedford, MA). The labeled SsuE protein was then mixed with 10 μ M SsuD in a total volume of 1 mL and incubated in the dark for 15 min. The reaction mixture was exposed to UV light at a distance of 5 cm for 15 min, followed by the addition of 20 mM dithiothreitol (DTT) (final concentration). A sample (10 μ L) was collected following each step for further analysis by nondenaturing and nonreducing polyacrylamide gel electrophoresis. Control experiments similar to those described above were performed using either SsuE or SsuD to determine which bands represent intrasubunit cross-linking.

The size of the biotin-labeled protein complex between SsuE and SsuD was verified by affinity chromatography. A 4 mL sample of biotin-labeled protein complex solution (without the addition of DTT) was loaded (2 mL at one time) onto a 5 mL

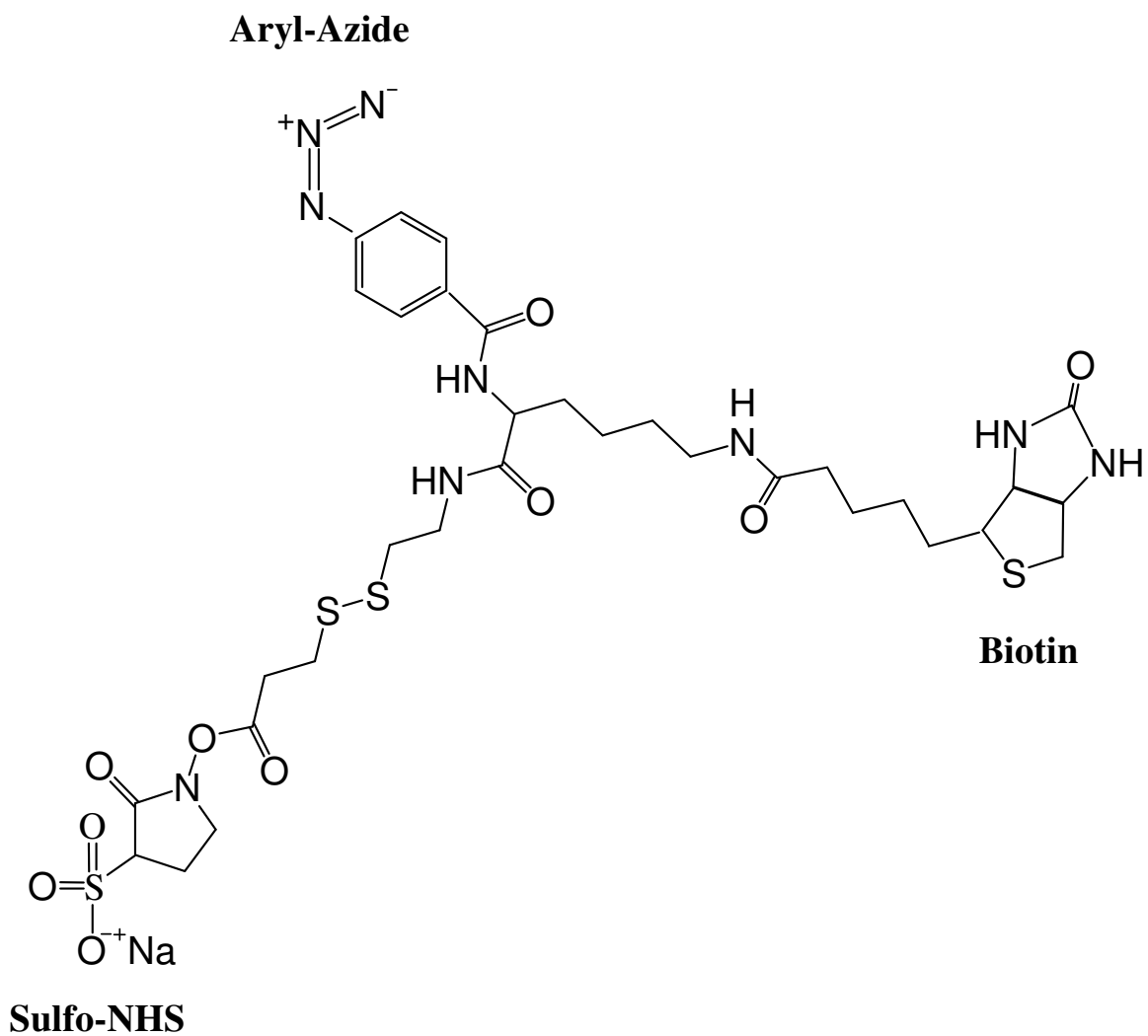


Figure 2.2. ProFound Label Transfer Sulfo-SBED {sulfosuccinimidyl[2,6-(biotinamido)-2-(*p*-azidobenzamido)-hexanoamido]-ethyl-1,3'-dithiopropionate} Protein:Protein Interaction Agent [149].

column containing streptavidin agarose matrix (Invitrogen, Carlsbad, CA). The column was washed with 50 mL of 25 mM potassium phosphate buffer (pH 7.5), and 10% glycerol. The protein complex was eluted with a 0-8 M urea gradient solution in 25 mM potassium phosphate buffer (pH 7.5), and 10% glycerol. The protein fractions were collected and analyzed by nondenaturing and nonreducing polyacrylamide gel electrophoresis.

2.11.2 Determination of amino acid residues involved in protein-protein interactions

Chemical cross-linking experiments were performed using EDC and sulfo-NHS (combination of the two reagents yield a zero-length spacer arm), BS³ (11.4 Å), and EGS (16.1 Å) cross-linking reagents (Figure 2.3) [149]. The EDC cross-linker has a functional group that reacts with a carboxyl group of protein 1. The semi-stable NHS ester intermediate reacts with the amino group of protein 2. Both BS³ and EGS are homobifunctional cross-linkers that react with amino groups of proteins. The reaction conditions and buffer solution used were based on manufacturer instructions with some modifications. The EDC and sulfo-NHS cross-linker reagents were freshly prepared separately in 100 mM MES buffer (pH 6.0) and 500 mM NaCl. The EDC and sulfo-NHS (10 mM and 20 mM, respectively) were mixed with sample of SsuE (10-50 μM) in 100 mM MES buffer (pH 6.0) and 500 mM NaCl in a total volume of 200 μL at room temperature for 15 minutes. The unreacted reagent was removed by washing the sample twice by centrifugation at 3,000 rpm for 15 min, utilizing a 10,000-molecular-weight-cutoff Amicon Ultra-4 centrifugation filter from Millipore (Bedford, MA). A 5-25 μM sample of SsuD in 100 mM sodium phosphate buffer (pH 7.5) and 150 mM NaCl was

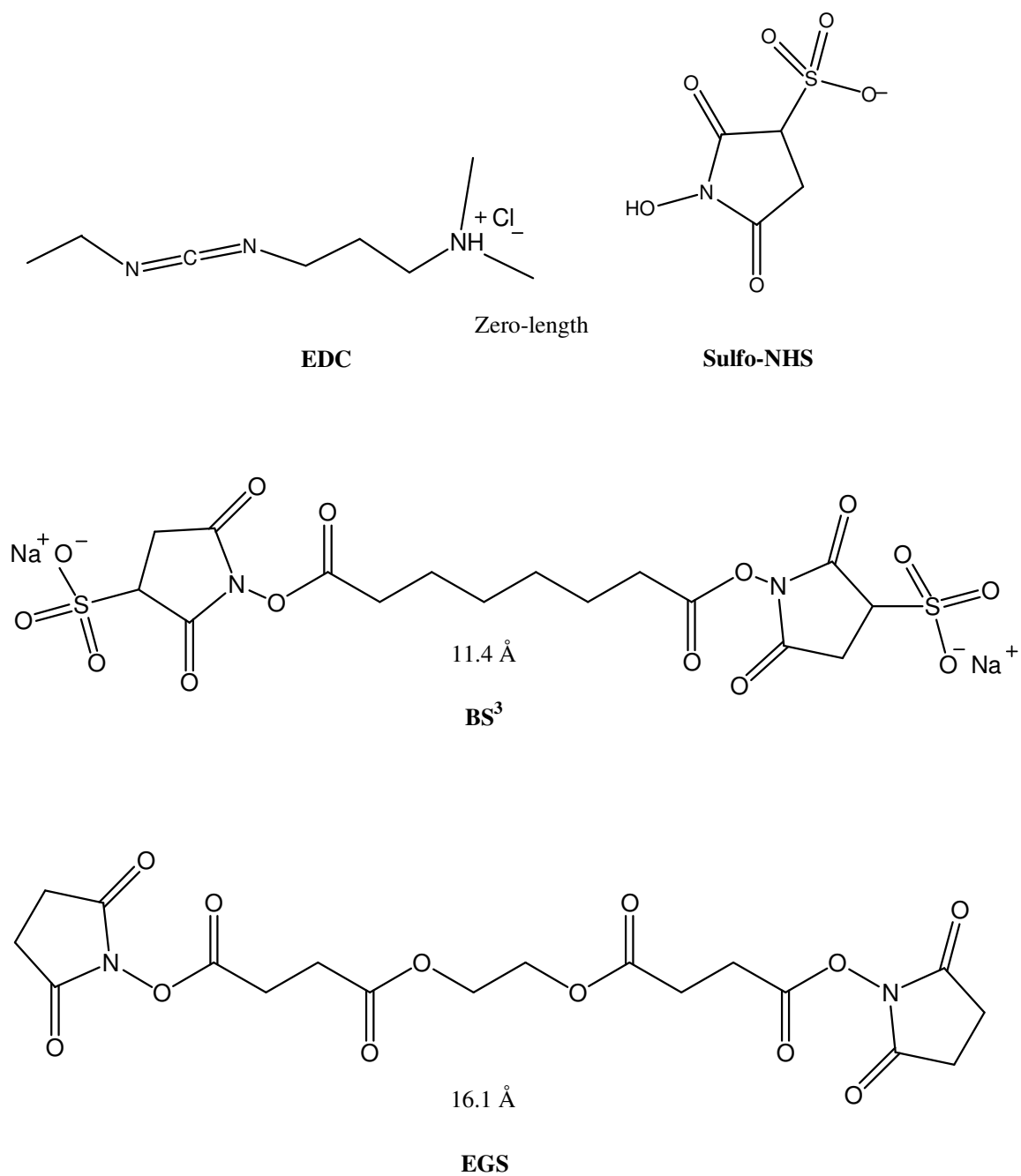


Figure 2.3. Cross-linking reagents used for determination of amino acid residues involved in protein-protein interactions between SsuE and SsuD [149].

then mixed with previously treated SsuE in a total volume of 200 μ L and incubated on ice for 2-3 hours (optional: the incubation reaction can also be done with gently shaking at 10 $^{\circ}$ C for 2-3 hrs). A 10-15 μ L reaction mixture was taken every 15 minutes to monitor the progress of the reaction. The reaction was terminated by adding glycine to the reaction mixture in a final concentration of 10 mM. The samples were analyzed on 10% SDS-PAGE and stained with either coomassie blue or silver-stain. The BS³ or EGS cross-linking reagents were freshly prepared in 25 mM potassium phosphate buffer (pH 7.5) and 150 mM NaCl. The BS³ or EGS cross-linker reagents (1-10 mM final concentration) was mixed with a 10 μ M solution of SsuE and SsuD protein in 25 mM potassium phosphate buffer (pH 7.5) and 100 mM NaCl in a total volume of 200 μ L and incubated at room temperature for 30-60 minutes, 18 $^{\circ}$ C for 60-90 minutes, or in ice for 120-180 minutes. A 10-15 μ L reaction mixture was taken every 15 minutes to monitor the progress of the reaction. The reaction was terminated by adding glycine to the reaction mixture in a final concentration of 10 mM. The samples were analyzed on 10% SDS-PAGE.

2.11.3 Matrix assisted laser desorption ionization-time of flight mass spectroscopy

Matrix assisted laser desorption ionization-time of flight mass spectroscopy (MALDI-TOF MS) experiments were performed on a Microflex™ MALDI-TOF mass spectrometer (Bruker Daltonic, Billerica, MA) equipped with a nitrogen laser operating at 337 nm. All MALDI-TOF MS results were obtained in the linear positive mode.

The SDS polyacrylamide gel containing proteins of interest, either native or potentially cross-linked protein products, were excised and placed in a microcentrifuge

tube. The gel pieces were washed twice with 50% acetonitrile, twice with 50% acetonitrile containing 50 mM ammonium bicarbonate, pH 8.0, and twice with 50% acetonitrile containing 10 mM ammonium bicarbonate, pH 8.0. The gel pieces were dried in a DNA Speed Vac (Thermo Savant, Holbrook, NY). Trypsin was dissolved in 25 mM ammonium bicarbonate (pH 8.0) to a final concentration of 1 µg/mL. A 50 µL trypsin solution was added to each tube allowing the gel to absorb the solution. Additional buffer solution was added to completely cover the gel slices, and the gel mixture was incubated overnight at 37 °C. The peptides were extracted by washing the gel pieces twice with 0.1% trifluoroacetic acid (TFA) in water for 20 minutes and the soluble fractions from each extraction were pooled. The gel pieces were extracted two additional times with 60% acetonitrile, and 0.1% TFA in water. All the fractions were pooled together and dried to reduce solvent contamination prior to analyses by MALDI-TOF MS.

The matrix solutions were prepared separately by dissolving 2 mg of either 2,5-dihydroxybenzoic acid (DHB), 3,5-dimethoxy-4-hydroxycinnamic acid (sinapinic acid, SA), or α -cyano-4-hydroxycinnamic acid (CHCA) in 100 µL of solvent containing 50% acetonitrile and 0.1% trifluoroacetic acid. Analytes were prepared by mixing a 1:1 ratio of protein sample (undigested or digested) and matrix solution on a MALDI plate followed by air drying at room temperature in a fume hood prior to analysis by MALDI-TOF mass spectrometer. Mass spectra for undigested proteins were externally calibrated with trypsinogen $[M+H]^+$ (23,982 Da), protein A $[M+H]^+$ (44,613 Da), albumin-bovin $[M+H]^+$ (66,431 Da), protein A $[M+2H]^{2+}$ (22,306 Da), and albumin-bovin $[M+2H]^{2+}$ (33,216 Da). Mass spectra for digested proteins were externally calibrated with

bradykinin (1-7) [M+H]⁺ (757.86 Da), angiotensin II [M+H]⁺ (1,047.19 Da), angiotensin I [M+H]⁺ (1,297.49 Da), substance P [M+H]⁺ (1,348.6 Da), bombesin [M+H]⁺ (1,620.9 Da), renin substrate [M+H]⁺ (1,760.03 Da), ACTH clip (1-17) [M+H]⁺ (2,094.43 Da), ACTH clip (18-39) [M+H]⁺ (2,466.68 Da), and somatostatin (28) [M+H]⁺ (3,149.57 Da). The percentage of error (% error) of the observed molecular weight for tryptically-digested fragments is calculated based on the following equation (Eq. 2.3):

$$\% \text{ error} = \frac{|\text{observed value} - \text{theoretical value}|}{\text{theoretical value}} \times 100\% \quad (\text{Eq. 2.3})$$

2.12 Pre-steady state kinetic experiments

Experiments monitoring the reductive half-reaction of FMN in single enzyme reactions were carried out using previously published procedures [113]. Rapid reaction kinetic analyses were performed on an Applied Photophysics SX.18 MV stopped-flow spectrophotometer. All experiments were performed under anaerobic conditions at 4 °C in single mixing mode and monitored at single wavelengths of 450 or 550 nm. The stopped-flow instrument was made anaerobic by repeated filling and emptying of one drive syringe with an oxygen scavenging system containing 25 mM phosphate buffer (pH 7.5), 10% glycerol, 100 mM NaCl, with 20 mM glucose and 10 units of glucose oxidase. The other drive syringe contained 10 mM Tris buffer (pH 8.5), 10% glycerol, 100 mM NaCl with 20 mM glucose and 10 units of glucose oxidase. The anaerobic solutions were prepared in a tonometer and made anaerobic by vacuum gas exchange followed by saturation with oxygen free argon for at least 20 cycles with two minute durations for each cycle.

2.12.1 Kinetic analyses of FMN reduction and charge transfer formation in the presence of SsuD

The kinetic analyses of SsuE in the presence of SsuD but in the absence of SsuD substrates (octanesulfonate and oxygen) were performed anaerobically in the stopped-flow spectrophotometer by mixing SsuE (25 μM) and SsuD (25 μM) in a tonometer with a substrate solution containing FMN (25 μM) and NADPH (250 μM) in an air-tight syringe. The concentrations are final concentrations after mixing in the stopped-flow instrument.

2.12.2 Kinetic analyses of FMN reduction and charge transfer formation with alternate additions of SsuD and substrates

Rapid reaction kinetic analyses were performed using alternate addition of the enzymes and substrates in the stopped-flow instrument. The SsuE (25 μM) protein solutions with or without SsuD (25 μM) and/or octanesulfonate (250 μM) were made anaerobic in a tonometer and mixed with a solution containing FMN (25 μM) and NADPH (250 μM) with or without oxygen (0-440 μM). The varied oxygen concentrations were made by mixing oxygen-saturated buffer with anaerobic buffer solution containing 10 mM Tris buffer (pH 8.5), 10% glycerol, 100 mM NaCl in an air-tight syringe. The oxygen-saturated buffer was made by bubbling the solution with 100% oxygen for 30 minutes. The first experiment was performed by mixing the solution containing SsuE (25 μM) and SsuD (25 μM) with the solution containing FMN (25 μM), NADPH (250 μM), and varied oxygen concentrations (0-440 μM). The second experiment was performed by mixing the solution containing SsuE (25 μM), SsuD (25

μM), and octanesulfonate (250 μM) with the solution containing FMN (25 μM), NADPH (250 μM), and varied oxygen concentrations (0-440 μM). In the third experiment, the solution containing SsuE (25 μM) and octanesulfonate (250 μM) was mixed with the solution containing FMN (25 μM), NADPH (250 μM), and oxygen at varied oxygen concentrations (0-440 μM). Additional experiment was carried out by mixing the solution containing SsuE (25 μM), SsuD (25 μM), and octanesulfonate (250 μM) with the solution containing FMN (25 μM) and NADPH (250 μM).

2.12.3 Data analysis

Initial analyses of the single wavelength stopped-flow traces at 450 and 550 nm were performed with the PROKIN software (Applied Photophysics, Ltd.) installed in the stopped-flow spectrophotometer. First, global analysis was applied to discern the steps involved in flavin reduction. Second, a three-step sequential reversible model of $A \rightarrow B \rightarrow C \rightarrow D$ was adopted during the fitting, and the kinetic traces were resolved into three distinct phases. All single wavelength traces at 450 and 550 nm were imported and fitted with Kaleidagraph software (Abelbeck Software, Reading, PA). The single-wavelength traces at 450 nm were best fitted to a double or triple exponential using the following equation (Eq. 2.4 and 2.5, respectively):

$$A = A_1 \exp(-k_1 t) + A_2 \exp(-k_2 t) + C \quad (\text{Eq. 2.4})$$

$$A = A_1 \exp(-k_1 t) + A_2 \exp(-k_2 t) + A_3 \exp(-k_3 t) + C \quad (\text{Eq. 2.5})$$

The single-wavelength traces at 550 nm were best fitted to a triple exponential using the following equation (Eq.2.6):

$$A = 1 - [A_1 \exp(-k_1 t) + A_2 \exp(-k_2 t)] + A_3 \exp(-k_3 t) + C \quad (\text{Eq. 2.6})$$

where k_1 , k_2 and k_3 are apparent rate constants for the first, second, or third phases, respectively, A is the absorbance at time t , A_1 , A_2 , A_3 are amplitudes of each phase, and C is the absorbance at the end of the reaction.

2.13 UV-visible spectroscopy of FMNH₂

UV-visible spectra for free FMNH₂ at 450 nm were obtained by measuring the absorbance of an FMNH₂ solution (25 μ M) in 25 mM potassium phosphate buffer (pH 7.5), 100 mM NaCl, and 10 % glycerol. UV-visible spectra for FMNH₂-bound SsuD were obtained by measuring the absorbance of an FMNH₂ (25 μ M) and SsuD (25 μ M) solution in 25 mM potassium phosphate buffer (pH 7.5), 100 mM NaCl, and 10 % glycerol. The anaerobic FMN solution was photoreduced by irradiation for at least 5 minutes. Anaerobic FMN solutions in the absence or in the presence of SsuD were prepared in a glass titration cuvette by at least 20 cycles of evacuation followed by equilibration with ultra high purity argon gas with two minutes duration for each cycle.

CHAPTER THREE

RESULTS

3.1 Construction and expression of double cloning expression system in E. coli

Construction of a coexpression vector system was performed to study protein-protein interactions between SsuE and SsuD through cross-linking experiments, affinity chromatography, and kinetic analyses. The *ssuD* gene (1.1 kb) (not shown) was subcloned into MCS2 of the pETDuet-1 plasmid and designated as pKAA-11 (6.5 kb) (Figure 3.1 and Figure 3.2, lane 4). The His-tagged *ssuE* gene (0.6 kb) (Figure 3.2, lane 1) was then subcloned into MCS1 of the pKAA-11 plasmid and designated as pKAA-12 (7.1 kb) (Figure 3.1 and Figure 3.2, lane 3). The gene construct was expressed first in *E. coli* BL21(DE3). The His-tagged SsuE (Figure 3.3A, lane 3, indicated by a dotted arrow) and SsuD (Figure 3.3A, lane 3, indicated by solid arrow) proteins were successfully expressed upon IPTG induction. It was shown that the molecular mass of His-tagged SsuE protein (Figure 3.3A, lane 3, indicated by dotted arrow) was slightly higher than the native SsuE protein (Figure 3.3A, lane 2, indicated by dotted arrow). However, the majority of proteins were found as inclusion bodies generating insoluble protein even at low temperature. The genes were then expressed in different *E. coli* strains to increase the solubility of each protein. Several genetically modified bacterial strains which are commercially available were used for protein expression to increase solubility of

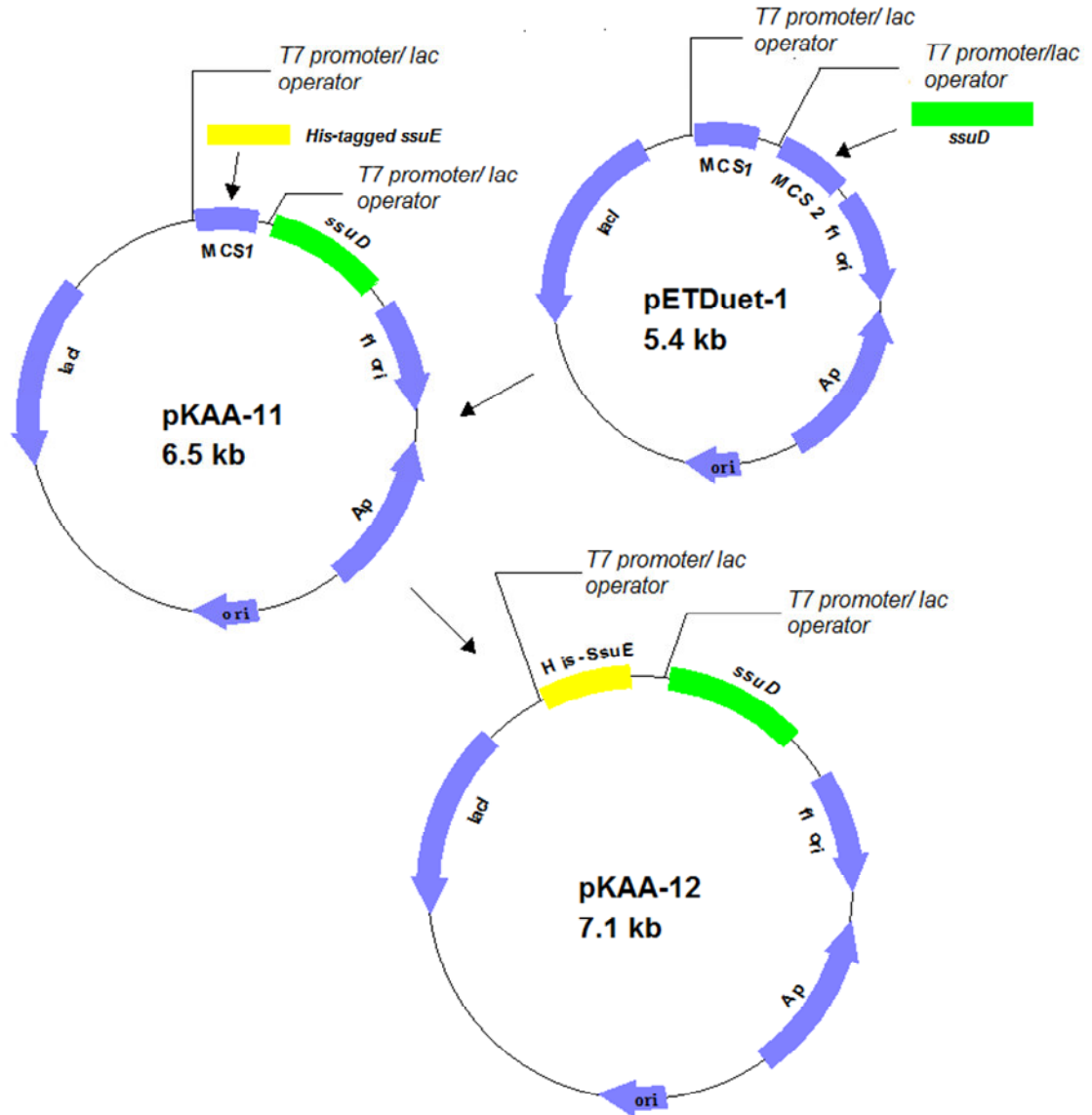


Figure 3.1. Subcloning of His-tagged *ssuE* and *ssuD* genes into double multiple cloning sites (MCS1 and MCS2) of pETDuet-1 plasmid.

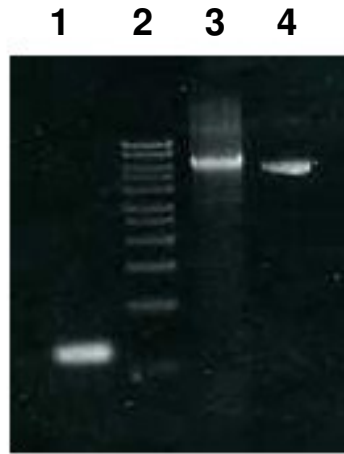


Figure 3.2. Agarose gel electrophoresis of doubly cloned His-tagged *ssuE* and *ssuD* genes into pETDuet-1 plasmid expression system.

recombinant proteins. In general, the solubility of difficult target proteins can be increased by controlling the level of expression of the proteins. Again, the results showed that both proteins, His-tagged SsuE (Figure 3.3B, indicated by dotted arrow) and SsuD (Figure 3.3B, indicated by solid arrow) expressed in these bacterial strains; Origami (lanes 3 and 4, cell lysate and supernatant, respectively), Tuner pLysS (lanes 5 and 6, cell lysate and supernatant, respectively), BL21(DE3)pLysS (lanes 7 and 8, cell lysate and supernatant, respectively), Tuner (lanes 11 and 12, cell lysate and supernatant, respectively), and BL21(DE3) (lanes 9 and 10, cell lysate and supernatant, respectively) were insoluble. SsuE in particular was shown to be almost completely insoluble (Figure 3.3B, lanes 4, 6, 8, 10, and 12, indicated by dotted arrow) in all cell lines utilized for expression.

3.2 Affinity chromatography

The transfer of reduced flavin between the two-component monooxygenase enzymes could occur either by a diffusion mechanism or by direct flavin transfer due to protein-protein interactions. Because dual expression was not a viable option, affinity chromatography experiments with individually expressed His-tagged SsuD and native SsuE were performed to identify static protein interactions. His-tagged SsuD in a cell lysate was loaded onto a Ni-NTA column. Following a phosphate buffer wash to remove unbound protein, native SsuE in a cell lysate was loaded onto the Ni-NTA column containing bound His-tagged SsuD. The column was first washed with 125 mM imidazole buffer to remove any unbound protein, followed by a second wash with 300 mM imidazole buffer to remove bound His-tagged SsuD. After applying the 125 mM

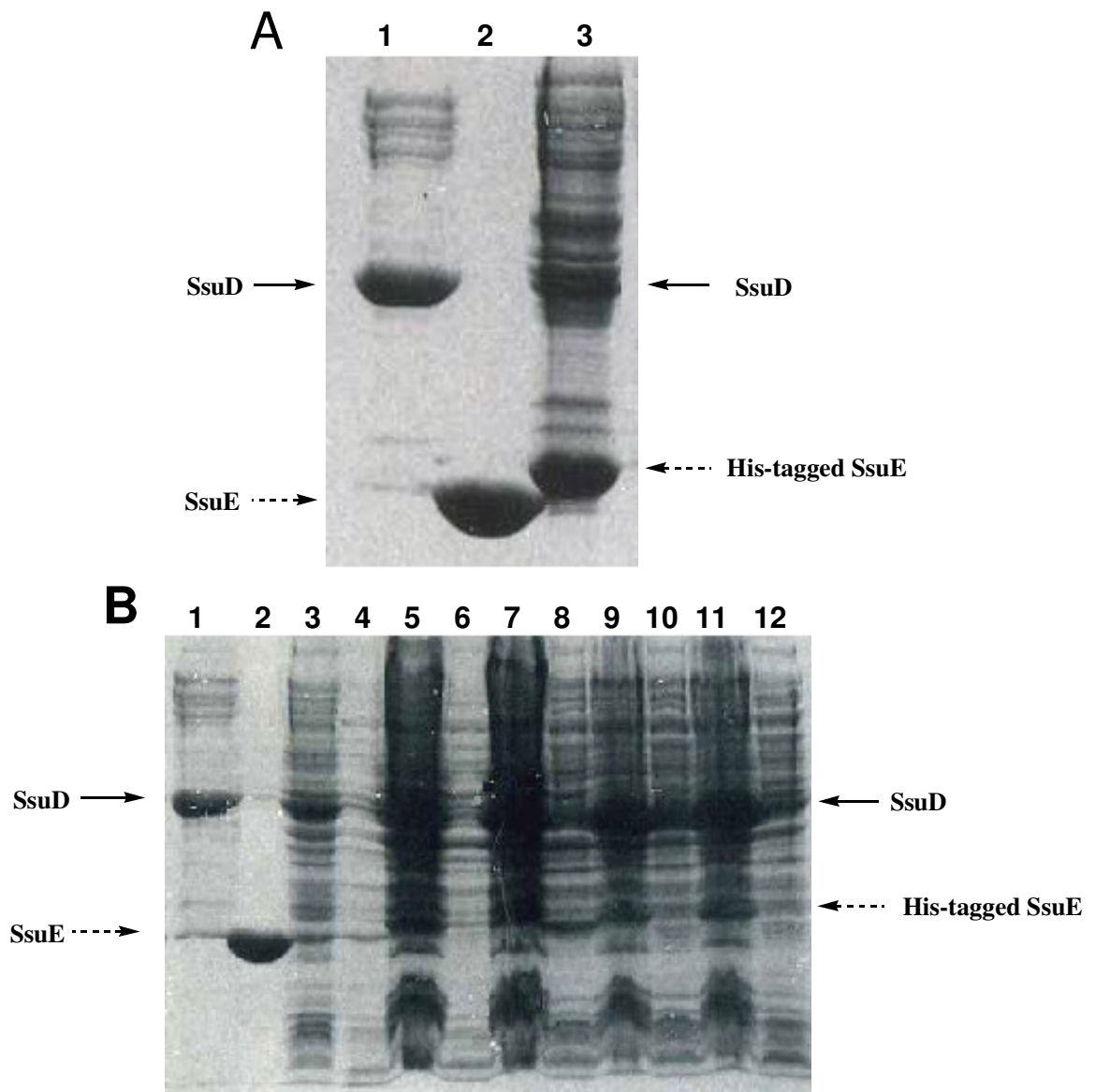


Figure 3.3. Expression of pKAA-12 plasmid expression system containing SsuD and His-tagged SsuE in different *E. coli* strains.

and 300 mM imidazole buffers, the fractions were collected from the column and analyzed by SDS PAGE (Figure 3.4A, lanes 2-9 and Figure 3.4B, lane 4, respectively). Native SsuE and SsuD are also shown (Figure 3.4A, lane 1 and Figure 3.4B, lane 3 and 2, respectively).

The results showed that His-tagged SsuD (Figure 3.4B, lane 4, indicated by dotted arrow) and native SsuE (Figure 3.4B, lane 4, indicated by solid arrow) coeluted from the column with 300 mM imidazole buffer. The data suggest that the native SsuE protein remains bound to the column after the 125 mM imidazole wash due to protein-protein interactions with His-tagged SsuD. Control experiments showed that native SsuE from a cell lysate was unable to bind to the Ni-NTA column in the absence of His-tagged SsuD. The SsuE protein was eluted off the column with 125 mM imidazole buffer (Figure 3.5A, lanes 2-9), and there was no protein detected on the gel following the 300 mM imidazole wash (Figure 3.5B, lanes 2-10). Native SsuE and SsuD are also shown (Figure 3.5A and 3.5B, lane 1). Similar control experiments performed with an unrelated protein, rat cysteine dioxygenase (CDO), and His-tagged SsuD did not result in the coelution of the two proteins with 300 mM imidazole buffer (Figure 3.6B, lanes 2-10). The CDO protein was eluted off the column with 125 mM imidazole buffer (Figure 3.6A, lanes 2-10). Protein markers with their corresponding molecular mass are shown (Figure 3.6A and 3.6B, lane 1). These results suggest that the interactions between SsuE and SsuD were specific and not caused by random aggregation.

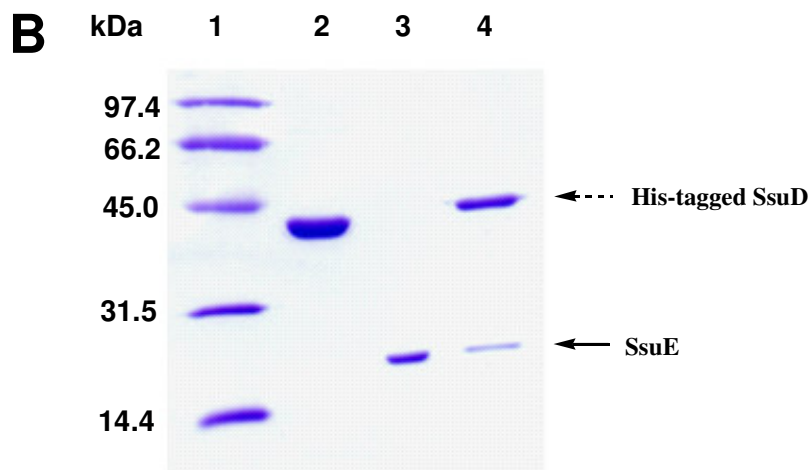
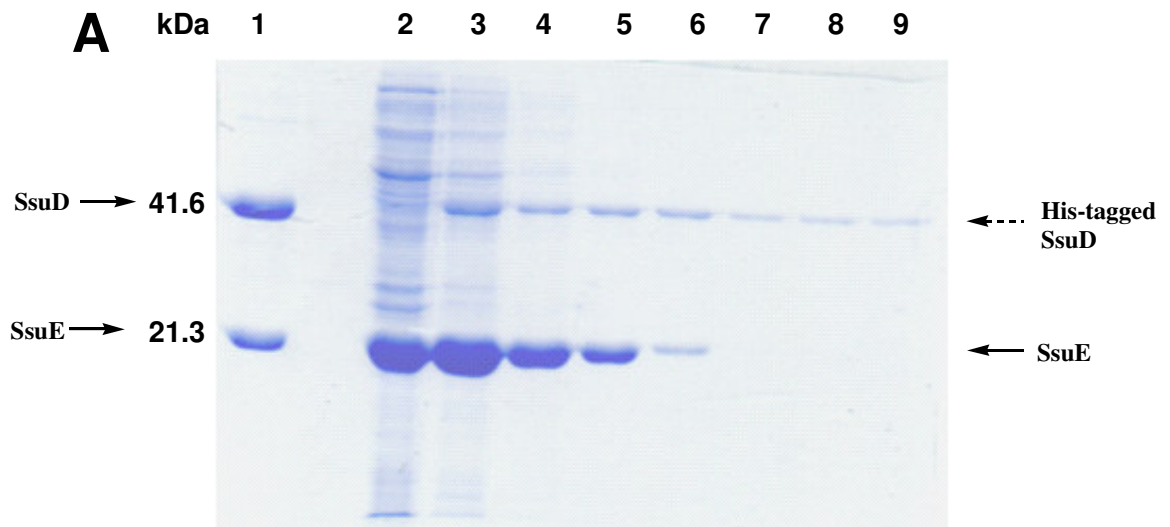


Figure 3.4. SDS-PAGE (10% acrylamide) from affinity chromatography experiments with SsuE and His-tagged SsuD.

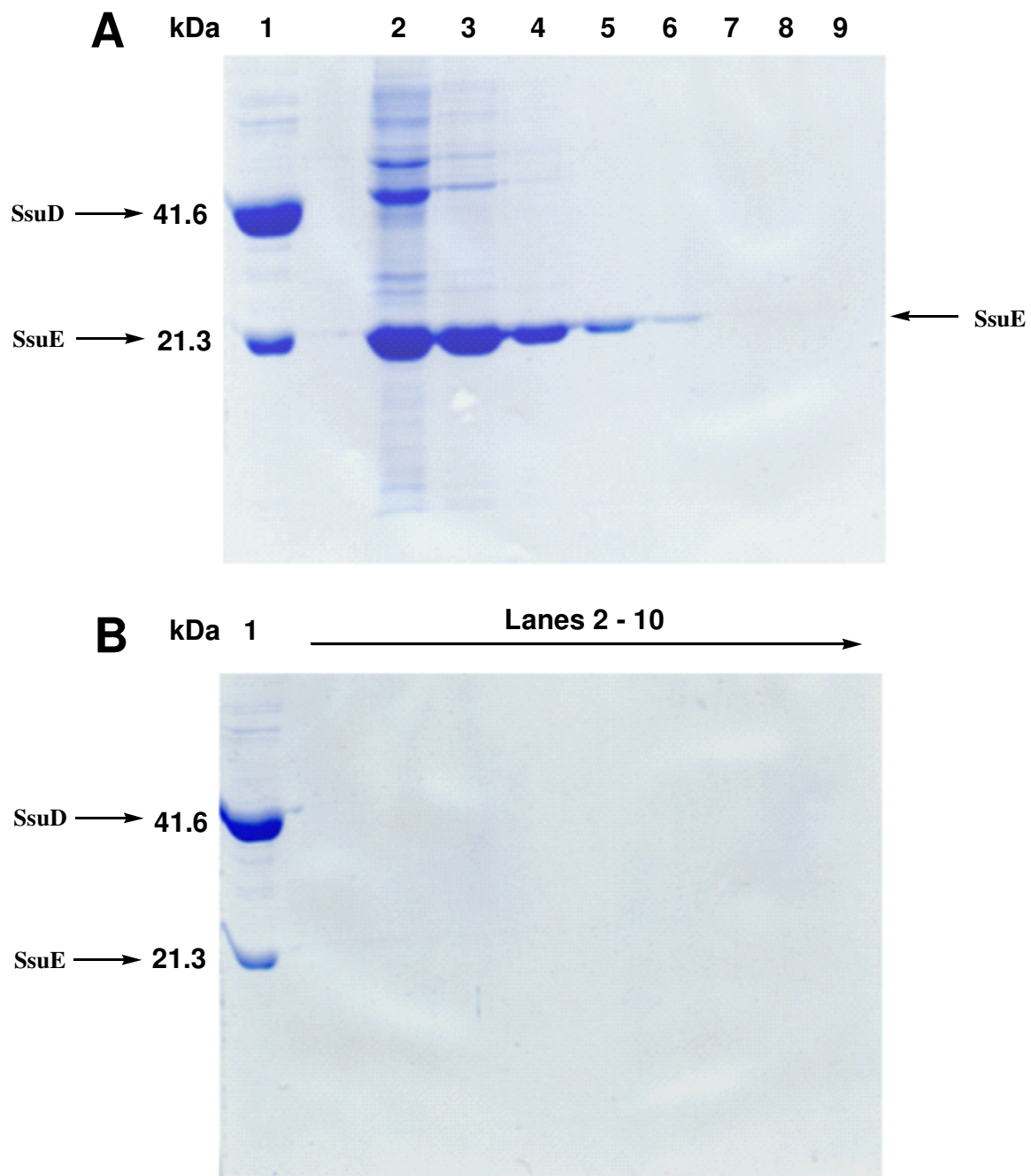


Figure 3.5. SDS-PAGE (10% acrylamide) from affinity chromatography experiments with SsuE in the absence of His-tagged SsuD.

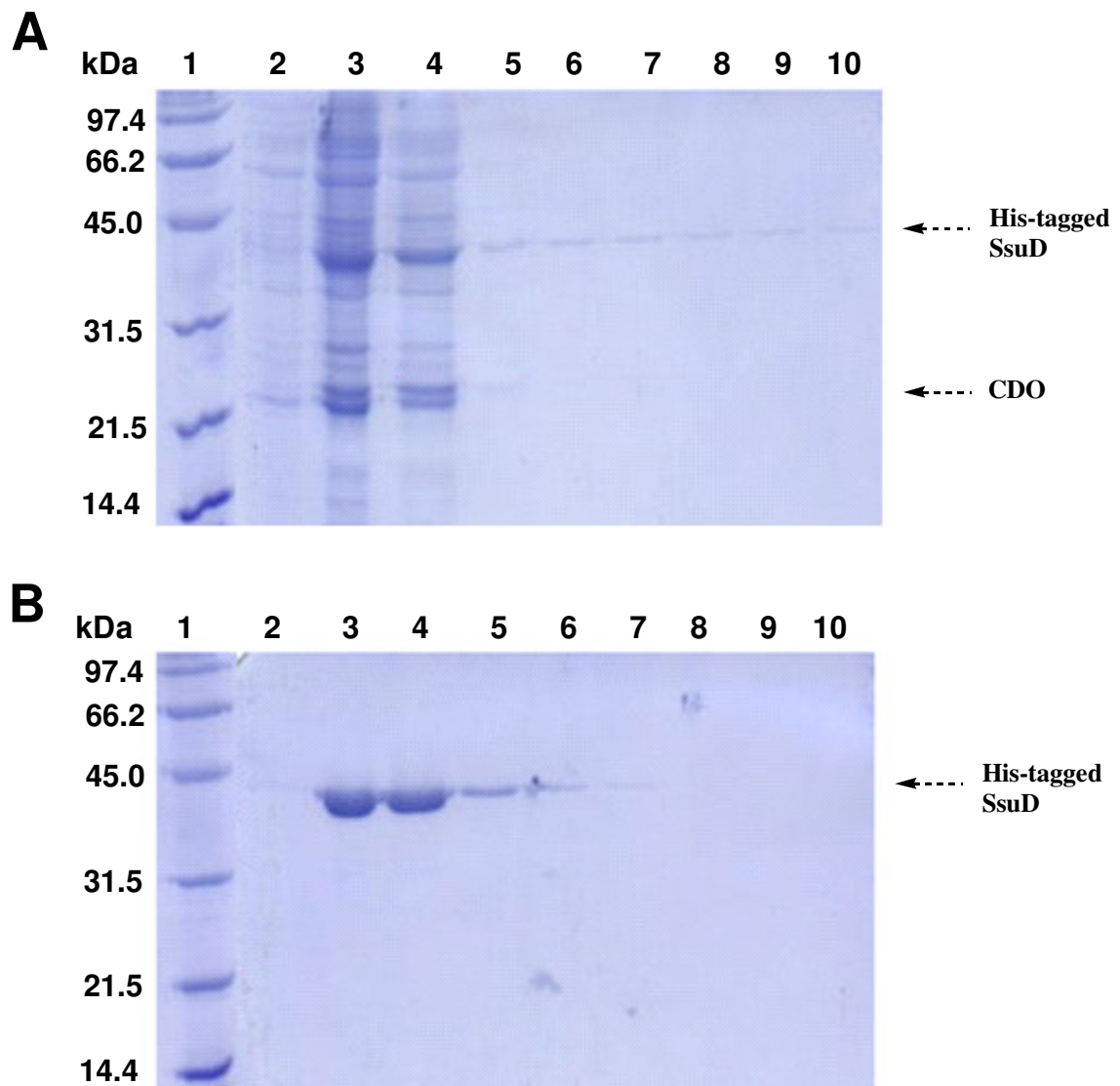


Figure 3.6. SDS-PAGE (10% acrylamide) from affinity chromatography experiments with rat cysteine dioxygenase and His-tagged SsuD.

3.3 Secondary structure changes due to protein-protein interactions

The circular dichroism (CD) spectroscopy experiments in the far-UV (190-250 nm) and visible (300-500 nm) regions were performed to monitor any changes in the gross secondary structure or flavin environment caused by interactions between FMN-bound SsuE and SsuD. The individual CD spectra of SsuE (Figure 3.7, solid line) and SsuD (Figure 3.7, dotted line) in the far UV region were initially obtained to determine if there were any observable alterations in the secondary structure of each protein compared to the spectrum obtained with both proteins. The results showed that there were no significant changes in the secondary structure, and the additive individual spectra of SsuE and SsuD (Figure 3.7, long dashed line) closely resemble the spectrum obtained with both proteins present (Figure 3.7, dashed line).

When spectra in the visible absorbance region were obtained, oxidized flavin (FMN) exhibited a characteristic spectrum with a weak signal typical for free FMN (solid line) (Figure 3.8). A significant change in the flavin spectrum was observed upon binding of FMN to SsuE (dashed line), providing an intense signal with both positive and negative ellipticity (Figure 3.8). When SsuD was included in the solution, the molar ellipticity between 300 to 375 nm decreased (dotted line) (Figure 3.8). This suggested that the flavin environment was affected by the presence of SsuD. However, the CD spectrum of FMN (Figure 3.9, solid line) did not significantly change in the presence of SsuD alone (Figure 3.9, dotted line). Therefore, the protein-protein interactions cause a slight change in the flavin environment but do not lead to significant changes in the overall gross secondary structure.

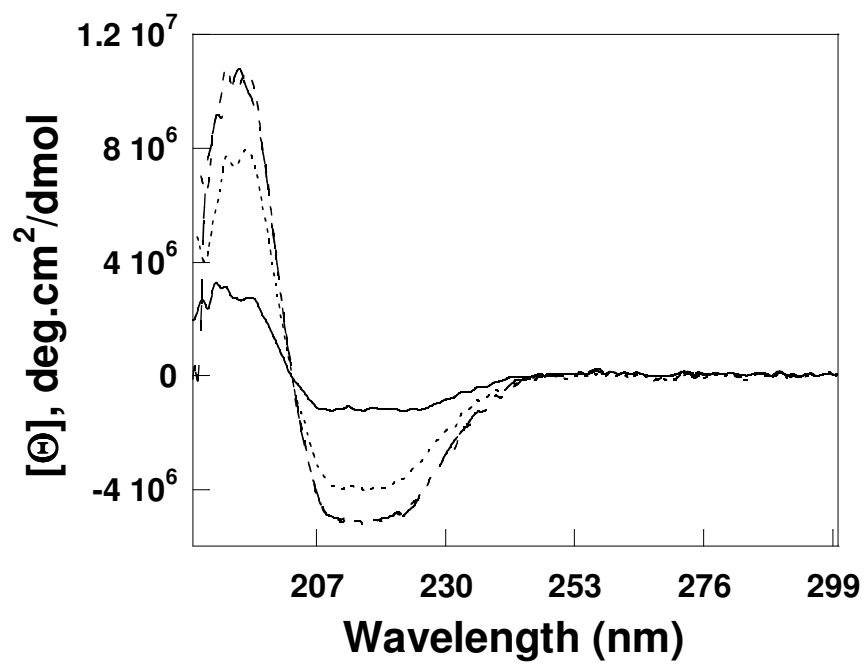


Figure 3.7. Far-UV CD spectroscopy of SsuE and SsuD.

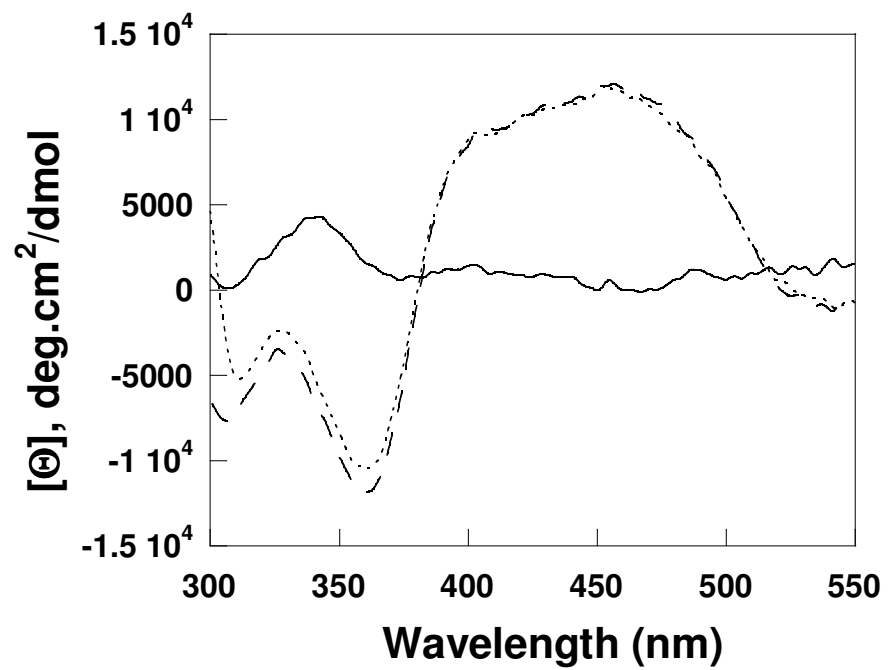


Figure 3.8. Visible CD spectra for FMN in the absence and presence of SsuE and SsuD.

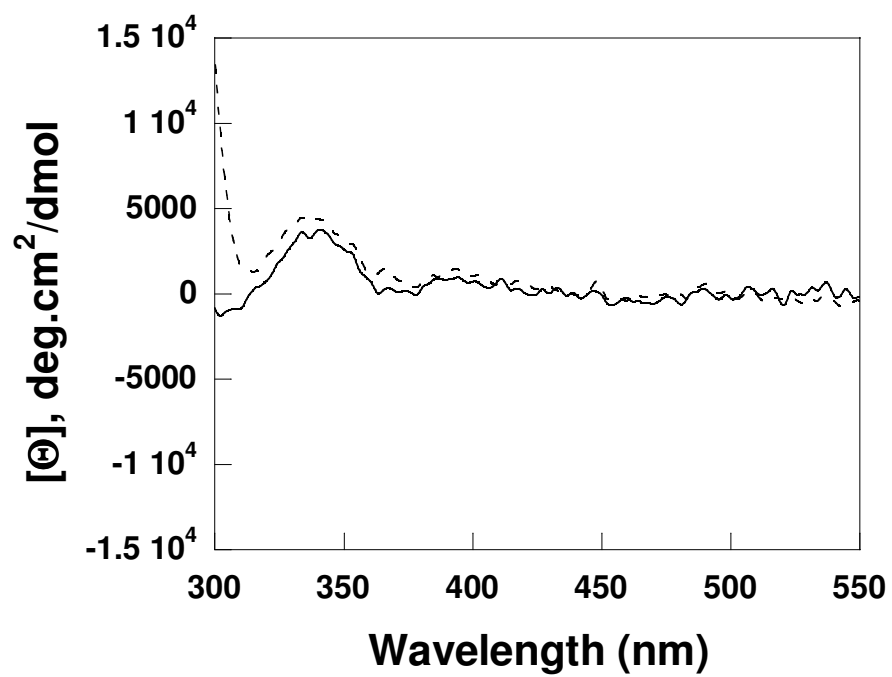


Figure 3.9. Visible CD spectra for FMN in the absence and presence of SsuD.

3.4 Binding of SsuD to FMN-bound SsuE

Fluorescence spectroscopy experiments were performed to determine the K_d for protein-protein interactions and binding stoichiometry. When FMN binds SsuE, there is a decrease in the flavin fluorescence at 520 nm (excitation wavelength of 450 nm) (Figure 3.10). The K_d value of SsuE binding to FMN was $0.015 \pm 0.004 \mu\text{M}$ indicating that oxidized flavin has a high affinity for the enzyme [78]. The K_d of SsuD binding to SsuE was determined by titrating the FMN-bound SsuE solution with SsuD. The increase in flavin fluorescence was monitored at an excitation wavelength of 450 nm following each addition of SsuD (Figure 3.11A). The concentration of SsuD bound was plotted against the total SsuD to obtain a K_d value of $0.002 \pm 0.001 \mu\text{M}$ (Figure 3.11B) with a 1:1 stoichiometric ratio between SsuE and SsuD.

The increase in fluorescence associated with SsuD binding to FMN-bound SsuE could be caused by release of the bound flavin. Filtration experiments utilizing a 10,000-molecular-weight-cutoff Amicon Ultra-4 centrifugation filter from Millipore (Bedford, MA) were performed to confirm that the flavin is still bound to SsuE following the addition of SsuD. If the flavin is still bound, then it should be retained with the protein in the retentate, while free flavin would be located in the filtrate. A UV-visible spectrum following filtration showed that the flavin was retained in the retentate, indicating that the FMN remains bound to SsuE in the presence of SsuD (Figure 3.12). The flavin was located in the filtrate in filtration experiments with free flavin only. These results confirmed that the increase in the intrinsic fluorescence associated with SsuD binding is due to protein-protein interactions.

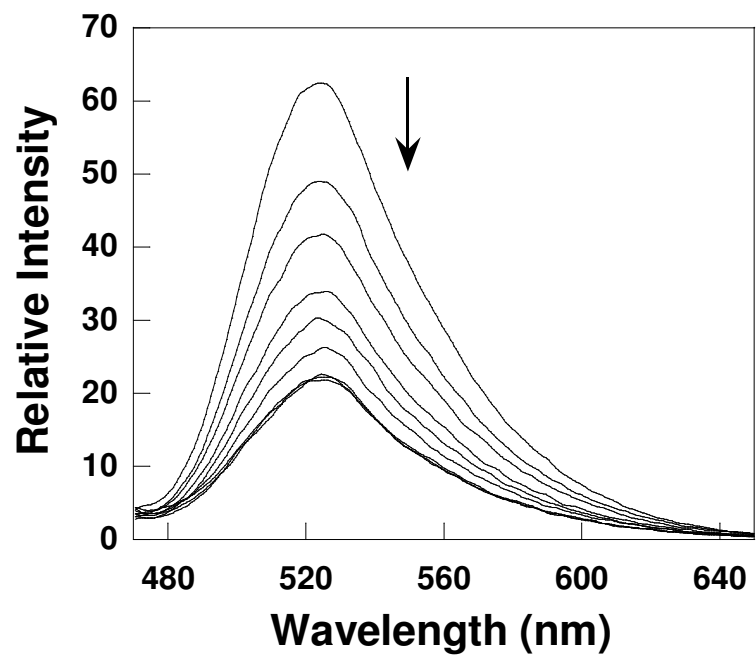


Figure 3.10. Fluorometric titration of SsuE to FMN.

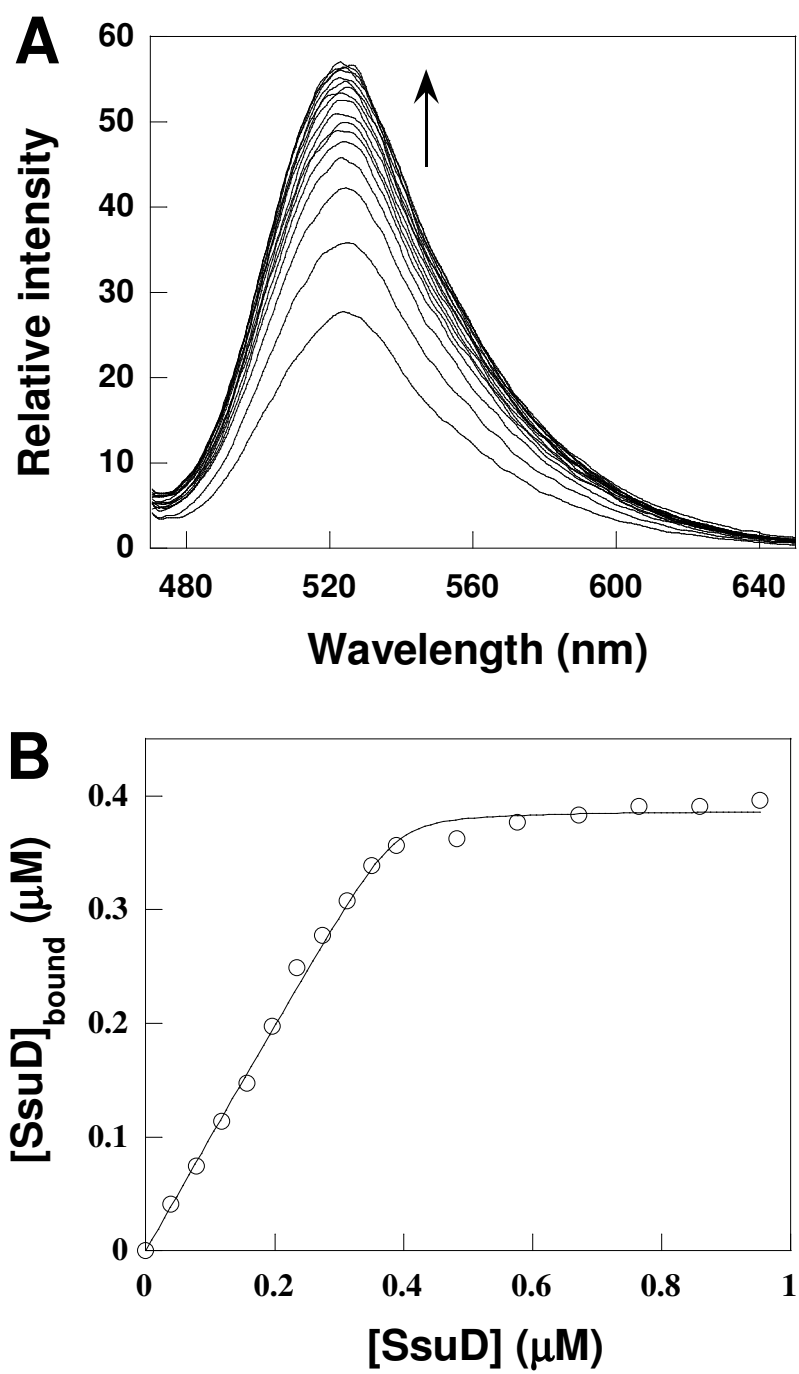


Figure 3.11. Fluorometric titration of SsuD to FMN-bound SsuE and determination of binding constant between SsuE and SsuD.

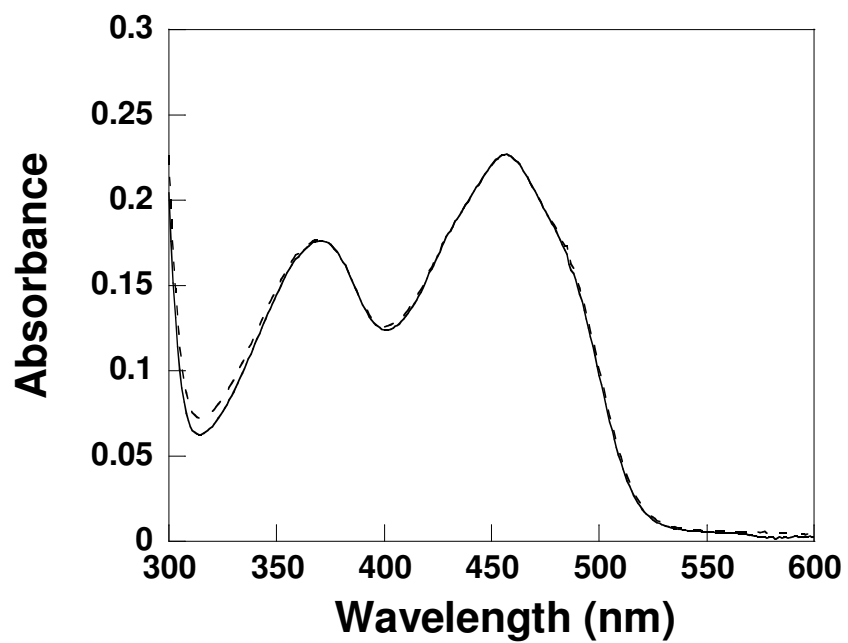


Figure 3.12. UV-visible spectra for filtration of FMN in the presence of SsuE and SsuD proteins.

3.5 Isothermal titration calorimetry

Isothermal titration calorimetry (ITC) experiments were performed to determine the thermodynamic properties for SsuE and SsuD binding by measuring the heat evolved during protein-protein interactions. The results from titration of SsuD into the cell containing the SsuE solution showed that the heat released to the solution decreased as the concentration of SsuD increased, which is normally observed during protein-protein interactions (Figure 3.13). The heat evolved due to protein-protein interactions should decrease as the two proteins reach equilibrium. Unfortunately, the data obtained was not reproducible and the heat evolved in the titration was relatively low. Therefore, the results could not be used for further analysis to determine the thermodynamic properties of SsuE and SsuD interactions.

3.6 Trifunctional chemical cross-linking

Cross-linking experiments were performed to investigate any physical interactions between SsuE and SsuD proteins, utilizing a trifunctional cross-linker. The trifunctional cross-linker (sulfo-SBED) contains an amine reactive site, an amine photoreactive arylazide, a biotin label, and a cleavable disulfide bond. The amine groups on SsuE were reacted first with the trifunctional cross-linker before the addition of SsuD. While SsuD contains no cysteine residues for cross-linking, analysis of the distribution of amino acids in the three-dimensional structure shows several surface-exposed amine-containing residues that are randomly distributed [74]. Following SsuE labeling, the SsuD protein was added and the sample exposed to UV light to cross-link SsuD with the photoreactive group (Figure 3.14). The addition of DTT following photoactivation cleaves the disulfide

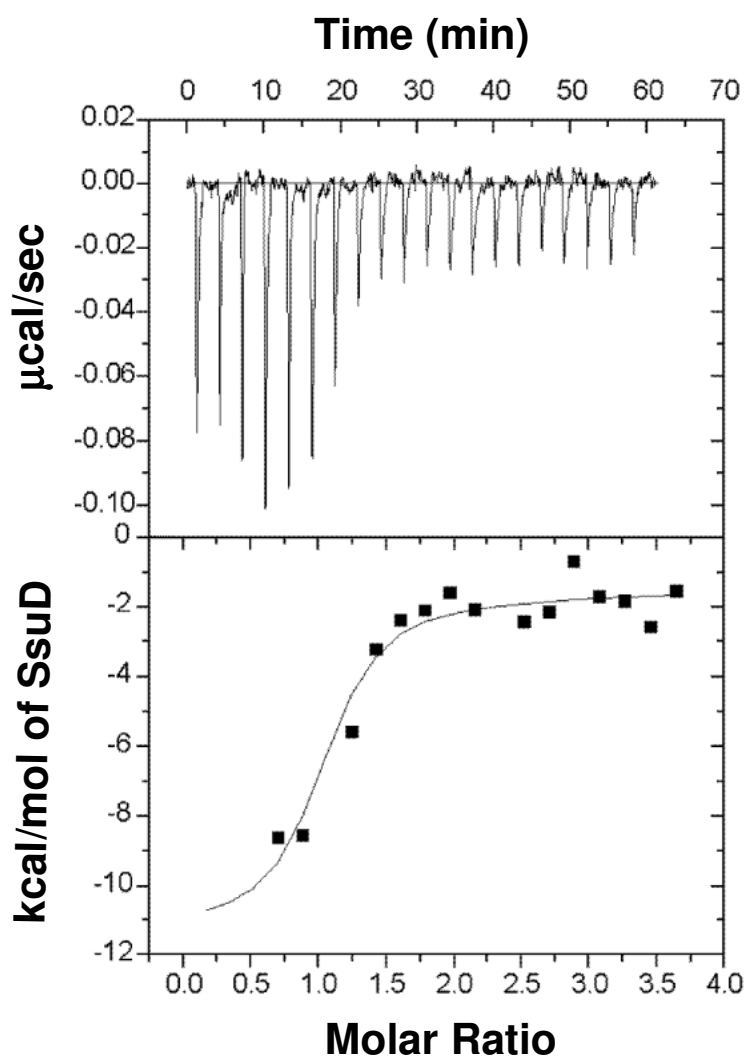


Figure 3.13. Isothermal titration calorimetry measurements to determine the thermodynamic properties of protein-protein interactions between SsuE and SsuD proteins.

bond in the amine reactive arm, resulting in biotin-labeled SsuD. Samples were taken after each step for analysis by native gel electrophoresis. Protein markers with their corresponding molecular mass and monomeric SsuE and SsuD are also shown on the gel (Figure 3.15A, lane 1 and lane 2, respectively). The sample after the activation of the photoreactive group contained a protein band with an apparent molecular mass of approximately 63 kDa corresponding to the monomeric cross-linking of SsuE (21.3 kDa) and SsuD (41.6 kDa) (Figure 3.15A, lanes 3-7, indicated by dotted arrow). The reagent-linked SsuE monomer was also observed (Figure 3.15A, lanes 3-7) with molecular masses slightly higher than native SsuE (Figure 3.15A, lane 2). The two bands observed in lanes 3-7 at approximately 43 and 80 kDa were due to dimerization of SsuE and SsuD, respectively, as similar results were observed in control experiments.

To ensure that the protein band with an apparent molecular mass of approximately 63 kDa is the biotin-labeled monomeric cross-linked SsuE and SsuD, the protein of interest was loaded onto a streptavidin agarose chromatography column. After applying the standard buffer containing 0-8 M of urea, the fractions were collected and analyzed by nonreducing polyacrylamide gel electrophoresis. The results showed that the protein with an apparent molecular mass of 63 kDa (Figure 3.15B, lanes 7-14, indicated by dotted arrow) was eluted from the streptavidin column only after coelution with a high concentration of urea. This indicated that the protein band was the biotin-labeled complex and was tightly bound to the column.

The sample following DTT treatment showed a decrease in the intensity of the 63 kDa band (Figure 3.16, lane 4) representing the putative cross-linked SsuE-SsuD species, with a concomitant increase in the intensity of the monomeric SsuE and SsuD

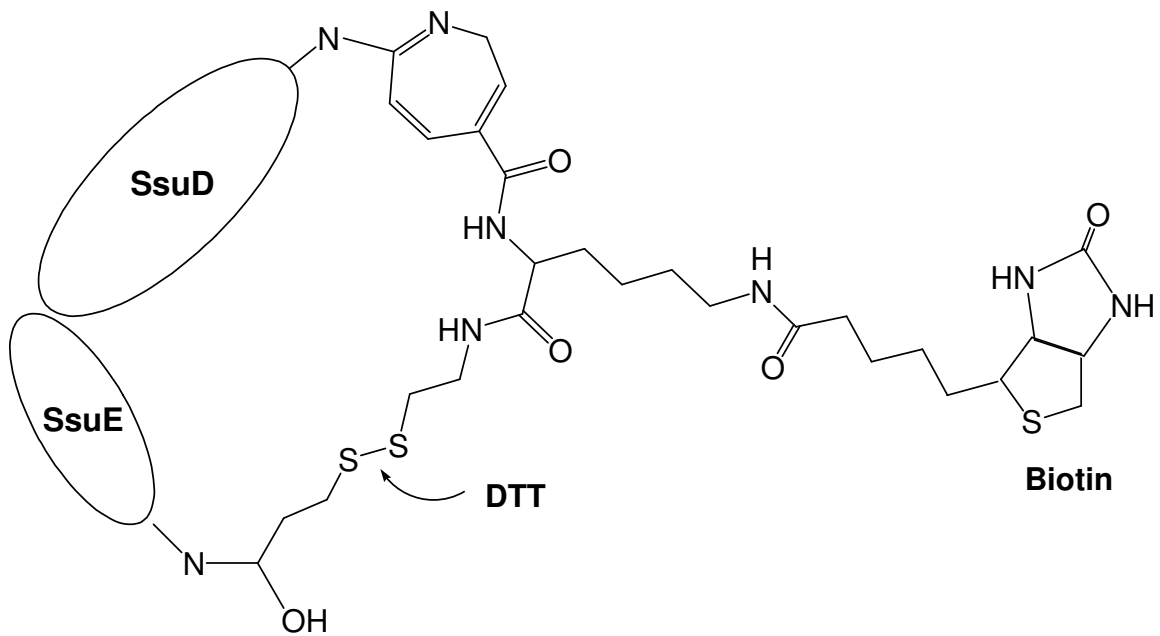


Figure 3.14. Complex formation between SsuE and SsuD by trifunctional cross-linking reagent. Biotin label was transferred from SsuE to SsuD following disulfide bond cleavage by DTT.

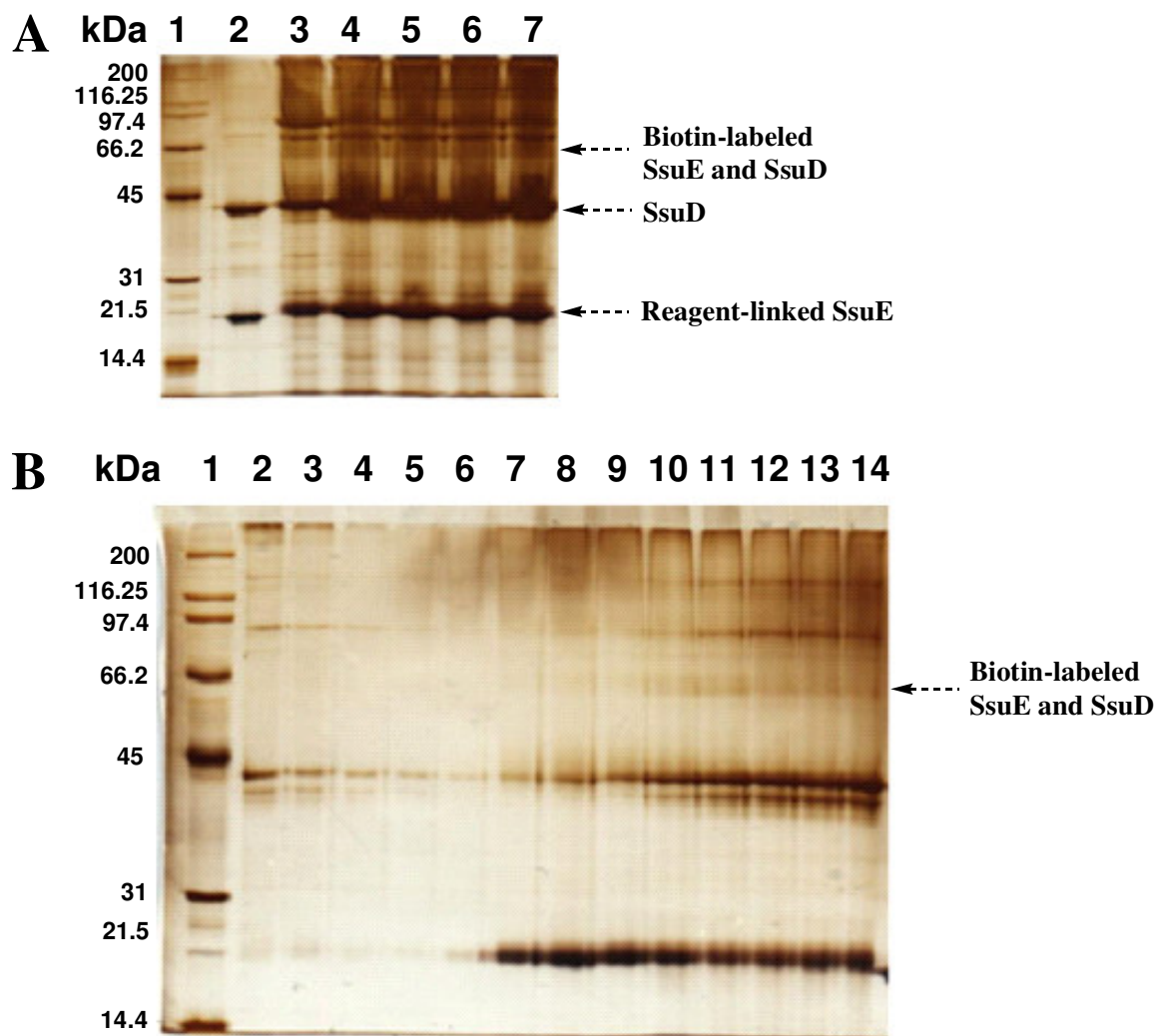


Figure 3.15. Silver-stained gel electrophoresis of cross-linking experiments between SsuE and SsuD proteins.

protein bands (Figure 3.16, lane 5). Protein markers with their corresponding molecular mass (Figure 3.16, lanes 1 and 6) and native SsuE and SsuD (Figure 3.16, lane 2) are also shown. Dimers of intrastrand cross-linked SsuE and SsuD proteins were shown at approximately 43 and 80 kDa respectively, when they were separated under nonreducing conditions (Figure 3.16, lane 7). However, the protein band with a molecular mass of 63 kDa was not observed in this control experiment. Experiments involving the cross-linking of only SsuE were performed to determine if a 63 kDa band was observed. A cross-linked trimer of SsuE would have a molecular mass similar to that of a cross-linked monomer of SsuE and SsuD. However, there was no band observed at 63 kDa with SsuE only, which indicated that the 63 kDa band represented the cross-linked monomers of SsuE and SsuD. In addition, cross-linking experiments with SsuE and bovine serum albumin were performed to verify that the higher molecular mass band was not caused by protein aggregation. The higher-molecular mass band at 63 kDa was not observed with any of the controls tested (data not shown), further confirming the formation of stable protein-protein interactions between SsuE and SsuD.

3.7 Determination of amino acid residues involved in protein-protein interactions between SsuE and SsuD proteins

Determining the amino acid residues involved in protein-protein interactions is important to further probe the structure-function relationship of SsuE and SsuD. Previous results using trifunctional cross-linking reagents have shown that the two proteins form a stable protein complex [103]. However, the trifunctional cross-linker cannot be used to identify the amino acid residues involved in protein associations. Cross-linking

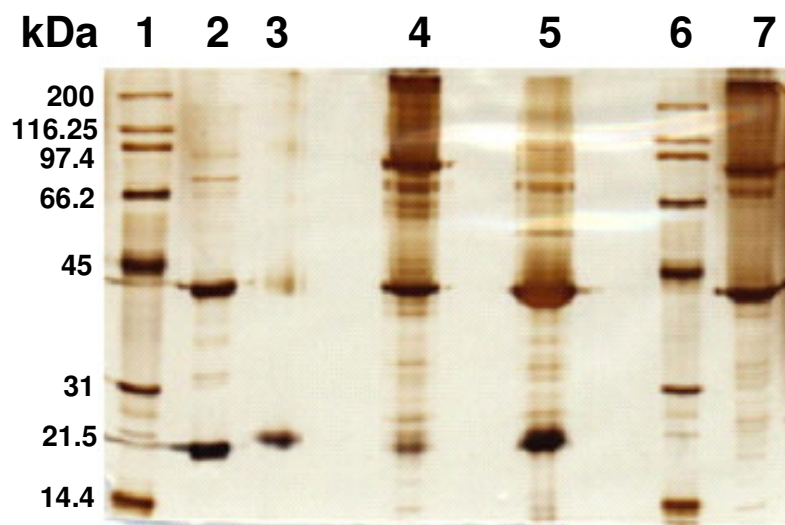


Figure 3.16. Silver-stained gel electrophoresis of DTT-treated cross-linked SsuE and SsuD.

experiments utilizing several bifunctional cross-linking reagents were performed to identify the binding sites of the two proteins involved in complex formation. The cross-linking reagents covalently link the interacting proteins by forming amide bonds with amino acid functional groups.

Four cross-linking reagents were used in this study that included 1-ethyl-3-(3-dimethylaminopropyl) carbodiimide hydrochloride (EDC), *N*-hydroxysulfosuccinimide (sulfo-NHS), bis(sulfosuccinimidyl) suberate (BS³), and ethylene glycol bis(succinimidylsuccinate) (EGS). Sulfo-NHS had been used in conjunction with EDC to stabilize the intermediate product (semi-stable amino reactive NHS ester) formed from the reaction of EDC with the carboxyl group of protein 1, while the functional group of the semi-stable amino reactive NHS ester will react with amino groups of protein 2 (Figure 3.17) [149]. The reactive groups of BS³ and EGS are only reactive towards amino group side chains of proteins. The general reaction involves the incubation of protein 1 with a cross-linking reagent (or combination of two different reagents, as in the case of EDC and sulfo-NHS reagents) followed by elimination of unreacted reagent(s) by filtration prior to addition of protein 2.

Analysis of the cross-linking experiments by SDS-PAGE showed that only EDC and sulfo-NHS reagents were able to covalently link SsuE and SsuD, while BS³ and EGS reagents both failed to yield a cross-linked product. In this reaction, SsuE was first reacted with EDC and sulfo-NHS followed by the addition of SsuD. The results showed that EDC/sulfo-NHS was able to covalently link SsuE and SsuD with an apparent molecular weight of cross-linked product at approximately 66 kDa (Figure 3.18, lanes 4-7). The molecular weight of the complex is slightly higher than the expected molecular

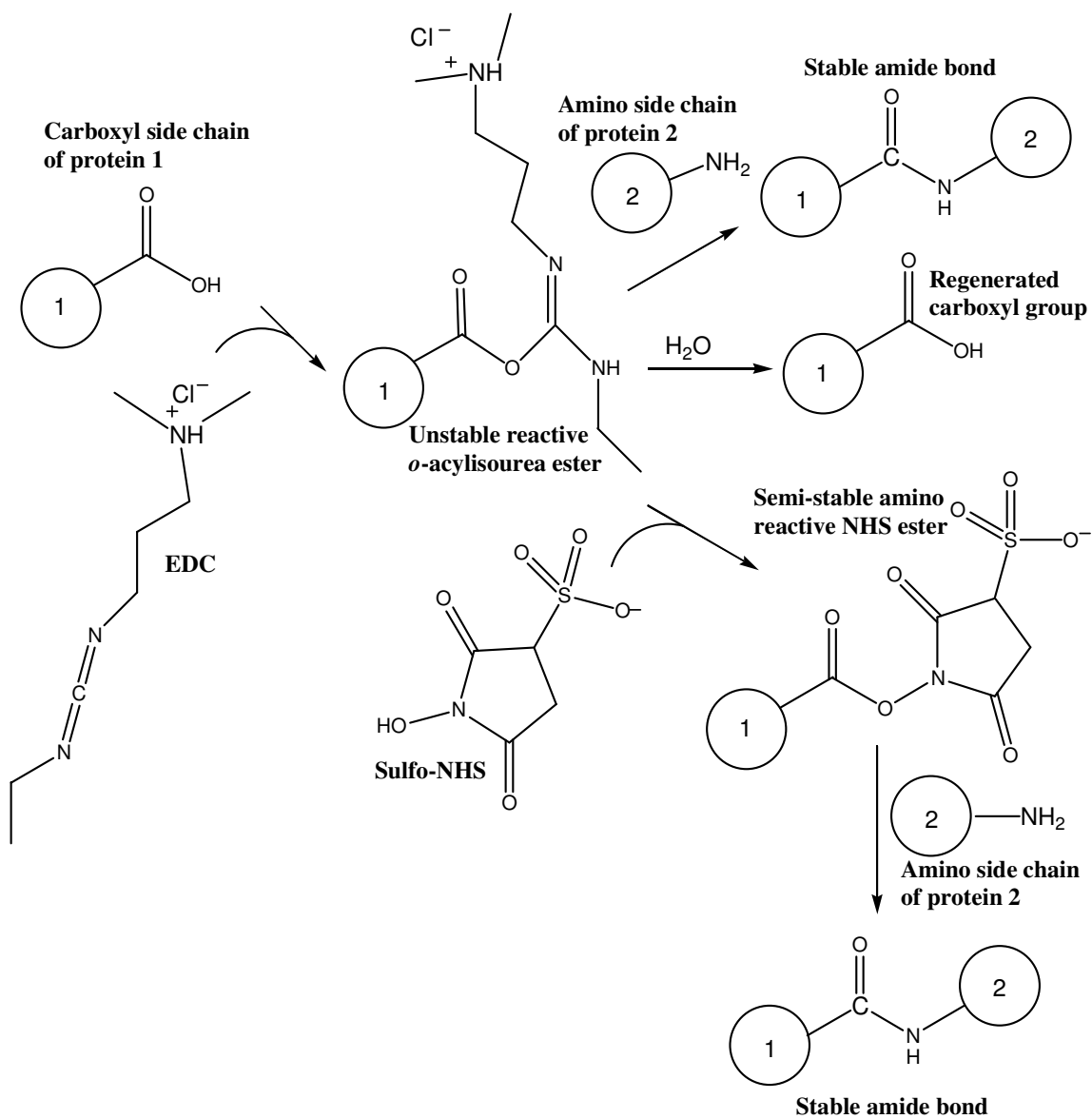


Figure 3.17. Reaction of EDC and sulfo-NHS cross-linking reagents with carboxyl group of protein 1 and amino group of protein 2 [149].

weight of 63 kDa as previously determined. This might be due to a change in the mobility of the cross-linked products on SDS-PAGE compared to the cross-linked products on the native gel. This band was not observed in the control with SsuE alone (Figure 3.18, lane 2).

Interestingly, when SsuD was mixed first with EDC and sulfo-NHS reagent followed by SsuE, the reagent failed to covalently link SsuD and SsuE. A protein band was observed at approximately 83 kDa representing a dimer of SsuD (Figure 3.18, lanes 8-11) as indicated by the control with SsuD alone (Figure 3.18, lane 3). Taken together, these results indicate that the EDC reagent first reacts with carboxyl groups of SsuE, followed by reaction of amine groups of SsuD with the semi-stable reactive NHS ester (Figure 3.19). In all experiments performed, the addition of FMN in a 1:1 molar ratio with SsuE were similar to the reactions without FMN.

The MALDI-TOF MS experiments were performed to further analyze the amino acid residues involved in complex formation between SsuE and SsuD. The matrices selected showed that 3,5-dimethoxy-4-hydroxycinnamic acid (sinapinic acid, SA) is the suitable matrix for the analyses of undigested proteins, while α -cyano-4-hydroxycinnamic acid (CHCA) is the suitable matrix for the analyses of digested proteins (peptide analyses). Protein standards were used for calibration of the MALDI-TOF MS instrument (Figure 3.20). In these experiments, the molecular weight of undigested SsuE and SsuD were 21.1 kDa (Figure 3.21) and 41.4 kDa (Figure 3.22), respectively. These results are slightly lower than the published molecular weight utilizing electrospray mass spectrometry, which are 21.3 and 41.6 kDa for SsuE and SsuD, respectively [78]. The results from mass spectrometric analyses of SsuD also showed the degradation product of

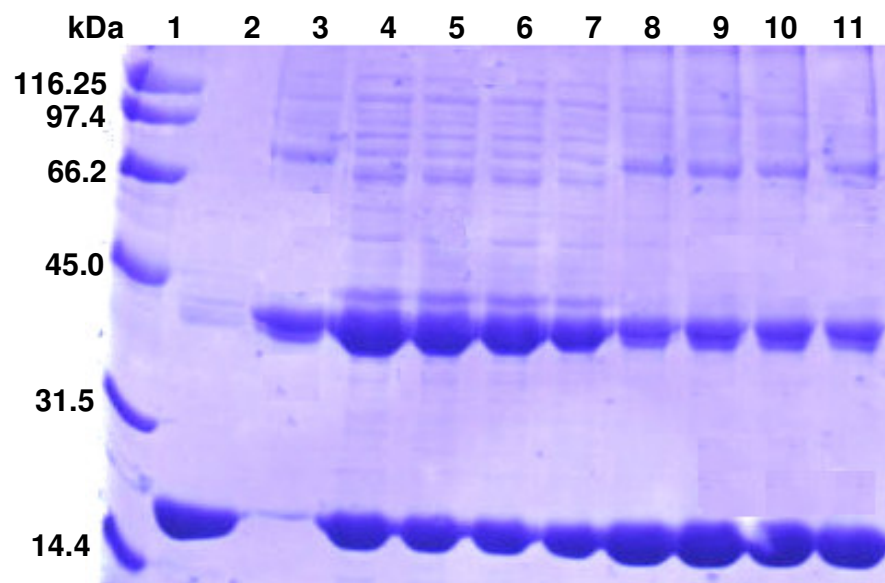


Figure 3.18. SDS-PAGE (10% acrylamide) from cross-linking experiments between SsuE and SsuD proteins with EDC and sulfo-NHS reagents.

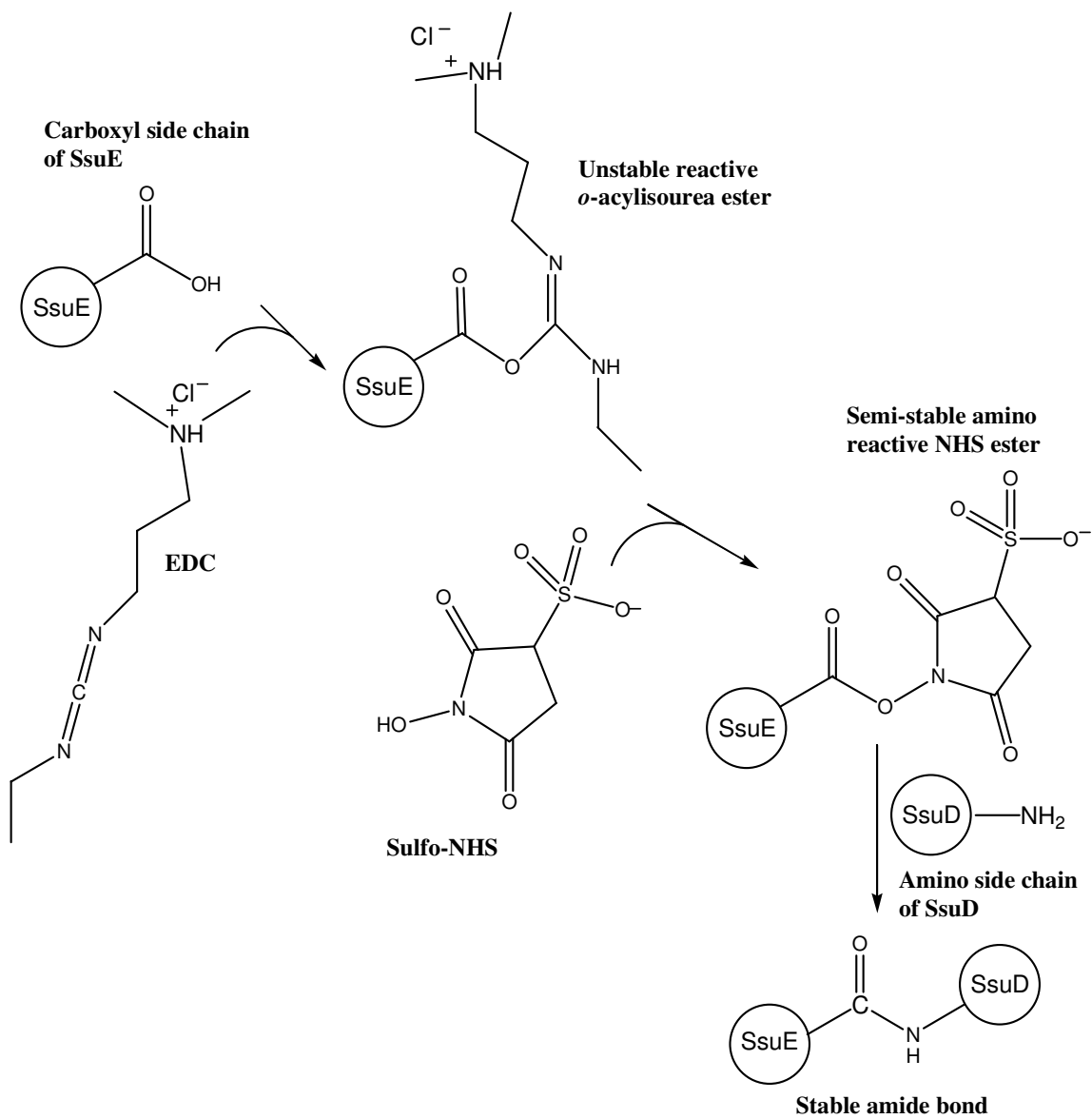


Figure 3.19. Reaction of EDC and sulfo-NHS cross-linking reagents with carboxyl groups of SsuE and amino groups of SsuD.

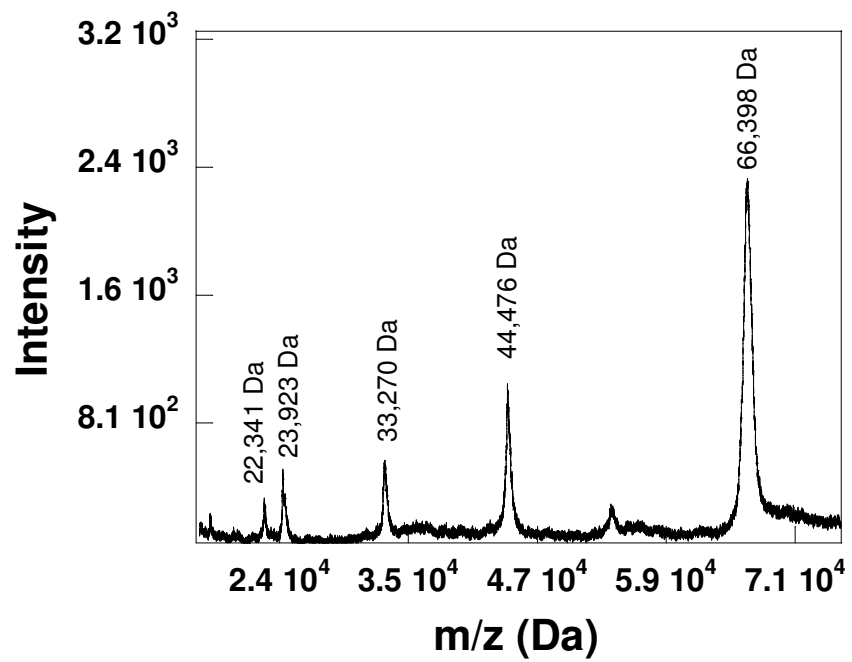


Figure 3.20. MALDI-TOF MS spectra for protein standards.

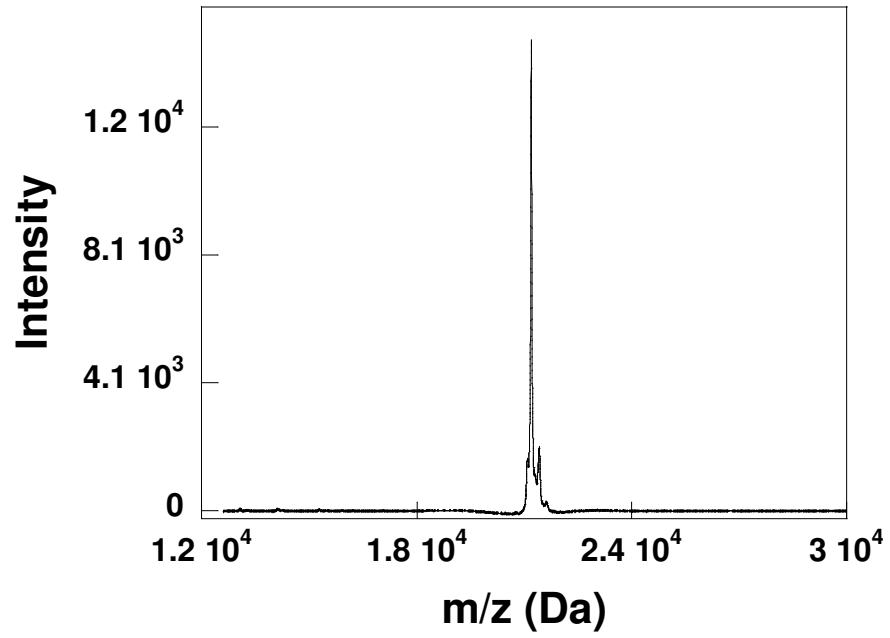


Figure 3.21. MALDI-TOF MS spectra for undigested SsuE protein.

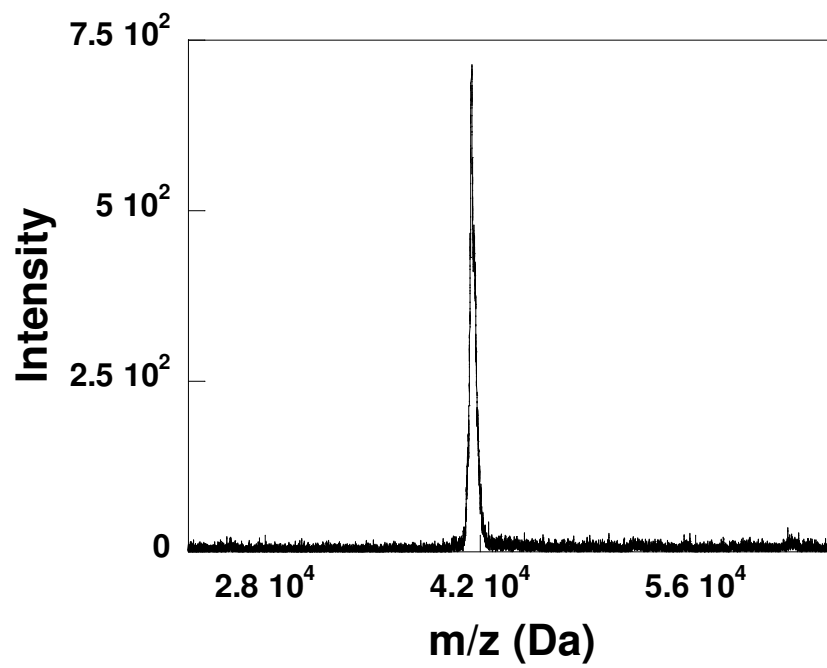


Figure 3.22. MALDI-TOF MS spectra for undigested SsuD protein.

SsuD by trypsin protease with a molecular weight of 20697 Da (21.0 kDa) (data not shown). Degradation product of SsuD was also observed on SDS-PAGE at a similar molecular weight (data not shown). Degradation product of SsuD was observed when the SsuD stock solution stored at 4 °C for several days was separated by SDS-PAGE.

Tryptic digests of native SsuE and SsuD proteins were analyzed by MALDI-TOF MS to obtain the molecular weights for peptides of each protein. These results were used as references for peptide analyses of the tryptically-digested protein complex, and peptide standards were used for calibration of the instrument (Figure 3.23). The results from MALDI-TOF MS analyses identified tryptically-digested SsuE peptides (Figure 3.24). The percentage of error (% error) of the tryptically-digested peptide was calculated according to Eq. 2.3. The results showed that the percent recovery of the peptide with a percent error of 1% or less was more than 50% as shown in the comparison between the observed and the theoretical molecular weight values (Table 3.1). MALDI-TOF MS analyses showed that peptides of tryptically-digested SsuD were also identified (Figure 3.25). The percent recovery of the peptide with a percent error of 1% or less was more than 57% as shown in the comparison between the observed and the theoretical molecular weight values (Table 3.2). The percentage recovery obtained from both SsuE and SsuD tryptically-digested peptides was reliable enough to be used for peptide analyses. Unfortunately, it was difficult to identify the cross-linked peptide. This might due to the low concentration of the cross-linked product extracted from SDS-PAGE. Therefore, there was not a sufficient amount of protein recovered from the gel for detailed analyses.

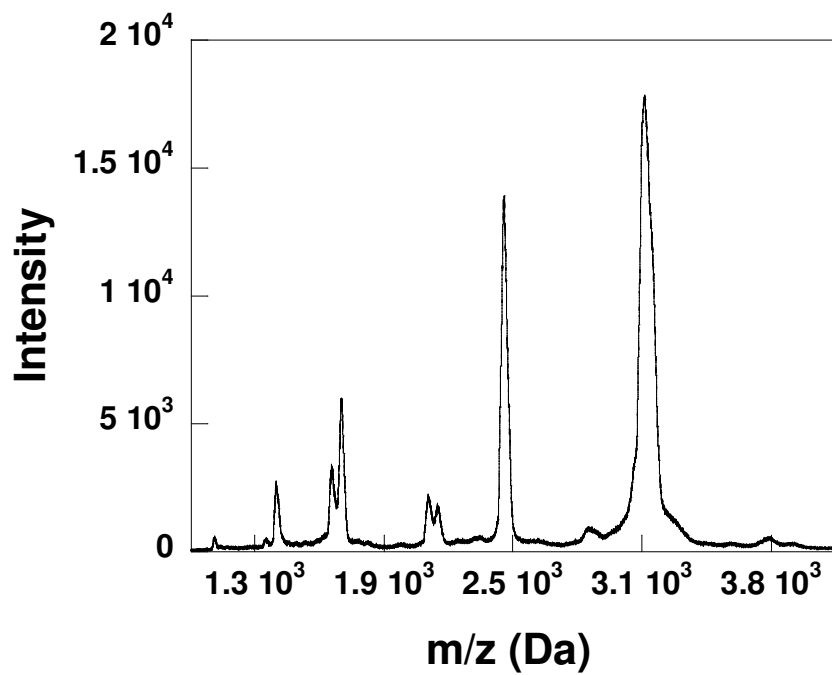


Figure 3.23. MALDI-TOF MS spectra for peptide standards.

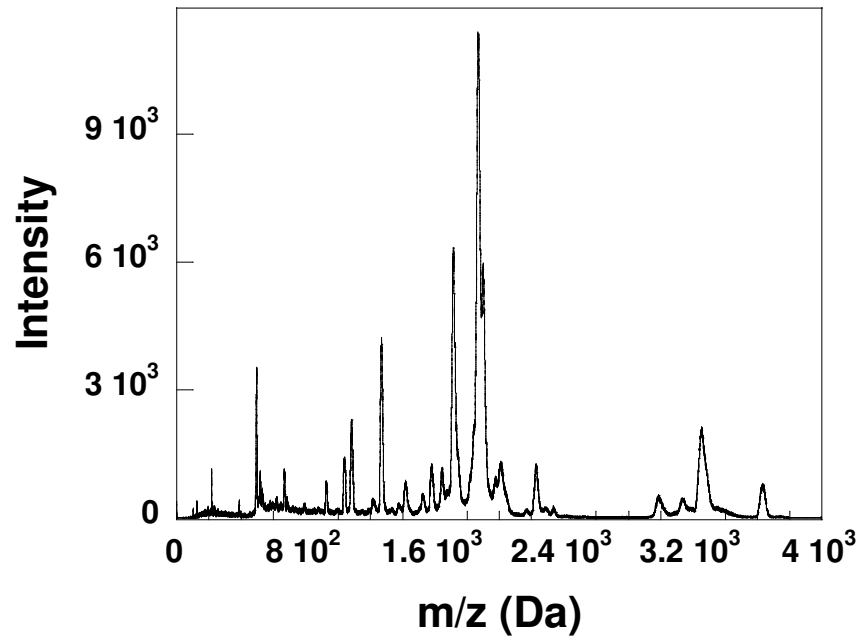


Figure 3.24. MALDI-TOF MS spectra for tryptically-digested SsuE.

Table 3.1. The molecular weight for the tryptically-digested SsuE peptide fragments.

Molecular weight (Da)		
Number of peptides	Theoretical value	Observed value ^a
1	175.1189	175.1935
2	276.1554	254.1
3	306.1594	- ^b
4	469.2153	-
5	506.2721	515.1
6	516.3140	518.3989
7	777.4141	-
8	780.4250	796.753
9	913.5465	921.7048
10	1025.5262	1032.702
11	1069.6251	1075.137
12	1254.7052	1271.439
13	1700.8754	1717.929
14	2222.1703	2223.157
15	2929.7488	-
16	2989.4842	2981.5
17	3632.7992	3633.6

^a Observed value of peptides recovered by MALDI-TOF MS presented are the value with percentage error $\leq 1\%$.

^b not detected.

The observed value with percentage error $1\% < \text{error} < 5\%$ are indicated with white on dark background color.

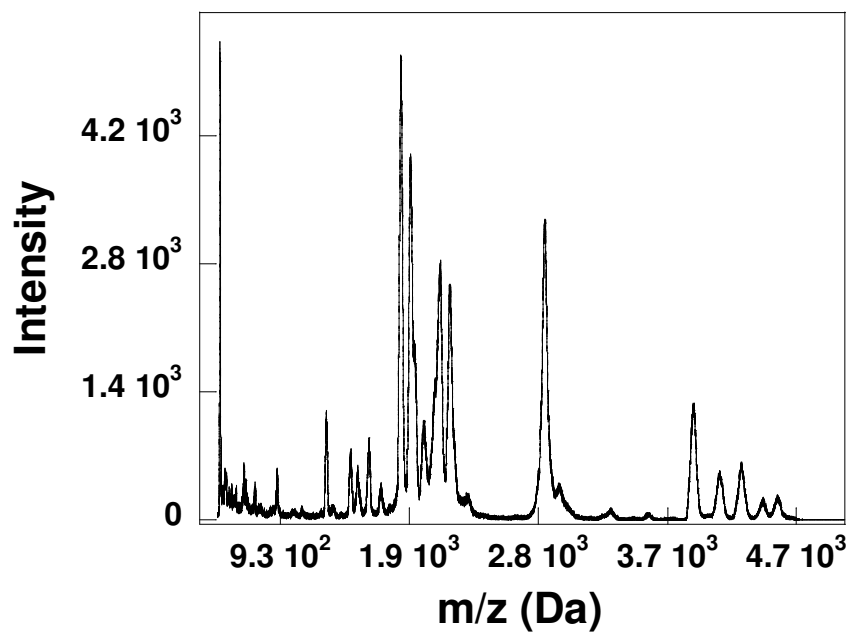


Figure 3.25. MALDI-TOF MS spectra for tryptically-digested SsuD.

Table 3.2. The molecular weight for the tryptically-digested SsuD peptide fragments.

Molecular weight (Da)		
Number of peptides	Theoretical value	Observed value ^a
1	147.1128	145.8878
2	175.1189	174.8736
3	218.1499	215.8348
4	260.1968	238.0093
5	275.1714	- ^b
6	276.1554	-
7	288.2030	300.9157
8	404.2140	388.8
9	492.2929	496.1233
10	529.3456	531.3
11	546.2994	533.9
12	582.3106	579.3
13	644.3726	642.1
14	661.3892	668.9
15	734.3944	748.1
16	736.4828	747.6404
17	774.4104	781.7
18	841.4349	821.1
19	890.4326	898.5
20	909.4312	907.0
21	1246.7154	1267.2
22	1354.7212	1381.6
23	1419.6135	1426.272
24	1469.7706	-
25	1486.6961	1486.5
26	1785.0381	1791.974
27	1852.9915	1868.6
28	1976.9568	1964.3
29	2787.3937	2792.4
30	3907.1003	3907.6
31	4514.1370	4512.3
32	4889.4963	-

^a Observed value of peptides recovered by MALDI-TOF MS presented are the value with percentage error $\leq 1\%$.

^b not detected.

The observed value with percentage error $1\% < \text{error} \leq 5\%$ are indicated with white on dark background color.

3.8 The effect of protein-protein interactions on SsuE-catalyzed flavin reduction

The reductive half-reaction of SsuE involves FMN reduction with reducing equivalents provided by NADPH. Previous work in our laboratory has shown that the mechanism for SsuE-catalyzed flavin reduction can be monitored at 450 and 550 nm [150]. An absorbance decrease at 450 nm represents time-dependent flavin reduction as the amount of oxidized flavin decreased over time. However, this flavin reduction reaction also involves SsuE-mediated charge transfer formation between FMN and NADPH that can be monitored at 550 nm. Charge transfer formation occurs as a distinct two phase absorbance increase followed by an absorbance decrease representing decay of the charge transfer complex. Two charge transfer complexes are generated; one between FMN and NADPH (CT-1), and the other between FMNH₂ and NADP⁺ (CT-2) (Figure 3.26) [150]. Charge transfer complex formation occurs within a similar time course as the absorbance trace obtained at 450 nm.

Previous studies have shown that the two proteins of the alkanesulfonate monooxygenase system form stable protein-protein interactions [103]. Here, the effects of protein-protein interactions on the reductive half-reaction by SsuE were further evaluated through pre-steady state kinetic analyses. Rapid reaction kinetic analyses were performed to determine if the rates for FMN reduction and charge transfer formation by SsuE were altered due to protein-protein interactions with SsuD. Alterations in enzymatic rates due to allosteric communication between active sites of two proteins have been observed in several coupled-enzyme reactions.

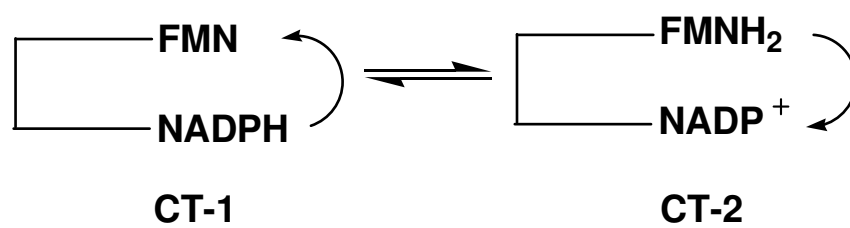


Figure 3.26. Charge transfer conversion between FMNH₂ and NADP⁺ in FMN reduction by SsuE [150].

3.8.1 The kinetics of flavin reduction by SsuE

The spectra for FMN reduction and charge transfer formation by SsuE in the absence of SsuD were obtained by single-wavelength absorbance at 450 and 550 nm. Time dependent spectra for FMN reduction at 450 nm (Figure 3.27A, closed circle) and charge transfer formation at 550 nm (Figure 3.27B, closed circle) were best fit to the sum of three exponentials representing three distinct phases (k_1 , k_2 and k_3) according to Eq. 2.5 and 2.6, respectively. The results showed that the initial phase for FMN reduction by SsuE at 450 nm had an observed rate of 124 s^{-1} (k_1), the second phase had an observed rate of 6.4 s^{-1} (k_2), and the third phase had an observed rate of 0.08 s^{-1} (k_3) (Table 3.3). The rates for charge transfer formation at 550 nm were also obtained with an observed rate of 243.3 s^{-1} (k_1) for the first phase, an observed rate of 10.7 s^{-1} (k_2) for the second phase, and an observed rate of 13.1 s^{-1} (k_3) for the third phase (Table 3.3). The rates obtained at 450 and 550 nm were very consistent with the results obtained from previous studies in our laboratory [150]. The initial fast phase at 550 nm (CT-1) corresponds to the majority of flavin still in the oxidized form when compared to the spectra at 450 nm. The second phase (CT-2) correlates to the last phase of the absorbance increase at 550 nm representing the charge-transfer formation between FMNH₂ and NADP⁺. The third phase represents the decay of the charge transfer complex indicated by the decrease in absorbance at 550 nm. This corresponds to the third phase at 450 nm representing complete flavin reduction or the release of the FMNH₂ product.

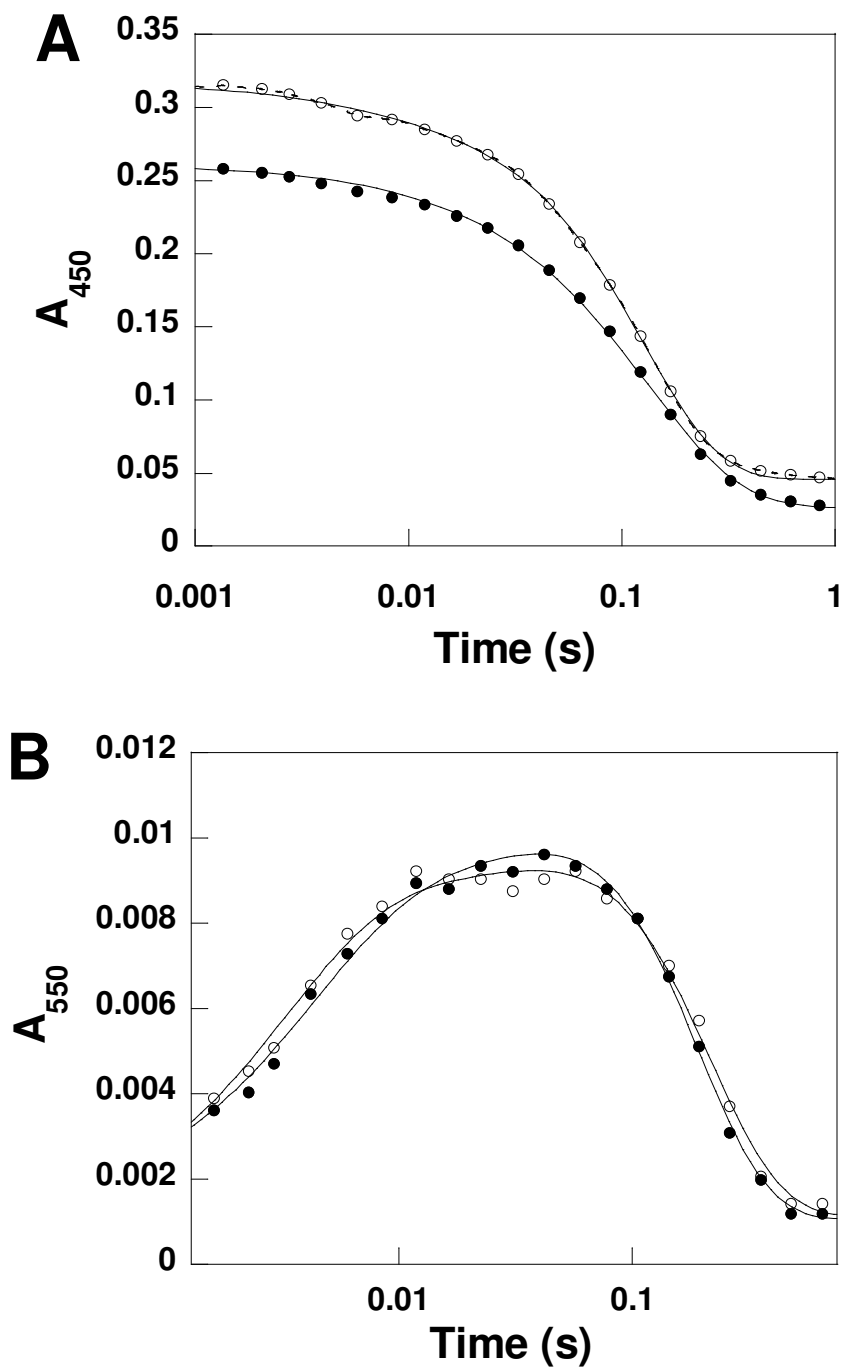


Figure 3.27. Spectra of FMN reduction and charge transfer formation in the absence and in the presence of SsuD.

Table 3.3. Rates for FMN reduction and charge transfer formation.

	450 nm (s ⁻¹)		
	k_1	k_2	k_3
SsuE + FMN / NADPH	124 ± 12	6.4 ± 0.1	0.08 ± 0.02
SsuE / SsuD + FMN / NADPH	161 ± 11	4.0 ± 0.1	17.3 ± 1.4
SsuE / SsuD / Octanesulfonate + FMN / NADPH	71.0 ± 7.7	6.4 ± 0.5	12.4 ± 2.3
SsuE / SsuD / Octanesulfonate + FMN / NADPH / O ₂	154 ± 27	13.2 ± 0.2	-0.120 ± 0.005
	550 nm (s ⁻¹)		
	k_1	k_2	k_3
SsuE + FMN / NADPH	243.3 ± 4.9	10.7 ± 1.7	13.1 ± 2.3
SsuE / SsuD + FMN / NADPH	311.4 ± 6.4	10.0 ± 3.0	11.2 ± 3.2
SsuE / SsuD / Octanesulfonate + FMN / NADPH	204.6 ± 6.1	3.1 ± 0.2	15.4 ± 1.4
SsuE / SsuD / Octanesulfonate + FMN / NADPH / O ₂	185.4 ± 9.6	34.9 ± 4.2	15.0 ± 0.9

3.8.2 The effect of SsuD on the kinetics of FMN reduction

The traces for FMN reduction and charge transfer formation by SsuE in the presence of SsuD were obtained at 450 and 550 nm (Figure 3.27A and 3.27B, open circle, respectively). The spectra at 450 and 550 nm were best fit to a triple exponential according to Eq. 2.5 and 2.6, respectively. A fit of the data at 450 nm showed that the observed rate (k_3) for FMN reduction by SsuE in the presence of SsuD increased 200-fold compared to the rate obtained for FMN reduction by SsuE alone (Table 3.3). However, the value for k_1 and the k_2 were not significantly altered (Table 3.3). A fit of the data at 550 nm for charge transfer formation by SsuE in the presence of SsuD did not change compared to the spectra in the absence of SsuD (Table 3.3).

UV-visible spectroscopy studies on free FMNH₂ and FMNH₂-bound SsuD were performed to investigate the subtle increase at the last phase of flavin reduction spectra that was observed at 450 nm in the presence of SsuD. The third phase (k_3) was previously shown to represent the flavin release step [150]. An alteration in the reduced flavin spectra in the absence and in the presence of SsuD would indicate that FMNH₂ binding to SsuD results in the observed change. The result showed that there was a spectral change at 450 nm (Figure 3.28, inset) between free FMNH₂ (Figure 3.28, solid line) and FMNH₂-bound SsuD (Figure 3.28, dashed line). This may suggest that the increase in absorbance at 450 nm at the end of the time course corresponds to the release of FMNH₂ and/or binding of FMNH₂ by SsuD that may correlate to the increase in k_3 at 450 nm.

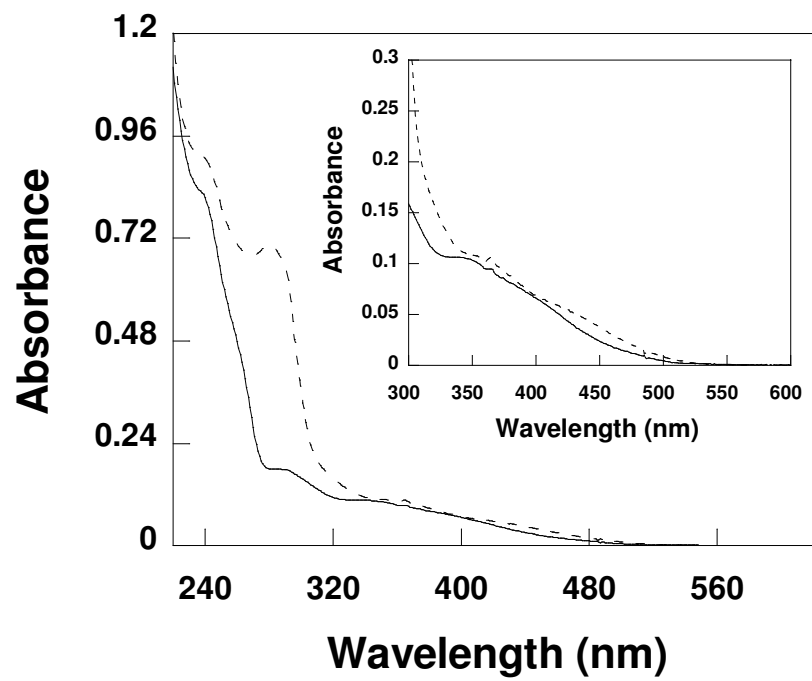


Figure 3.28. UV-visible spectra for free FMNH₂ and FMNH₂-bound SsuD.

3.8.3 Kinetics of FMN reduction and charge transfer formation by SsuE in the presence of SsuD, oxygen, and octanesulfonate

The effect of SsuD, octanesulfonate (250 μM), and dioxygen (440 μM) on FMN reduction and charge transfer formation were monitored by single-wavelength analyses at 450 and 550 nm, respectively. The trace at 450 nm for the reaction (Figure 3.29A, open circle) showed a notable change in the second and the third phases of flavin reduction compared to the reaction without dioxygen (Figure 3.29A, closed circle). A fit of the data at 450 nm showed that the rate of the second phase (k_2) increased more than two-fold in the reaction with dioxygen (440 μM) (Table 3.3), while the third phase (k_3) gave a negative value (Table 3.3). The negative value indicates that either the flavin is oxidized by SsuD or FMNH₂ is bound rapidly by SsuD (Figure 3.29A, open circle). Furthermore, the results from data analyses at 550 nm also showed that in the fully coupled-enzyme system the second phases (k_2) was more than 10-fold higher (Table 3.3 and Figure 3.29B, open circle) compared to the reaction without oxygen (Table 3.3 and Figure 3.29B, closed circle). However, the values for k_1 and k_3 were relatively unaffected by increased oxygen concentration (Table 3.3 and 3.4). It was previously determined that the second phase of flavin reduction by SsuE represents the electron transfer step from NADPH to FMN, which is believed to be the rate-determining step for FMN reduction by SsuE [150].

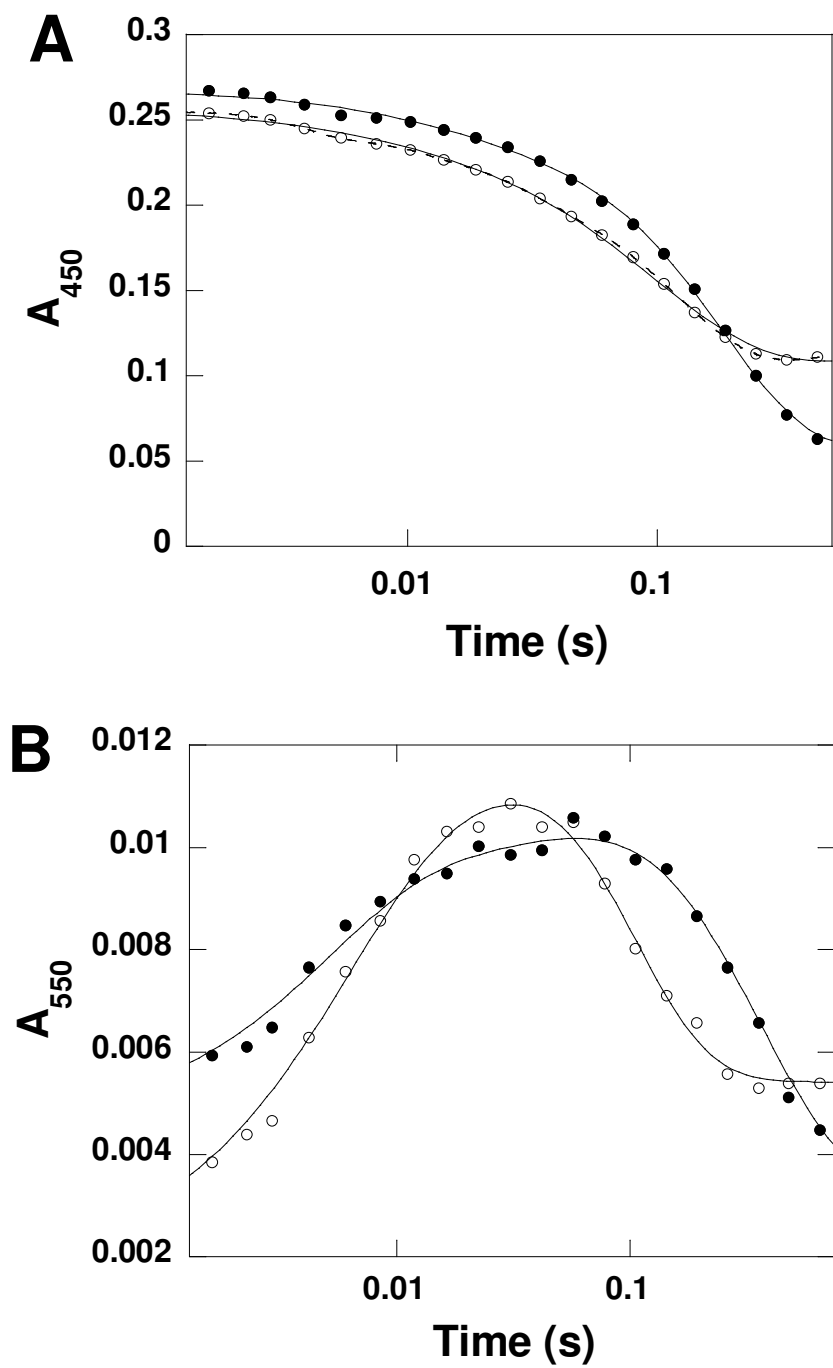


Figure 3.29. Spectra of FMN reduction and charge transfer formation by SsuE in the presence of SsuD, octanesulfonate, and oxygen.

Table 3.4. Rates for charge transfer formation in coupled-enzyme reactions with different oxygen concentration.

[Oxygen] (μM)	k_1 (s^{-1})	k_2 (s^{-1})	k_3 (s^{-1})
0	204.6 ± 6.1	3.1 ± 0.2	15.4 ± 1.4
110	225.3 ± 4.9	7.4 ± 0.3	20.4 ± 1.5
330	182.8 ± 4.9	18.4 ± 6.2	14.4 ± 4.0
440	185.4 ± 9.6	34.9 ± 4.2	15.0 ± 0.9

3.8.4 Kinetics of FMN reduction and charge transfer formation by SsuE in the presence of oxygen and octanesulfonate without SsuD

Rapid reaction kinetics analyses were performed at 450 and 550 nm in the presence of octanesulfonate (250 μM) and/or dioxygen (440 μM) excluding SsuD to further investigate whether the changes in rates were due to substrate-bound SsuD or if the substrates alone affect SsuE-catalyzed FMN reduction. The single traces at 450 and 550 nm with octanesulfonate alone (Figure 3.30A and 3.30B, closed circle, respectively) or in the presence of octanesulfonate and dioxygen (Figure 3.30A and 3.30B, open circle, respectively) were similar to reaction with SsuE alone. These results indicated that octanesulfonate and dioxygen in the absence of SsuD did not affect the SsuE-catalyzed flavin reduction or charge transfer formation as shown in the fully-coupled enzyme system.

3.8.5 Kinetics of FMN reduction and charge transfer formation in the presence of SsuD and dioxygen or octanesulfonate

Rapid reaction kinetic analyses of FMN reduction by SsuE were performed in the presence of SsuD and either dioxygen or octanesulfonate to investigate whether SsuD and individual substrates may affect the rates of FMN reduction when there is no reaction taking place at the SsuD active site. The effect of dioxygen on the rate of FMN reduction and charge transfer formation by SsuE in the presence of SsuD were performed by rapid reaction kinetic analyses at 450 and 550 nm, respectively. The results showed that the rates of the reaction at 450 and 550 nm in the presence of dioxygen (440 μM) and SsuD (Figure 3.31A and 3.31B, open circle, respectively) were not significantly

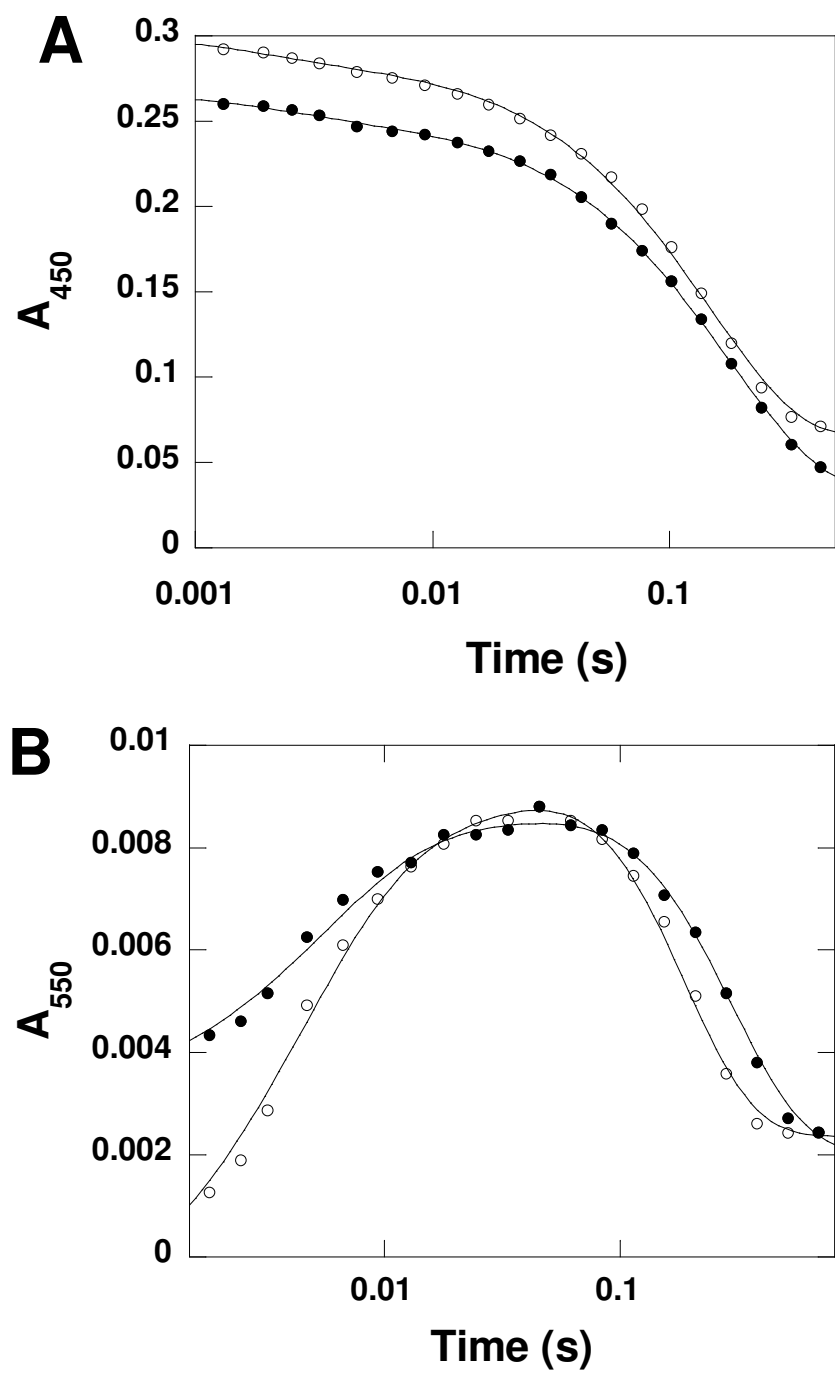


Figure 3.30. Spectra of FMN reduction and charge transfer formation by SsuE in the presence of oxygen and octanesulfonate without SsuD.

changed compared to the rates of the reaction with SsuD alone (Figure 3.31A and 3.31B, closed circle, respectively). Other control experiments that were performed without oxygen in the solution, in the presence of SsuD with octanesulfonate also resulted in no effect on the rates at both 450 and 550 nm compared to SsuD alone (data not shown). These results indicated that the alteration in the rates of FMN reduction were affected by the binding of both substrates at the SsuD active site. Taken together, these results further confirmed that the alteration of the rate of charge transfer formation by SsuE was affected by substrate-bound SsuD, and support a mechanism involving allosteric communication between the active sites.

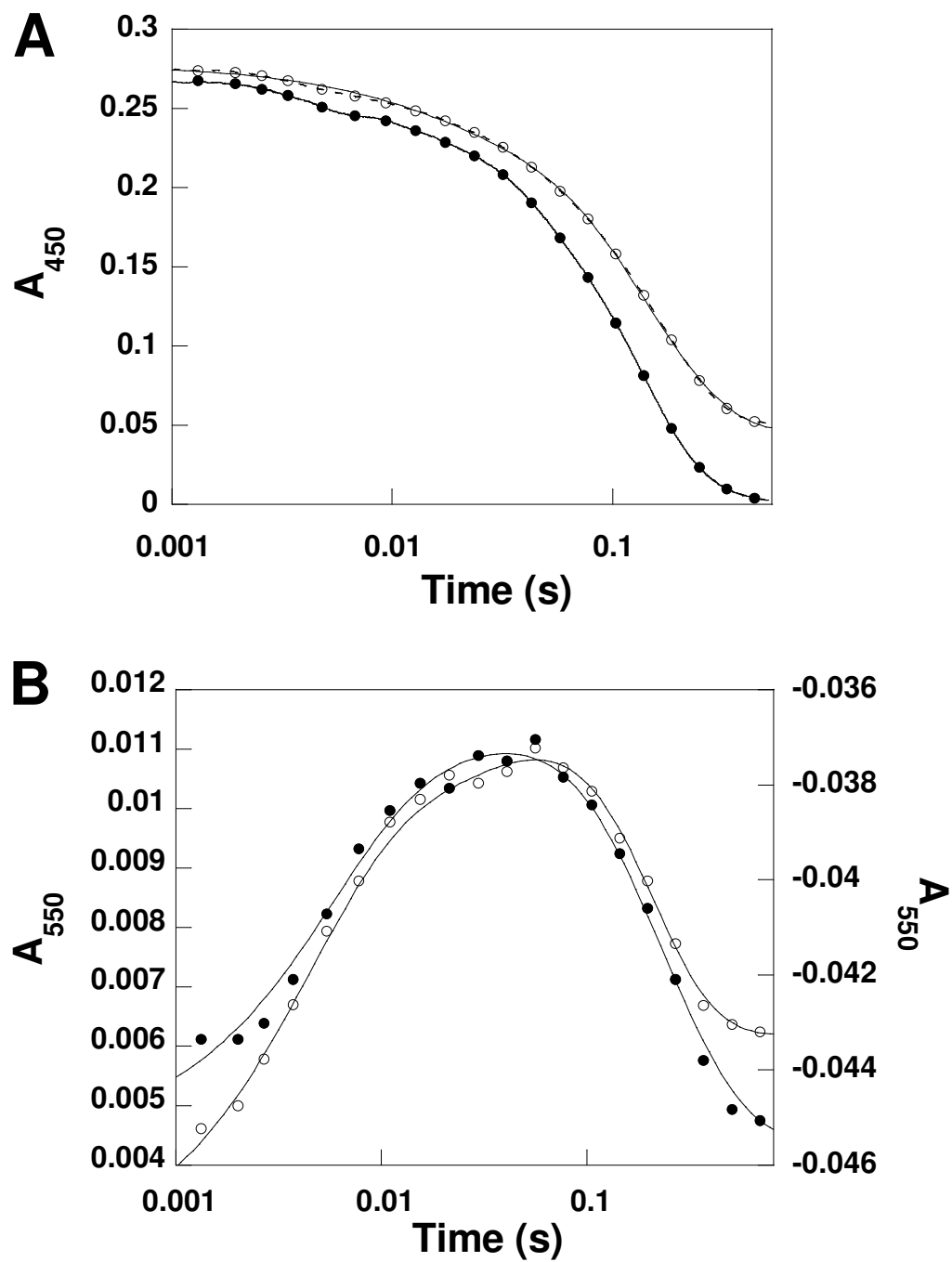


Figure 3.31. Spectra of FMN reduction and charge transfer formation by SsuE in the presence of SsuD and oxygen, but in the absence of octanesulfonate.

CHAPTER FOUR

DISCUSSION

Reduced flavins are utilized by various organisms for a wide range of biological processes. For most flavoproteins the reductive and oxidative half-reactions of the flavin occur within the same protein. Interestingly, the production and utilization of this intermediate species in certain microbial systems involve both a reductase and an oxygenase enzyme that independently catalyze each half-reaction. Although the role of reduced flavin in redox reactions has been known for some time, the mechanism of reduced flavin transfer in two-component enzyme systems is still poorly understood. Therefore, understanding the mechanism of reduced flavin transfer is extremely important to explore the role of reduced flavin in cellular systems. Free reduced flavin is typically considered unstable under aerobic conditions and is easily oxidized, generating hydrogen peroxide [66,94,151]. The hydrogen peroxide generated can be further oxidized leading to the production of oxygen radicals that can damage cellular macromolecules. Due to its unique properties, it is important to stabilize the reduced flavin from unproductive oxidation. In most flavoproteins the flavin is a bound prosthetic group, and the active site of the protein protects the reduced flavin from further oxidation. In systems where the reductive and oxidative half-reactions occur in separate proteins, a

possible mechanism of reduced flavin transfer is through protein-protein interactions between the reductase and oxygenase components. A channeling mechanism would protect the reduced flavin from futile oxidation before catalysis can occur.

The focus of these studies was to investigate the role of protein-protein interactions between the alkanesulfonate monooxygenase proteins through several biophysical approaches. These include the effects of protein associations on the SsuE-catalyzed reactions, the mechanism of reduced flavin transfer from the reductase to the monooxygenase, and identification of amino acid residues involved in complex formation.

4.1 Formation of insoluble proteins in the coexpression of SsuE and SsuD

Coexpression of SsuE and SsuD proteins was performed to provide a means to detect protein-protein interactions through cross-linking experiments, affinity chromatography, and kinetic analyses. The results showed that His-tagged SsuE and SsuD were successfully expressed, however, the two proteins were insoluble (Figure 3.3A). In bacteria, overexpression of recombinant proteins in foreign hosts often results in the formation of insoluble protein aggregates called inclusion bodies [152]. This may be due to protein misfolding which is dependent on several factors such as concentration, pH, temperature, ionic strength, and the redox environment [153,154]. There is also kinetic competition between the correctly folded and misfolded forms of proteins, which may or may not result in the formation of aggregates [153]. The formation of inclusion bodies often represents a major obstacle in the expression of proteins. With proteins that are known to form relatively strong protein-protein interactions, coexpression may even

prove more problematic. This can sometimes be overcome by reducing the induction time, since the formation of inclusion bodies is also time-dependent [155]. Different growth conditions, such as pH and temperature can also be applied during growth and induction [156]. Formation of inclusion bodies may also be caused by the production of toxic molecules or a high level of protein expression.

In this study, several bacterial *E. coli* strains were used as an expression host to overcome the insolubility of the coexpressed His-tagged SsuE and SsuD proteins in the BL21(DE3) *E. coli* strain (refer to Table 2.1 in materials and methods). The *E. coli* (DE3) strain expresses T7 polymerase upon IPTG induction, thus enhancing the expression of genes under the T7 promoter. The pLysS plasmid contains the T7 lysozyme gene (*lysS*) encoding the T7 lysozyme protein that binds the T7 RNA polymerase and inhibits expression from the T7 promoter. Thus, it is usually used to reduce basal level expression of the gene of interest, and is suitable for expression of toxic gene products. In addition, pLysS contains the p15A origin that allows for compatibility with plasmids containing the ColE1 or pMB1 origin (i.e. pUC- or pBR322-derived plasmids). Tuner cells contain a mutation in the lac permease (*lacZY*) gene. The lac permease (*lacY*) mutation allows uniform entry of IPTG into all cells in the population, which produces a concentration-dependent homogeneous level of induction. By adjusting the concentration of IPTG, expression of proteins can be regulated from very low to high levels. Lower level expression may enhance the solubility and activity of difficult target proteins. The origami host strain contains mutations in both the thioredoxin reductase (*trxB*) and glutathione reductase (*gor*) genes, which greatly enhances disulfide bond formation in the cytoplasm. However, the results still showed

that none of the host strains utilized in these studies remedied the formation of inclusion bodies (Figure 3.3B). Despite the difficulties caused by the formation of insoluble proteins from this coexpression system, this dual expression system offers an intriguing model to explore the molecular basis of misfolded protein-protein interactions [153,157]. However, further studies need to be performed to identify the cause of the insolubility of this coexpression system before it can be used for future work.

4.2 Detection of protein-protein interactions in the alkanesulfonate monooxygenase system

Various biophysical methods have been performed to detect the formation of protein complexes between SsuE and SsuD. Both native and His-tagged SsuE or SsuD proteins were used for these studies. Results from affinity chromatography experiments showed that the two proteins interact with a relatively strong binding affinity, as the proteins were shown to coelute from the column (Figure 3.4B, lane 4). This result is convincing as a large volume of buffer (10 to 20 times the column volume) was used to wash the column prior to elution. The possibility that SsuE and SsuD coelute due to nonspecific protein interactions and binding was examined in control experiments. If SsuD was not preloaded on the Ni-NTA column, the SsuE protein eluted from the column with a lower concentration of imidazole buffer (125 mM). In addition, a catalytically unrelated protein was unable to interact with SsuD. This supports the argument that the coelution of SsuE and SsuD was due to protein interactions and was not caused by protein aggregation or nonspecific interactions of SsuE with the column. While the amount of SsuE was not equimolar with SsuD, this would be expected if the

protein binding sites on SsuD were inaccessible due to alternative arrangements of SsuD on the column.

Although the two proteins are shown to interact in the absence of substrates, this interaction was not caused by any major conformational changes in the secondary structure of each protein as indicated by far-UV CD spectroscopy. Any changes that occur due to protein-protein interactions may lead to only minor perturbations in the protein structure that would not be translated to overall secondary structural changes. Several groups have utilized visible CD spectroscopy to analyze perturbations in the flavin environment within the active site [158,159]. The 100-fold greater affinity for oxidized flavin to SsuE over SsuD provided an ideal means to analyze changes in the FMN-bound SsuE active site upon SsuD binding [78]. While there were no major changes in the visible absorbance from 375 to 550 nm, a slight decrease in the negative molar ellipticity was observed between 300 and 375 nm with SsuD present. The change was not due to protein aggregation, because bovine serum albumin did not elicit the same decrease. These results suggest that the change in the flavin environment was due to specific protein interactions between SsuE and SsuD and not to random aggregations. This argument was supported by the data that the flavin environment did not change in the presence of SsuD alone (Figure 3.9). An alteration in the flavin environment would be expected if SsuE exists in a more open conformation in the presence of SsuD.

The decreased molar ellipticity observed by visible CD spectroscopy suggested that there was a change in the flavin environment that could be further analyzed by fluorescence spectroscopy. There is an observed decrease in fluorescence upon flavin binding to SsuE, which was previously used to determine the K_d for binding of the

oxidized flavin to SsuE. Titration of FMN-bound SsuE with SsuD resulted in an increase in fluorescence that reached a saturation point. Independent filtration experiments confirmed that the flavin was still bound to SsuE in the presence of SsuD, and therefore the increase in absorbance was not caused by the release of the bound flavin. The K_d value determined from these studies was $0.002 \pm 0.001 \mu\text{M}$, which indicates a relatively strong interaction between these proteins. Analytical ultracentrifugation studies have shown that SsuE is a dimer and SsuD is a tetramer at the concentration used in these studies [78]. Therefore, the 1:1 stoichiometric ratio for monomeric binding between SsuE and SsuD supports a structural model involving four dimers of SsuE bound to a tetramer of SsuD (Figure 4.1). Isothermal titration calorimetry (ITC) experiments had been performed prior to the fluorometric titration experiments to monitor the heat change due to protein-protein interactions. The results from these studies suggest that the heat change (ΔH) released from titration between SsuE ($1 \mu\text{M}$) with SsuD ($50 \mu\text{M}$) was relatively low ($\sim 10 \text{ kcal/mol SsuD}$) and the results were not readily reproducible (Figure 3.13). The low enthalpy changes can be explained by the low dissociation constant value ($0.002 \pm 0.001 \mu\text{M}$) obtained from fluorometric titration experiments. This value is much lower than the concentration of SsuE and SsuD required for the ITC experiments (μM range). Protein binding would occur rapidly when the high concentration of SsuE was titrated by an even higher SsuD concentration. Thus the binding had already reached equilibrium in the early stages of titration.

The results obtained suggest that static interactions occur between SsuE and SsuD and that these interactions may play a role in the transfer of reduced flavin. The existence of protein-protein interactions between SsuE and SsuD supports a mechanism

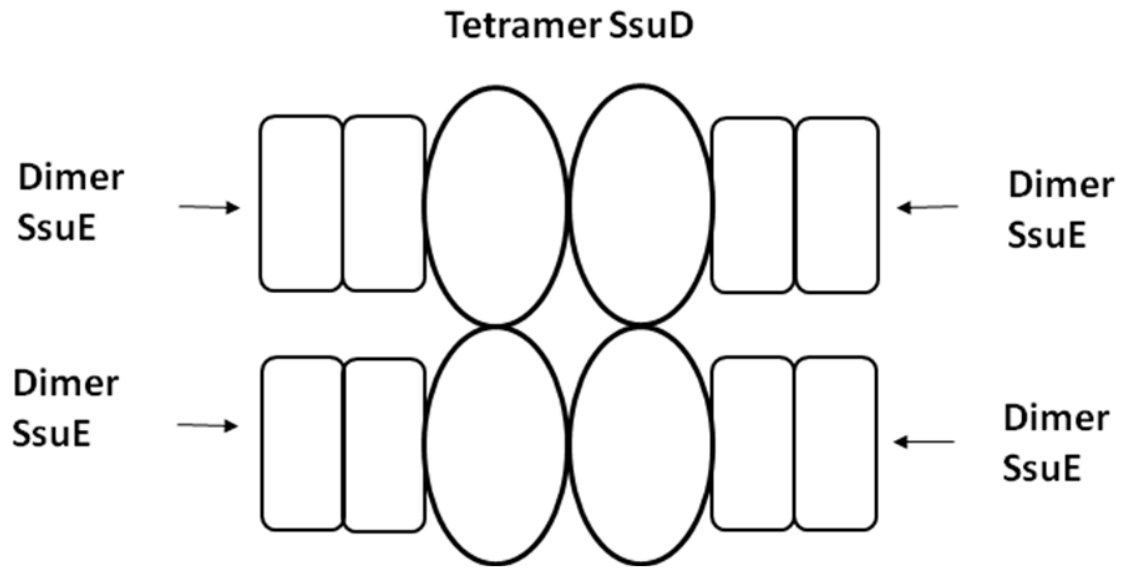


Figure 4.1. Proposed model for protein complex formation between SsuE and SsuD proteins.

where the flavin is channeled or shared by the two proteins but eliminates the possibility of a diffusion mechanism. Direct reduced flavin transfer through a substrate channeling mechanism and the involvement of the active sites of SsuE and SsuD in allosteric communication were further investigated through pre-steady state kinetic analyses.

4.3 Amino acid residues involved in protein-protein interactions between SsuE and SsuD

Our previous studies with affinity chromatography and fluorescent spectroscopy have shown that SsuE and SsuD are able to form a stable complex. The identification of SsuE and SsuD interactions were also analyzed with a trifunctional cross-linker. The silver-stained gel showed a protein band at approximately 63 kDa, which correlates with monomers of SsuE and SsuD covalently bound with the cross-linker reagent. In control experiments with SsuE or SsuD only, there was no higher molecular mass band observed at 63 kDa. Therefore, the band observed likely corresponds to the SsuE and SsuD proteins. The results from these studies further support the presence of protein interactions between SsuE and SsuD and provide an approach to determine the locations and identities of specific amino acids involved in protein interactions. The trifunctional cross-linker cannot be used for the identification of amino acids involved in protein-protein interactions. The reagent does not link the SsuE and SsuD amino acids involved in binding, but separately captures proteins through reactive functional groups following complex formation.

Several cross-linking reagents were used to identify amino acid residues involved in protein-protein interactions between SsuE and SsuD. Two of the cross-linking reagents used, BS³ and EGS, are homobifunctional cross-linkers with spacer arm lengths

of 11.4 and 16.1 Å, respectively. Homobifunctional cross-linkers have the same reactive functional groups at both end of their arms that react with protein amino groups. The combination of EDC and sulfo-NHS are considered heterobifunctional cross-linking reagents with a zero length spacer arm that react with a carboxyl group of the first incubated protein and with an amino group of the second protein. Results from cross-linking experiments showed that only the combination of EDC and sulfo-NHS was able to covalently link SsuE and SsuD (Figure 3.18). The reaction order was important, since the cross-linking product could only be detected when SsuE was first reacted with the cross-linking reagents followed by SsuD. These results indicate that the amino acid residues of SsuE involved in protein cross-linking may involve acidic amino acid residues (Asp or Glu). Alternatively, basic amino acid residues of SsuD (Arg, His, or Lys) may be involved in protein-protein interactions. SsuE and SsuD proteins were unable to form a complex when SsuD was incubated first with the reagents followed by SsuE. The reactivity of BS³ and EGS with protein amino groups only may explain why there was no cross-linked product observed with these reagents. The fact that only a combination of EDC and sulfo-NHS were able to covalently cross-link SsuE and SsuD is an interesting result (Figure 3.18 and 3.19). Usually, the longer the spacer arm of the cross-linker, the greater the probability of forming protein complexes. This also increases the non-specific cross-linking between proteins, which is a disadvantage in the use of cross-linking reagents [160]. The most reliable information is derived from zero-length reagents that induce a direct covalent link between cross-linked sites as in the case of EDC and sulfo-NHS reagents. This has been shown by quantitative evaluation of the lengths of homobifunctional protein cross-linking reagents [161]. Similar results have

been shown by the stearyl-acyl carrier protein desaturase where the combination of EDC and sulfo-NHS cross-linking were able to covalently link the component of the protein complexes only in a specific incubation order [162]. Therefore, this result strongly suggests that the SsuE and SsuD complex formation occurs between carboxyl groups of SsuE and the amino groups of SsuD.

Despite the low amino acid sequence identity among the flavin reductases, they show a notable structural similarity. The crystal structure of *E. coli* flavin reductase, Fre, showed that the enzyme structure is similar to the structures of the ferredoxin reductase family, FNR [163]. Ferredoxin reductase is the prototype of a family of flavin-dependent reductases (more than 20 different enzymes) that function as transducers between nicotinamide dinucleotides (two-electron carriers) and one-electron carriers [164-168]. All of the members of the family display a two domain motif, the N-terminal (FAD-binding) domain and the C-terminal (NADP⁺-binding) domain [165-168]. A conserved RXXS sequence motif found in the Fre and FNR proteins is believed to be involved in flavin binding [164]. Two Gly residues located in the NAD(P)H binding site are conserved among the FNR family [163,164]. In addition, there are highly conserved regions within this family of enzymes that may be involved in substrate binding or protein interactions with the monooxygenase component although the latter has not been well established. Most flavin reductase superfamily members have a carboxylate side chain close to the edge of the isoalloxazine ring where the methyl groups are located [163]. In FNR, a catalytically important serine residue is hydrogen bonded to the carboxylate of a glutamate residue (Glu312 in spinach FNR and Glu301 in *Anabaena* FNR) [164]. Further studies indicated that substitution of this residue with alanine

resulted in a significant decrease in the observed electron-transfer rate between FNR and its substrates [169]. In FNR, this residue is exposed to the solvent and has been proposed to be catalytically involved in proton transfer coupled to electron transfer during catalysis. In Fre, the structurally homologous aspartate points in the direction of Ser49 and is close to one edge of the isoalloxazine ring [163]. To date, very limited structural information is known for SsuE. However, there are highly conserved regions found in Fre and FNR that are also found in SsuE.

In the case of SsuD, the reaction of its amino group with the amino reactive NHS ester of the cross-linker can be explained by exploring the three-dimensional structure of this protein. SsuD contains approximately 10% positively charged amino group residues and many of them are on the surface of SsuD adjacent to the putative active site. For example, an Arg297 residue is protruding on the enzyme surface flanking the flavin binding pocket (Figure 1.14A and 1.14B). Interestingly, this residue is highly conserved in all two-component monooxygenase enzymes [37,81,85,86]. In the *p*-hydroxyphenylacetate hydroxylase (HPAH) from *Acinetobacter baumannii*, Arg263 is believed to be involved in substrate binding [170]. Structural comparison of the HPAH in the presence and absence of reduced flavin and *p*-hydroxyphenylacetate (HPA), suggested that admission of HPA into the active site likely involves movement of the Arg263 side chain that directly interacts with the carboxylate group of HPA and act as a gate to the active site [170]. However, mutation analyses for the Arg263 of the HPAH have not been carried out. Amino acid substitutions of Arg297 of SsuD have been generated and are currently being analyzed to determine the role of this residue in protein interactions and flavin transfer.

The positive results obtained from cross-linking experiments were examined by MALDI-TOF MS to identify which amino acid residues were responsible for protein cross-linking. Unfortunately, the MALDI-TOF MS experiments failed to identify the amino acid residues involved in cross-linking. Both the undigested and digested cross-linking products were unable to be detected by this method. This might be due to the low amount of protein complex produced in the cross-linking experiments. The low amount of protein complex might be due to the instability of SsuE in the cross-linker activation buffer. In the experiment, the EDC and sulfo-NHS cross-linker are activated in a buffer solution at pH 6.0. Under these conditions, the SsuE protein was shown to precipitate during the course of the incubation. One way to overcome this obstacle is by using a cross-linking reagent that works similarly as EDC and sulfo-NHS that can be activated in a buffer solution with a higher pH to maintain the structural integrity of SsuE (~pH 7.5). Further studies are being performed to identify the role of specific amino acid residues that may be involved in protein-protein interactions.

4.4 The importance of protein-protein interactions for efficient flavin reduction and reduced flavin transfer

Previous results have shown that SsuE and SsuD proteins were able to form stable protein-protein interactions. Pre-steady state kinetic analyses utilizing stopped-flow spectroscopy were performed to investigate the effects of protein-protein interactions on SsuE-catalyzed reactions at 450 and 550 nm. The absorbance at 450 nm monitors flavin reduction, while the absorbance at 550 nm monitors charge transfer formation. A change in the rate for SsuE-catalyzed flavin reduction or charge transfer formation in the

presence of SsuD and/or its biological substrates, dioxygen and octanesulfonate, would indicate that protein-protein interactions affect the SsuE-catalyzed reaction. Results from single-wavelength studies at 450 nm showed that the rate of the third phase (k_3) increased 200-fold in the presence of SsuD compared to FMN reduction by SsuE alone while the rates for the first and second phase remain unaffected. The third phase was previously shown to represent the release of FMNH₂ or the binding of FMNH₂ by SsuD. This result is consistent with previous studies which showed that SsuD has a relatively strong binding affinity towards FMNH₂ [171]. These results also suggest that when SsuD is present the FMNH₂ is efficiently transferred to SsuD following flavin reduction by SsuE. In the absence of SsuD, FMNH₂ is released into the solution at a slower rate, and reacts with dioxygen under aerobic conditions generating reactive oxygen species. Thus, the overall reaction of FMN reduction has become less effective. These results support previous observations that protein-protein interactions are essential for efficient transfer and protection of FMNH₂ from autoxidation by dioxygen. Results from rapid reaction kinetic analyses at 550 nm showed that the presence of SsuD alone did not alter the formation of the charge-transfer complex. The charge-transfer complex has been observed in several flavin reductases such as Fre, a general flavin reductase from *E. coli*, phthalate dioxygenase reductase from *Pseudomonas cepacia*, and flavin reductase ActVB from *Streptomyces coelicolor* [160,172,173].

The effect of SsuD and its substrates on flavin reduction and charge transfer formation by SsuE was also investigated. Results from rapid reaction kinetic analyses showed that flavin reduction and charge transfer formation were affected in the presence of SsuD and substrates (Figure 3.29A and 3.29B). It was shown that the rate (k_2) for

charge transfer formation (CT-2) increased 10-fold. The increased rate of CT-2 only when SsuD, dioxygen and octanesulfonate are present indicates that the SsuE-catalyzed charge transfer formation is affected by the binding of dioxygen and octanesulfonate to SsuD. This suggests that the binding of dioxygen and octanesulfonate to SsuD may result in a conformational change that affects SsuE-catalyzed charge transfer formation. Similar experiments at 450 nm also showed a two-fold rate increase in k_2 , which correlates with the observed increase in k_2 at 550 nm. Interestingly, data analyses have shown that the third phase at 450 nm cannot be detected under these reaction conditions. The absence of a third phase at 450 nm further suggests that FMNH₂ is rapidly transferred to the SsuD active site in the fully coupled-system. In the coupled-enzyme system the FMNH₂ may be directly channeled to the SsuD active site eliminating the binding or release step. Alternatively, the flavin may be bound by both enzymes eliminating the binding step between FMNH₂ and SsuD. The altered kinetic properties of the SsuE-catalyzed reaction between the single and coupled-enzyme reaction may imply that in the coupled-enzyme system, the formation of a molecular channel between SsuE and SsuD eliminates the release step. This allows the FMNH₂ to be efficiently transferred and utilized for the desulfonation reaction of octanesulfonate by SsuD.

The mechanism for the substrate binding order in the SsuE-catalyzed reaction has been previously determined at 550 nm (Figure 4.2) [150]. Michaelis complex formation between NADPH, FMN, and SsuE (MC-1) occurs very rapidly before the first detectable step. The initial phase (k_1) represents the interaction of NADPH with FMN (CT-1) at 550 nm, and corresponds to the first phase (k_1) of flavin reduction at 450 nm. The second phase (k_2) at 550 nm represents the formation of a charge-transfer complex between

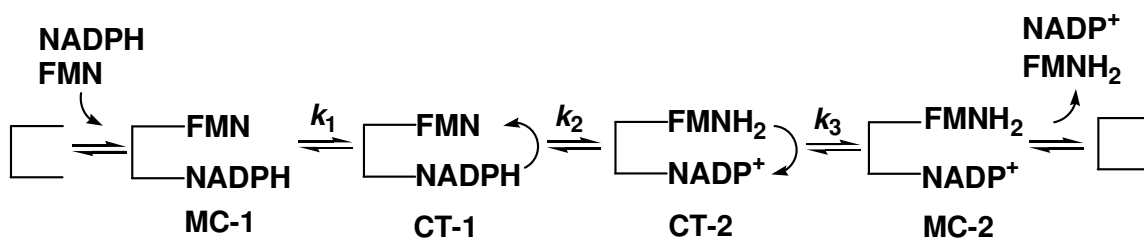


Figure 4.2. Charge-transfer complex of FMNH₂ and NADP⁺ [150].

FMNH₂ with NADP⁺ (CT-2). The formation of CT-2 was suggested to be the rate-determining step for flavin reduction by SsuE [150]. This corresponds to the actual flavin reduction step (k_2) at 450 nm. The third phase (k_3) at 550 nm represents a decay of the charge-transfer complex, and corresponds to the third phase (k_3) at 450 nm representing complete flavin reduction or the release of the FMNH₂ product.

Control experiments were performed to analyze whether changes in the rates of the SsuE-catalyzed reaction were due to the interaction of SsuD-bound substrates or the presence of the substrates only. It was previously reported that in *p*-hydroxyphenylacetate hydroxylase (HPAH) from *Acinetobacter baumannii* the kinetic of flavin reduction of the reductase is altered from two phases to one phase in the presence of *p*-hydroxyphenylacetate, the substrate for the oxygenase component [174]. This suggests that the substrate for the oxygenase alone affects the flavin reduction by the flavin reductase. Rapid reaction kinetic analyses were conducted in the presence of octanesulfonate but in the absence of SsuD to determine if octanesulfonate alone leads to the previously observed rate changes in flavin reduction by SsuE as shown in fully-coupled enzyme. The results showed that there were no notable rate changes in flavin reduction or charge transfer formation compared to the rates of flavin reduction or charge transfer formation by SsuE alone. Experiments were also performed in the presence of octanesulfonate and dioxygen but in the absence of SsuD to determine if both SsuD substrates would affect flavin reduction or charge transfer formation. The results showed that the SsuE-catalyzed reaction is not affected by the presence of octanesulfonate and dioxygen. Alternative experiments were also performed with SsuD and dioxygen in the absence of octanesulfonate or in the presence of SsuD and octanesulfonate without

dioxygen. The results showed that in both experiments, the rates of flavin reduction and charge transfer formation were not altered compared to the rates of flavin reduction or charge transfer formation by SsuE in the presence of SsuD alone. These results indicated that octanesulfonate and/or dioxygen in the absence of SsuD or the presence of SsuD in the absence of one of substrates did not affect the overall SsuE-catalyzed reaction as observed in fully-coupled enzyme system.

The rate increase in the second phase in the fully coupled-enzyme system suggests that the binding of dioxygen and octanesulfonate to SsuD affects the SsuE-catalyzed reaction. This binding may modulate flavin reduction at the SsuE active site through allosteric communication triggering the activation of the SsuE-catalyzed reaction. Previous results have shown that in the absence of reduced flavin, octanesulfonate alone is unable to bind to SsuD [171]. Interestingly, results from these studies show that the presence of SsuD, dioxygen, and octanesulfonate affect the SsuE-catalyzed flavin reduction. This suggests that in the presence of SsuE, dioxygen and octanesulfonate are able to bind to SsuD in the absence of reduced flavin. The binding of dioxygen and octanesulfonate may result in a conformational change that is transmitted to the active site of SsuE triggering flavin reduction. In the presence of dioxygen and octanesulfonate, the conformational change may lead to a more open conformation of the SsuD active site so it can readily accept reduced flavin from SsuE. Previous results have shown that in the presence of reduced flavin, the binding of substrates to SsuD results in a conformational change [171].

The rapid reaction kinetic results support the steady-state kinetic findings that the catalytic mechanism of SsuE is altered in the presence of SsuD [78]. A change in the

catalytic mechanism between a single enzyme and an enzyme-coupled reaction is often an indicator of protein channeling and allosteric communication [105]. The SsuD enzyme expressed in crude cell lysate is able to accept reduced flavins from other flavin reductases in addition to SsuE under normal cellular conditions suggesting that there is no specificity for flavin transfer between SsuE and SsuD [37]. However, it is not known if other flavin reductases are expressed to any significant level under sulfur starvation conditions. The SsuE and SsuD proteins are expressed under the control of the same operon during sulfur starvation providing SsuD with direct access to reduced flavin. Alternatively, the ability of monooxygenase enzymes from two-component systems to accept reduced flavin from oxidoreductases associated with other systems could suggest a common binding motif unique to this family of enzymes. Steady-state kinetic studies and fluorescence spectroscopy have also provided evidence for protein interactions between FMN reductase and bacterial luciferase from *Vibrio harveyi* [65]. The flavin reductases specific for bacterial luciferase show little amino acid sequence identity with SsuE. However, bacterial luciferase and SsuD show very similar overall structures even though they only possess 15% amino acid identity. Further analysis has shown that many of the conserved residues located in the active site of bacterial luciferase are also found in the putative active site of SsuD [85]. The conserved structural motif of these proteins may suggest that they share a common mechanism for flavin transfer between the reductase and oxygenase components.

Similar results supporting a substrate channeling mechanism and allosteric communication is found in tryptophan synthase from *Salmonella enterica* serovar *typhimurium*, where the metabolic intermediate (indole) is channeled from the active site

of the α subunit to the active site of the β subunit [140,175-177). The transfer of the indole intermediate is highly efficient such that the indole cannot be observed in a single enzyme turnover of the $\alpha\beta$ reaction. The reaction of serine with pyridoxal 5'-phosphate at the β site modulates the formation of indole at the α site or in the tunnel [178,179]. Allosteric communication and substrate channeling has also been well characterized in carbamoyl phosphate synthetase (CPS), a protein with three distinct active sites [144,180-183]. The nucleotide binding site within the N-terminal half of the large subunit is required for the phosphorylation of bicarbonate and formation of carbamate. The nucleotide binding site within the C-terminal domain of the large subunit catalyzes the phosphorylation of carbamate to the final product, carbamoyl phosphate. The ammonia produced within the active site of the small subunit is the substrate for reaction with the carboxy phosphate intermediate that is formed in the active site found within the N-terminal half of the large subunit of CPS. The formation of a molecular channel in this enzyme had been observed as an escape route for the ammonia intermediate. Here, ammonia is not released until carboxy phosphate is ready to form carbamate. Rapid-quench experiments indicated that during the synthesis of carbamoyl phosphate, the formation of carboxy phosphate triggers a conformational change that is transmitted to the small subunit where the hydrolysis of glutamine is stimulated [144,148]. The enhanced rate of ATPase in the presence of glutamine reflects the faster rate of attack on the carboxyl phosphate by the ammonia intermediate relative to water. [180].

Substrate channeling has become a recognized concept to explain the direct transfer of metabolites between sequential enzymes that often requires structural organization of the enzymes involved in the reactions [65,141,175,184,185]. Such

organization depends on the stability of protein-protein interactions. The association of enzymes may be substrate induced leading to a conformational change in the interacting enzymes. There are at least two different mechanisms where the intermediate can be transferred in metabolite channeling [181,186-189]. First, the intermediates can be covalently linked to a swinging arm and then gated via a tunnel through the interior of the acceptor protein. Second, a favorable electrostatic field between the adjacent active sites can be used to constrain the intermediate within the channeling path along the surface of the proteins. The structural analysis of the protein associations assembling the channeling complex requires detailed structural studies of the protein partners. The information obtained from these studies can be further utilized to observe any organizational changes of the protein complex.

As mentioned, the formation of a molecular channel has certain physiological advantages for cellular systems, including the protection of unstable intermediates from the solvent or breakdown due to side reactions during transfer [185]. It has been established that reduced flavin is a very reactive intermediate and is easily oxidized in the presence of molecular oxygen, generating species toxic to the cells. There are advantages for substrate channeling that are relevant to the properties of reduced flavin, including the protection of a reactive intermediate from the solvent, preventing the generation of toxic molecules such as hydrogen peroxide, oxygen or hydroxyl radical, and the improvement of catalytic efficiency [140,141,146,185]. In this study, the metabolite channeling mechanism for FMNH₂ from SsuE to SsuD enzymes is supported through rapid reaction kinetic analyses. The transfer of FMNH₂ is highly efficient such that the rate for this step cannot be detected in a single enzyme turnover reaction. In addition, the rapid reaction

kinetic studies also indicate that SsuE and SsuD showed an allosteric communication through the active sites of the proteins.

4.5 Conclusion

An increasing number of two-component flavin-dependent enzyme systems have been identified in bacterial species. Therefore, understanding the mechanism of reduced flavin transfer is extremely important. However, the principle governing the mechanism of reduced flavin transfer from the flavin reductase to the monooxygenase has not been well established. In this study, the mechanism of reduced flavin transfer in the alkanesulfonate monooxygenase was investigated through several approaches. The identification of stable protein-protein interactions was initially analyzed in these studies. The results from affinity chromatography and cross-linking experiments support the formation of a stable complex between the FMN reductase (SsuE) and monooxygenase (SsuD). Interactions between the two proteins do not lead to overall conformational changes in protein structure, as indicated by the results from circular dichroism spectroscopy in the far-UV region. However, subtle changes in the flavin environment of FMN-bound SsuE that occur in the presence of SsuD were identified by circular dichroism spectroscopy in the visible region. These data are supported by the results from fluorescent spectroscopy experiments, where a dissociation constant of $0.002 \mu\text{M} \pm 0.001 \mu\text{M}$ was obtained for the binding of SsuE to SsuD. Based on these studies, the stoichiometry for protein-protein interactions is proposed to involve a 1:1 monomeric association of SsuE with SsuD. [103]. Further studies were performed to determine if protein-protein interactions are essential for efficient reduced flavin transfer through

substrate channeling and allosteric communication. Results from rapid reaction kinetic analyses have shown that the SsuE-catalyzed reaction is affected by the binding of dioxygen and octanesulfonate to SsuD, providing additional evidence that the active sites of SsuE and SsuD enzymes are involved in allosteric communication. In coupled-enzyme system, the rate of SsuE-catalyzed FMN reduction at 450 nm changed from a triple to a double exponential due to rapid reduced flavin transfer to SsuD, and the rate of charge transfer formation (CT-2) at 550 nm increased 10-fold. In summary, the results from these studies have shown that protein-protein interactions between SsuE and SsuD occur and such interactions are essential for direct reduced flavin transfer. Furthermore, the active sites of SsuE and SsuD proteins are involved in allosteric communication which alters the mechanism of flavin reduction.

The alkanesulfonate monooxygenase system is an excellent model to study the mechanism of reduced flavin transfer due to the unique characteristics and function of this enzyme system. First, this enzyme system utilizes flavin as a cosubstrate rather than a tightly bound prosthetic group. Second, the enzyme system is composed of two distinct proteins that are cooperatively involved in a consecutive reaction that makes this enzyme system ideal model to study allosteric communication between the two active sites. Third, the mechanism of C-S bond cleavage of organosulfur compounds for sulfur assimilation is distinct from the C-S bond cleavage of organosulfur for utilization of carbon as energy sources in bacteria. Overall, the fact that this enzyme system is synthesized only during sulfur starvation indicates that the enzyme system has a novel mechanism and function.

REFERENCES

- [1] **Kertesz, M. A.** 1999. Riding the sulfur cycle-metabolism of sulfonates and sulfate esters in gram-negative bacteria. *FEMS Microbiol. Rev.* **24**:135-175.
- [2] **Brosnan, J. T., and M. E. Brosnan.** 2006. The sulfur-containing amino acids: an overview. *J. Nutr.* **136**:1636s-1640s.
- [3] **Levine, R. L., L. Mosoni, B. S. Berlett, and E. R. Stadtman.** 1996. Methionine residues as endogenous antioxidants in proteins. *Proc. Natl. Acad. Sci. USA* **93**:15036-15040.
- [4] **Moskovitz J.** 2005. Methionine sulfoxide reductases: ubiquitous enzymes involved in antioxidant defense, protein regulation, and prevention of aging-associated diseases. *Biochim. Biophys. Acta* **1703**:213-219.
- [5] **Stipanuk, M.** 2004. Sulfur amino acid metabolism: pathways for production and removal of homocysteine and cysteine. *Annu. Rev. Nutr.* **24**:539-577.
- [6] **Moran L. K., J. M. C. Gutteridge, and G. J. Quinlan.** 2001. Thiols in cellular redox signalling and control. *Curr. Med. Chem.* **8**:763-772(10).
- [7] **Meister, A.** 1994. Glutathione, ascorbate, and cellular protection. *Cancer Res.* **54**:1969s-1975s.
- [8] **John, H., and L. McLellan.** 1999. Glutathione and glutathione-dependent enzymes represent a co-ordinately regulated defence against oxidative stress. *Free Radic. Res.*

31:273-300(28).

[9] **Cotgreave, I. A., and R. G. Gerdes.** 1998. Recent trends in glutathione biochemistry-glutathione-protein interactions: A molecular link between oxidative stress and cell proliferation? *Biochem. Biophys. Res. Commun.* **242**:1-9.

[10] **Galter, D., S. Mihm, and W. Dröge.** 1994. Distinct effects of glutathione disulphide on the nuclear transcription factors κ B and the activator protein-1. *Eur J. Biochem.* **221**:639-648.

[11] **Jakobsson, P.-J., S. Thorén, R. Morgenstern, and B. Samuelsson.** 1999. Identification of human prostaglandin E synthase: A microsomal, glutathione-dependent, inducible enzyme, constituting a potential novel drug target. *Proc. Natl. Acad. Sci. USA* **96**:7220-7225.

[12] **Lopes, S., A. Jurisicova, J.-G. Sun, and R. F. Casper.** 1998. Reactive oxygen species: potential cause for DNA fragmentation in human spermatozoa. *Human Reproduct.* **13**:896-900.

[13] **Stipanuk, M. H.** 2004. Role of the liver in regulation of body cysteine and taurine levels: A brief review. *Neurochem. Res.* **29**:105-110.

[14] **Sturman, J. A.** 1986. Nutritional taurine and central nervous system development. *Ann. NY. Acad. Sci.* **477**:196-213.

[15] **Cammarata, P. R., G. Schafer, S. W. Chen, Z. Guo, and R. E. Reeves.** 2002. Osmoregulatory alterations in taurine uptake by cultured human and bovine lens epithelial cells. *Invest. Ophthalmol. Vis. Sci.* **43**:425-433.

[16] **Uchida, S., H. M. Kwon, A. Yamauchi, A. S. Preston, F. Marumo, and J. S. Handler.** 1992. Molecular cloning of the cDNA for an MDCK cell Na^+ - and

Cl⁻-dependent taurine transporter that is regulated by hypertonicity. Proc. Natl. Acad. Sci. USA **89**:8230-8234.

[17] **Kang, Y. S., S. Ohtsuki, H. Takanaga, M. Tomi, K. Hosoya, and T. Terasaki.** 2002. Regulation of taurine transport at the blood–brain barrier by tumor necrosis factor- α , taurine and hypertonicity. J. Neurochem. **83**:1188-1195.

[18] **Janeke, G., W. Siefken, S. Carstensen, G. Springmann, O. Bleck, H. Steinhart, P. Höger, K.-P. Wittern, H. Wenck, F. Stäb, G. Sauermann, V. Schreiner, and T. Doering.** 2003. Role of taurine accumulation in keratinocyte hydration. J. Invest. Dermatol. **121**:354-361.

[19] **Pasantes-Morales, H., C. E. Wright, G. E. Gaull.** 1985. Taurine protection of lymphoblastoid cells from iron-ascorbate induced damage. Biochem. Pharmacol. **34**:2205-2207.

[20] **Oja, S. S., and P. Saransaari.** 1996. Taurine as osmoregulator and neuromodulator in the brain. Metab. Brain. Dis. **11**:153-164.

[21] **Xu, Y. X., A. Wagenfeld, C. H. Yeung, W. Lehnert, and T. G. Cooper.** 2003. Expression and location of taurine transporters and channels in the epididymis of infertile c-ros receptor tyrosine kinase-deficient and fertile heterozygous mice. Mol. Reprod. Dev. **64**:144-151.

[22] **Heafield, M. T., S. Fearn, G. B. Steventon, R. H. Waring, A. C. Williams, S. G. Sturman.** 1990. Plasma cysteine and sulphate levels in patients with motor neurone, Parkinson's and Alzheimer's disease. Neurosci. Lett. **110**:216-220.

[23] **Dorszewska J., J. Florczak, A. Rozycka, B. Kempisty, J. Jaroszevska-Kolecka, K. Chojnacka, W. H. Trzeciak, and W. Kozubski.** 2007. Oxidative DNA damage and

level of thiols as related to polymorphisms of MTHFR, MTR, MTHFD1 in Alzheimer's and Parkinson's diseases. *Acta. Neurobiol. Exp. (Wars)*. **67**:113-129.

[24] **Cooper, A. J. L.** 1983. Biochemistry of sulfur-containing amino acids. *Ann. Rev. Biochem.* **52**:187-222.

[25] **Giovanelli, J., S. H. Mudd, and A. M. Datko.** 1980. Natural sulfur compounds: novel biochemical and structural aspects. New York: Plenum, pp. 81-92.

[26] **Krebs, H.A., R. Hems, and B. Tyler.** 1976. The regulation of folate and methionine metabolism. *Biochem J.* **158**:341-353.

[27] **Wakil, S. J.** 1989. Fatty acid synthase, a proficient multifunctional enzyme. *Biochemistry* **28**:4523-4530.

[28] **Wakil, S. J., J. K. Stoops, and C. V. Joshi.** 1983. Fatty Acid Synthesis and its Regulation. *Ann. Rev. Biochem.* **52**:537-579.

[29] **Mattevi, A., A. de Kok, and R. N. Perham.** 1992. The pyruvate dehydrogenase multienzyme complex. *Curr. Opin. Struct. Biol.* **2**:877-887.

[30] **Thauer, R. K.** 1998. "Biochemistry of methanogenesis: a tribute to Marjory Stephenson". *Microbiology* **144**:2377-2406.

[31] **Utter, M. F., and D. B. Keech.** 1960. Formation of Oxaloacetate from Pyruvate and CO₂. *J. Biol. Chem.* **235**:17-18.

[32] **Owen, O. E., M. S. Patel, B. S. B. Block, T. H. Kreulen, F. A. Reichle, and M. A. Mozzoli.** 1976. In *Gluconeogenesis* (Hanson, R. W. and Mehlman, M. A., eds.) pp.533-558, John Wiley & Sons, New York.

[33] **Knowles, J. R.** 1989. The Mechanism of Biotin-Dependent Enzymes. *Ann. Rev. Biochem.* **58**:195-221.

- [34] **Reed, L. J., B. G. DeBusk, I. C. Gunsalus, and C. S. Hornberger Jr.** 1951. "Crystalline alpha-lipoic acid; a catalytic agent associated with pyruvate dehydrogenase". *Science* **114**:93-94.
- [35] **Johnson, D. C., D. R. Dean, A. D. Smith, and M. K. Johnson.** 2005. Structure, function, and formation of biological iron-sulfur clusters. *Annu. Rev. Biochem.* **74**:247-281.
- [36] **Ding, H., and R. J. Clark.** 2004. Characterization of iron binding in IscA, an ancient iron-sulphur cluster assembly protein. *Biochem J.* **379**:433-440.
- [37] **van der Ploeg, J. R., E. Eichhorn, and T. Leisinger.** 2001. Sulfonate-sulfur metabolism and its regulation in *Escherichia coli*. *Arch. Microbiol.* **176**:1-8.
- [38] **Thomas, D., R. Barbey, and Y. Surdin-Kerjan.** 1990. Gene-enzyme relationship in the sulfate assimilation pathway of *Saccharomyces cerevisiae*. Study of the 3'-phosphoadenylylsulfate reductase structural gene. *J. Biol. Chem.* **265**:15518-15524.
- [39] **Perna, N. T., G. Plunkett, III, V. Burland, B. Mau, J. D. Glasner, D. J. Rose, G. F. Mayhew, P. S. Evans, J. Gregor, H. A. Kirkpatrick, G. Pósfai, J. Hackett, S. Klink, A. Boutin, Y. Shao, L. Miller, E. J. Grotbeck, N. W. Davis, A. Lim, E. T. D., K. D. Potamosis, J. Apodaca, T. S. Anantharaman, J. Lin, G. Yen, D. C. Schwartz, R. A. Welch, and F. R. Blattner.** 2001. Genome sequence of enterohaemorrhagic *Escherichia coli* O157:H7. *Nature* **409**:529-533.
- [40] **Hayashi, T., K. Makino, M. Ohnishi, K. Kurokawa, K. Ishii, K. Yokoyama, C.-G. Han, E. Ohtsubo, K. Nakayama, T. Murata, M. Tanaka, T. Tobe, T. Iida, H. Takami, T. Honda, C. Sasakawa, N. Ogasawara, T. Yasunaga, S. Kuhara, T. Shiba, M. Hattori, and H. Shinagawa.** 2001. Complete genome sequence of

enterohemorrhagic *Escherichia coli* O157:H7 and genomic comparison with a laboratory strain K-12. *DNA Res.* **8**:11-22.

[41] **Sirko, A., M. Hryniewicz, D. Hulanicka, and A. Böck.** 1990. Sulfate and thiosulfate transport in *Escherichia coli* K-12: nucleotide sequence and expression of the *cysTWAM* gene cluster. *J. Bacteriol.* **172**:3351-3357.

[42] **Roberts, R. B., P. H. Abelson, D. B. Cowie, E. T. Bolton, and R. J. Britten (Eds.).** 1955. Sulfur metabolism. pp. 318-405. Carnegie Institution, Washington D. C.

[43] **Eichhorn, E., J. R. van der Ploeg, M. A. Kertesz, and T. Leisinger.** 1997. Characterization of α -Ketoglutarate-dependent Taurine Dioxygenase from *Escherichia coli* *J. Biol. Chem.* **272**:23031-23036.

[44] **Hummerjohann, J., E. Kuttel, M. Quadroni, J. Ragaller, T. Leisinger, and M. A. Kertesz.** 1998. Regulation of the sulfate starvation response in *Pseudomonas aeruginosa*: role of cysteine biosynthetic intermediates. *Microbiology* **144**:1375-1386.

[45] **Kertesz, M.A., T. Leisinger, and A. M. Cook.** 1993. Proteins induced by sulfate limitation in *Escherichia coli*, *Pseudomonas putida*, or *Staphylococcus aureus*. *J. Bacteriol.* **175**:1187-1190.

[46] **Quadroni, M., W. Staudenmann, M. Kertesz, and P. James.** 1996. Analysis of global responses by protein and peptide fingerprinting of proteins isolated by two-dimensional gel electrophoresis. Application to the sulfate-starvation response of *Escherichia Coli*. *Eur. J. Biochem.* **239**:773-781.

[47] **Dainese, P., W. Staudenmann, M. Quadroni, C. Korostensky, G. Gonnet, M. Kertesz, and P. James.** 1997. Probing protein function using a combination of gene knockout and proteome analysis by mass spectrometry. *Electrophoresis* **18**:432-442.

- [48] **Quadroni, M., P. James, P. Dainese-Hatt, and M. A. Kertesz.** 1999. Proteome mapping, mass spectrometric sequencing and reverse transcription-PCR for characterization of the sulfate starvation-induced response in *Pseudomonas aeruginosa* PAO1. Eur. J. Biochem. **266**:986-996.
- [49] **Cook, A. M., H. Laue, and R. Junker.** 1999. Microbial desulfonation. FEMS Microbiol. Rev. **22**:399-419.
- [50] **Linton, K. J., and C. F. Higgins.** 1998. The *Escherichia coli* ATP-binding cassette (ABC) proteins. Mol. Microbiol. **28**:5-13.
- [51] **van der Ploeg, J. R., M. A. Weiss, E. Saller, H. Nashimoto, N. Saito, M.A. Kertesz, and T. Leisinger.** 1996. Identification of sulfate starvation-regulated genes in *Escherichia coli*: a gene cluster involved in the utilization of taurine as a sulfur source. J. Bacteriol. **178**:5438-5446.
- [52] **van der Ploeg, J. R., R. Iwanicka-Nowicka, M. A. Kertesz, T. Leisinger, and M. M. Hryniewicz.** 1997. Involvement of CysB and Cbl regulatory proteins in expression of the tauABCD operon and other sulfate starvation-inducible genes in *Escherichia coli* J. Bacteriol. **179**:7671-7678.
- [53] **van der Ploeg, J. R., R. Iwanicka-Nowicka, T. Bykowski, M. M. Hryniewicz, and T. Leisinger.** 1999. The *Escherichia coli* *ssuEADCB* gene cluster is required for the utilization of sulfur from aliphatic sulfonates and is regulated by the transcriptional activator Cbl. J. Biol. Chem. **274**:29358-29365.
- [54] **Eichhorn, E., J. R. van der Ploeg, and T. Leisinger.** 1999. Characterization of a two-component alkanesulfonate monooxygenase from *Escherichia coli*. J. Biol. Chem. **274**:26639-26646.

- [55] **Iwanicka-Nowicka, R., and M. M. Hryniewicz.** 1995. A new gene, *cbl*, encoding a member of the LysR family of transcriptional regulators belongs to *Escherichia coli* *cys* regulon. *Gene* **166**:11-17.
- [56] **Kredich, N. M.** 1996. Biosynthesis of cystein. In: *Escherichia coli* and *Salmonella*, 2nd edn. (F. C. Neidhardt, R. Curtiss, J. L. Ingraham, E. C. C. Lin, K. B. Low, B. Magasanik, W. S. Reznikoff, M. Riley, M. Schaechter, and H. E. Umbarger, Eds.), pp 514-527. ASM Press, Washington DC.
- [57] **Tyrrell, R., K. H. G. Verschueren, E. J. Dodson, G. N. Murshudov, C. Addy, and A. J. Wilkinson.** 1997. The structure of the cofactor-binding fragment of the LysR family member, CysB: a familiar fold with a surprising subunit arrangement. *Structure* **5**:1017-1032.
- [58] **Blyth, A. W.** 1879. The composition of cows' milk in health and disease. *J. Chem. Soc., Trans.* **35**:530 – 539.
- [59] **Meah, Y., and V. Massey.** 2000. Old yellow enzyme: stepwise reduction of nitroolefins and catalysis of aci-nitro tautomerization. *Proc. Natl. Acad. Sci.* **97**:10733-10738.
- [60] "**Theorell, Axel Hugo Teodor.**" *Encyclopaedia Britannica*. 2007. *Encyclopaedia Britannica Online*. 10 Sept. 2007.
- [61] **Muller, F.,** Ed. 1990-1992. *Chemistry and biochemistry of flavoenzymes*. CRC Press: Boca Raton, Vols. 1-3.
- [62] **Massey, V., and G. Palmer.** 1966. On the existence of spectrally distinct classes of flavoprotein semiquinones. A new method for the quantitative production of flavoprotein semiquinones. *Biochemistry* **5**:3181-3189.

- [63] **Massey, V.** 2000. The Chemical and biological versatility of riboflavin. *Biochem. Soc. Trans.* **28**:283-296.
- [64] **Murataliev, M. B.** 1999. Application of electron spin resonance (ESR) for detection and characterization of flavoprotein. In: *Flavoprotein protocols* (S. K. Chapman, and G. A. Reid. Eds.) **131**:97-101. Humana Press Inc. Totowa, New Jersey.
- [65] **Tu, S.-C.** 2001. Reduced flavin: donor and acceptor enzymes and mechanisms of channeling. *Antioxid. Redox Signal.* **3**:881–897.
- [66] **Walsh, C.** 1978. Chemical approaches to the study of enzymes catalyzing redox transformations. *Ann. Rev. Biochem.* **47**:881-931.
- [67] **Fontecave, M., J. Coves, and J. L. Pierre.** 1994. Ferric reductases or flavin reductases? *Biometals* **7**:3-8.
- [68] **Covès, J., B. Delon, I. Climent, B.-M. Sjöberg, and M. Fontecave.** 1995. Enzymic and chemical reduction of the iron center of the *Escherichia coli* ribonucleotide reductase protein R2. The role of the C-terminus. *Eur. J. Biochem.* **233**:357-363.
- [69] **Fontecave, M., R. Eliasson, and P. Reichard.** 1989. Enzymatic regulation of the radical content of the small subunit of *Escherichia coli* ribonucleotide reductase involving reduction of its redox centers. *J. Biol. Chem.* **264**:9164-9170.
- [70] **Nivière, V., M. A. Vanoni, G. Zanetti, and M. Fontecave.** 1998. Reaction of the NAD(P)H:flavin oxidoreductase from *Escherichia coli* with NADPH and riboflavin: identification of intermediates. *Biochemistry* **37**:11879-11887.
- [71] **Nivière, V., F. Fieschi, J.-L. Décout, and M. Fontecave.** 1999. The NAD(P)H:flavin oxidoreductase from *Escherichia coli*. Evidence for a new mode of binding for reduced pyridine nucleotides. *J. Biol. Chem.* **274**:18252-18260.

- [72] **Ballou, D. P.** 1984. Flavoprotein monooxygenases. In: Flavin and flavoproteins (R. C. Bray, P. C. Engel, and S. G. Mayhew, Eds.), pp. 605-618.
- [73] **Massey, V.** 1994. Activation of molecular oxygen by flavins and flavoproteins. *J. Biol. Chem.* **269**:22459-22462.
- [74] **Ballou, D. P., B. Entsch, and L. J. Cole.** 2005. Dynamics involved in catalysis by single-component and two-component flavin-dependent aromatic hydroxylases. *Biochem. Biophys. Res. Commun.* **338**:590-598.
- [75] **Valton, J., L. Filisetti, M. Fontecave, and V. Nivière.** 2004. A two-component flavin-dependent monooxygenase involved in actinorhodin biosynthesis in *Streptomyces coelicolor*. *J. Biol. Chem.* **279**:44362-44369.
- [76] **Thibaut, D., N. Ratet, D. Bisch, D. Faucher, L. Debussche, and F. Blanche.** 1995. Purification of the two-enzyme system catalyzing the oxidation of the D-proline residue of pristinamycin IIB during the last step of pristinamycin IIA biosynthesis *J. Bacteriol.* **177**:5199-5205.
- [77] **Gisi, M. R., and L. Xun.** 2003. Characterization of chlorophenol 4-monooxygenase (TftD) and NADH:flavin adenine dinucleotide oxidoreductase (TftC) of *Burkholderia cepacia* AC1100. *J. Bacteriol.* **185**:2786-2792.
- [78] **Gao, B., and H. R. Ellis.** 2005. Altered mechanism of the alkanesulfonate FMN reductase with the monooxygenase enzyme. *Biochem. Biophys. Res. Commun.* **331**:1137-1145.
- [79] **Fieschi, F., V. Nivière, C. Frier, J.-L. Décout, and M. Fontecave.** 1995. The mechanism and substrate specificity of the NADPH:flavin oxidoreductase from *Escherichia coli*. *J. Biol. Chem.* **270**:30392-30400.

- [80] **Bruns, C. M., and P. A. Karplus.** 1995. Refined crystal structure of spinach ferredoxin reductase at 1.7 Å resolution: oxidized, reduced and 2'-phospho-5'-AMP bound states. *J. Mol. Biol.* **247**:125-145.
- [81] **Eichhorn, E., C. A. Davey, D. F. Sargent, T. Leisinger, and T. J. Richmond.** 2002. Crystal structure of *Escherichia coli* alkanesulfonate monooxygenase SsuD. *J. Mol. Biol.* **324**:457-468.
- [82] **Thibaut, D., N. Ratet, D. Bisch, D. Faucher, L. Debussche, and F. Blanche.** 1995. Purification of the two-enzyme system catalyzing the oxidation of the D-proline residue of pristinamycin IIB during the last step of pristinamycin IIA biosynthesis. *J. Bacteriol.* **177**:5199-5205.
- [83] **Uetz, T., R. Schneider, M. Snozzi, and T. Egli.** 1992. Purification and characterization of a two-component monooxygenase that hydroxylates nitrilotriacetate from "*Chelatobacter*" strain ATCC 29600. *J. Bacteriol.* **174**:1179-1188.
- [84] **Farber, G. K., and G. A. Petsko.** 1990. The evolution of α/β barrel enzymes *Trends. Biochem. Sci.* **15**:228-234.
- [85] **Fisher, A. J., T. B. Thompson, J. B. Thoden, T. O. Baldwin, and I. Rayment.** 1996. The 1.5-Å resolution crystal structure of bacterial luciferase in low salt conditions. *J. Biol. Chem.* **271**:21956-21968.
- [86] **Shima, S., E. Warkentin, W. Grabarse, M. Sordel, M. Wicke, R. K. Thauer and U. Ermler.** 2000. Structure of coenzyme F₄₂₀ dependent methylenetetrahydromethanopterin reductase from two methanogenic archaea. *J. Mol. Biol.* 2000. **300**:935-950.
- [87] **Reichenbecher, W., and J. C. Murrell.** 1999. Linear alkanesulfonates as carbon

and energy sources for gram-positive and gram-negative bacteria. Arch.Microbiol. **171**:430-438.

[88] **Kertesz, M. A.** 1996. Desulfonation of aliphatic sulfonates by *Pseudomonas aeruginosa* PAO. FEMS Microbial. Lett. **137**:221-225.

[89] **Chikuba, K., T. Yubisui, K. Shirabe, and M. Takeshita.** 1994. Cloning and nucleotide sequence of a cDNA of the human erythrocyte NADPH-flavin reductase. Biochem. Biophys. Res. Commun. **198**:1170-1176.

[90] **Gaudu, P., D. Touati, V. Niviere, and M. Fontecave.** 1994. The NAD(P)H:flavin oxidoreductase from *Escherichia coli* as a source of superoxide radicals J. Biol. Chem. **269**:8182-8188.

[91] **Covès, J., B. Delon, I. Climent, B.-M. Sjöberg, and M. Fontecave.** 1995. Enzymic and chemical reduction of the iron center of the *Escherichia coli* ribonucleotide reductase protein R2. The role of the C-terminus. Eur. J. Biochem. **233**:357-363.

[92] **Fontecave, M., R. Eliasson, and P. Reichard.** 1987. NAD(P)H:flavin oxidoreductase of *Escherichia coli*. A ferric iron reductase participating in the generation of the free radical of ribonucleotide reductase. J. Biol. Chem. **262**: 12325-12331.

[93] **Fontecave, M., R. Eliasson, and P. Reichard.** 1989. Enzymatic regulation of the radical content of the small subunit of *Escherichia coli* ribonucleotide reductase involving reduction of its redox centers. J. Biol. Chem. **264**:9164-9170.

[94] **Imlay, J. A.** 2003. Pathways of oxidative damage. Annu. Rev. Microbiol. **57**:395-418.

[95] **Eberlein, G., and T. C. Bruice.** 1983. The chemistry of a 1,5-diblocked flavin. 2. Proton and electron transfer steps in the reaction of dihydroflavins with oxygen. J. Am.

Chem. Soc. **105**:6685-6697.

[96] **Cabiscol E., J. Tamarit, and J. Ros.** 2000. Oxidative stress in bacteria and protein damage by reactive oxygen species. *Inter. Microbiol.* **3**:3-8.

[97] **Gibson, Q. H., and J. W. Hasting.** 1962. The oxidation of reduced flavin mononucleotide by molecular oxygen. *Biochem. J.* **83**:368-377.

[98] **Massey, V., S. Strickland, S. G. Mayhew, L. G. Howell, P. C. Engel, R. G. Matthews, M. Schuman, and P. A. Sullivan.** 1969. The production of superoxide anion radicals in the reaction of reduced flavins and flavoproteins with molecular oxygen. *Biochem. Biophys. Res. Commun.* **36**:891-97.

[99] **Messner, K. R., and J. A. Imlay.** 1999. The identification of primary sites of superoxide and hydrogen peroxide formation in the aerobic respiratory chain and sulfite reductase complex of *Escherichia coli*. *J. Biol. Chem.* **274**:10119-10128.

[100] **Louie, T. M., X. S. Xie, and L. Xun.** 2003. Coordinated production and utilization of FADH₂ by NAD(P)H-flavin oxidoreductase and 4-hydroxyphenylacetate 3-monooxygenase. *Biochemistry* **42**:7509–7517.

[101] **Galán, B., E. Díaz, M. A. Prieto, and J. L. García.** 2000. Functional analysis of the small component of the 4-hydroxyphenylacetate 3-monooxygenase of *Escherichia coli* W: a prototype of a new flavin:NAD(P)H reductase subfamily. *J. Bacteriol.* **182**:627-636.

[102] **Valton, J., L. Filisetti, M. Fontecave, and V. Nivière.** 2004. A two-component flavin-dependent monooxygenase involved in actinorhodin biosynthesis in *Streptomyces coelicolor*. *J. Biol. Chem.* **279**:44362-44369.

- [103] **Abdurachim, K., and H. R. Ellis.** 2006. Detection of protein-protein interactions in the alkanesulfonate monooxygenase system from *Escherichia coli*. *J. Bacteriol.* **188**:8153-8159.
- [104] **Jeffers, C. E., and S.-C. Tu.** 2001. Differential transfers of reduced flavin cofactor and product by bacterial flavin reductase to luciferase. *Biochemistry* **40**:1749-1754.
- [105] **Jeffers, C. E., J. C. Nichols, and S.-C. Tu.** 2003. Complex formation between *Vibrio harveyi* luciferase and monomeric NADPH:FMN oxidoreductase. *Biochemistry* **42**:529-534.
- [106] **Lei, B., and S.-C. Tu.** 1998. Mechanism of reduced flavin transfer from *Vibrio harveyi* NADPH-FMN oxidoreductase to luciferase. *Biochemistry* **37**:14623–14629.
- [107] **Kantz, A., F. Chin, N. Nallamotheu, T. Nguyen, and G. T. Gassner.** 2005. Mechanism of flavin transfer and oxygen activation by the two-component flavoenzyme styrene monooxygenase. *Arch. Biochem. Biophys.* **442**:102–116.
- [108] **Jones, S., and J. M. Thornton.** 1996. Principles of protein-protein interactions. *Proc. Natl. Acad. Sci.* **93**:13-20.
- [109] **Phizicky, E. M., and S. Fields.** 1995. Protein-protein interactions: methods for detection and analysis. *Microbiol. Rev.* **59**:94-123.
- [110] **Bogan, A. A., and K. S. Thorn.** 1998. Anatomy of hot spots in protein interfaces. *J. Mol. Biol.* **280**:1-9.
- [111] **Johnson, J. E.** 1996. Functional implications of protein-protein interactions in icosahedral viruses. *Proc. Natl. Acad. Sci.* **93**:27-33.
- [112] **Finzel, B. C., P. C. Weber, K. D. Hardman, and F. R. Salemme.** 1985. Structure of ferricytochrome *c'* from *Rhodospirillum rubrum* at 1.67 Å resolution. *J. Mol.*

Biol. **186**:627-643.

[113] **Daviss, B.** 2005. "Growing pains for metabolomics." *The Scientist*. **19**:25-28.

[114] **Tsunogae, Y., I. Tanaka, T. Yamane, J. Kikkawa, T. Ashida, C. Ishikawa, K. Watanabe, S. Nakamura, and K. Takahashi.** 1986. Structure of the trypsin-binding domain of Bowman-Birk type protease inhibitor and its interaction with trypsin. *J. Biochem. (Tokyo)* **100**:1637-1646.

[115] **Sheriff, S., E. W. Silverton, E. A. Padlan, G. H. Cohen, S. J. Smith-Gill, B. C. Finzel, and D. R. Davies.** 1987. Three-dimensional structure of an antibody-antigen complex. *Proc. Natl. Acad. Sci.* **84**:8075-8092.

[116] **Keskin, O., B. Ma, and R. Nussinov.** 2005. Hot regions in protein-protein interactions: the organization and contribution of structurally conserved hot spot residues. *J. Mol. Biol.* **345**:1281-1294.

[117] **Keskin, O., C.-J. Tsai, H. Wolfson, and R. Nussinov.** 2004. A new, structurally nonredundant, diverse data set of protein-protein interfaces and its implications. *Protein Sci.* **13**:1043-1055.

[118] **Tsai, C.-J., S. L. Lin, H. J. Wolfson, and R. Nussinov.** 1996. A dataset of protein-protein interfaces generated with a sequence-order-independent comparison technique. *J. Mol. Biol.* **260**:604-620.

[119] **Janin, J.** 1997. Specific versus non-specific contacts in protein crystals. *Nature. Struct. Biol.* **4**:973-974.

[120] **Horton, N., and M. Lewis.** 1992. Calculation of the free energy of association for protein complexes. *Protein Sci.* **1**:169-181.

[121] **Chothia, C., and J. Janin.** 1975. Principles of protein-protein recognition. *Nature*

256:705-708.

[122] **Janin, J., and C. Chothia.** 1990. The structure of protein-protein recognition sites. *J. Biol. Chem.* **265:16027-16030.**

[123] **Clackson, T., and J. A. Wells.** 1995. A hot spot of binding energy in a hormone-receptor interface. *Science* **267:383-386.**

[124] **Cunningham, B. C., and J. A. Wells.** 1991. Rational design of receptor-specific variants of human growth hormone. *Proc. Natl. Acad. Sci.* **88:3407-3411.**

[125] **Tsai, C. J., S. L. Lin, H. J. Wolfson, and R. Nussinov.** 1997. Studies of protein-protein interfaces: A statistical analysis of the hydrophobic effect. *Protein Sci.* **6:53-64.**

[126] **Ma, B., T. Elkayam, H. Wolfson, and R. Nussinov.** 2003. Protein-protein interactions: structurally conserved residues distinguish between binding sites and exposed protein surfaces. *Proc. Natl. Acad. Sci.* **100:5772-5777.**

[127] **Lee, B., and F. M. Richards.** 1971. The interpretation of protein structures: estimation of static accessibility. *J. Mol. Biol.* **55:379-380.**

[128] **Jones, S., and M. Janet.** 1995. Protein-protein interactions: a review of protein dimer structures. *Prog. Biophys. Mol. Biol.* **63:31-59.**

[129] **Chothia, C.** 1974. Hydrophobic bonding and accessible surface area in proteins. *Nature (London)* **248:338-339.**

[130] **Vakser, I. A., C. Aflalo.** 1994. Hydrophobic docking: A proposed enhancement to molecular recognition techniques. *Proteins: Struct. Funct. Genet.* **20: 320-329.**

[131] **Lawrence, M. C., and P. M. Colman.** 1993. Shape complementarity at protein/protein interfaces. *J. Mol. Biol.* **234:946-950.**

- [132] **Janin, J., S. Miller, and C. Chothia.** 1988. Surface, subunit interfaces and interior of oligomeric proteins. *J. Mol. Biol.* **204**:155-164.
- [133] **Lee, F. S., D. S. Auld, and B. L. Vallee.** 1989. Tryptophan fluorescence as a probe of placental ribonuclease inhibitor binding to angiogenin. *Biochemistry* **28**:219-224.
- [134] **Lee, F. S., R. Shapiro, and B. L. Vallee.** 1989. Tight-binding inhibition of angiogenin and ribonuclease A by placental ribonuclease inhibitor. *Biochemistry* **28**:225-230.
- [135] **Shapiro, R., and B. L. Vallee.** 1991. Interaction of human placental ribonuclease with placental ribonuclease inhibitor. *Biochemistry* **30**:2246-2255.
- [136] **Spivey, H. O., and J. Ovadi.** 1999. Substrate channeling. *Methods* **19**:306-321.
- [137] **Anderson, K. S.** 1999. Fundamental mechanisms of substrate channeling. *Methods Enzymol.* **308**:111-145.
- [138] **Srere, P. A.** 1987. Complexes of sequential metabolic enzymes. *Annu. Rev. Biochem.* **56**:89-124.
- [139] **Easterby, J. S.** 1981. A generalized theory of the transition time for sequential enzyme reactions. *Biochem J.* **199**:155-161.
- [140] **Westerhoff, H. V., and G. R. Welch.** 1992. Enzyme organization and the direction of metabolic flow: physicochemical considerations. *Curr. Top. Cell. Regul.* **33**:361-390.
- [141] **Rudolph, J., and J. Stubbe.** 1995. Investigation of the mechanism of phosphoribosylamine transfer from glutamine phosphoribosylpyrophosphate amidotransferase to glycylamide ribonucleotide synthetase. *Biochemistry* **34**:2241-2250.
- [142] **Ushiroyama, T., T. Fukushima, J. D. Styre, and H. O. Spivey.** 1992. Substrate

channeling of NADH in mitochondrial redox processes. *Curr. Top. Cell. Regul.* **33**:291-307.

[143] **Ovadi, J., Y. Huang, and H. O. Spivey.** 1994. Binding of malate dehydrogenase and NADH channelling to complex I. *J. Mol. Recognit.* **7**:265-272.

[144] **Raushel, F. M., J. B. Thoden, and H. M. Holden.** 2003. Enzymes with molecular tunnels. *Acc. Chem. Res.* **36**:539–548.

[145] **Trujillo, M., R. Duncan, and D. V. Santi.** 1997. Construction of a homodimeric dihydrofolate reductase-thymidylate synthase bifunctional enzyme. *Protein Eng.* **10**:567-573.

[146] **Miles, E. W.** 2001. Tryptophan synthase: a multienzyme complex with an intramolecular tunnel. *Chem. Rec.* **1**:140-151.

[147] **Ngo, H., N. Kimmich, R. Harris, D. Nicks, L. Blumenstein, V. Kulik, T. R. Barends, I. Schlichting, and M. F. Dunn.** 2007. Allosteric regulation of substrate channeling in tryptophan synthase: modulation of the L-serine reaction in stage I of the β -reaction by α -site ligands. *Biochemistry* **46**:7740-7753.

[148] **Miles, B. W., and F. M. Raushel.** 2000. Synchronization of the three reaction centers within carbamoyl phosphate synthetase. *Biochemistry* **39**:5051-5056.

[149] **Pierce Biotechnology Inc.** 2006. Cross-linking reagents technical handbook. Rockford, Illinois.

[150] **Gao, B., and H. R. Ellis.** 2007. Mechanism of flavin reduction in the alkanesulfonate monooxygenase system. *Biochim. Biophys. Acta.* **1774**:359-367.

[151] **Bruice, T. C.** 1982. A progress report on studies of the activation of molecular oxygen by dihydroflavins. In: flavins and flavoproteins (V. Massey and C. H. Williams,

Eds.), pp. 265–277. Elsevier North-Holland, Inc., New York.

[152] **Marston, F. A. O.** 1986. The purification of eukaryotic polypeptides synthesized in *Escherichia coli*. *Biochem. J.* **240**:1-12.

[153] **Yon, J. M.** 1996. The specificity of protein aggregation. *Nature Biotechnol.* **14**:1231.

[154] **Thomas, J. G., and Baneyx, F.** 1996. Protein misfolding and inclusion body formation in recombinant *Escherichia coli* cells overexpressing heat-shock proteins. *J. Biol. Chem.* **271**:11141-11147.

[155] **Carrió, M. M., J. L. Corchero, A. Villaverde.** 1998. Dynamics of *in vivo* protein aggregation: building inclusion bodies in recombinant bacteria. *FEMS Microbiol. Lett.* **169**:9-15.

[156] **Strandberg, L., and S.-O Enfors.** 1991. Factors influencing inclusion body formation in the production of a fused protein in *Escherichia coli*. *Appl. Environ. Microbiol.* **57**:1669-1674.

[157] **Speed, M. A., Wang, D. I. C. and King, J.** 1996. Specificity aggregation of partially folded polypeptide chains: The molecular basis of inclusion body composition. *Nature Biotechnol.* **14**:1284-1287.

[158] **Auer, H. E., and F. E. Frerman.** 1980. Circular dichroism studies of acyl-CoA dehydrogenase and electron transfer flavoprotein. *J. Biol. Chem.* **255**:8157-8163.

[159] **Goetzman, E. S., M. He, T. V. Nguyen, and J. Vockley.** 2006. Functional analysis of acyl-CoA dehydrogenase catalytic residue mutants using surface plasmon resonance and circular dichroism. *Mol. Gen. Metabol.* **87**:233-242.

[160] **Filisetti, L., M. Fontecave, and V. Nivière.** 2003. Mechanism and substrate

specificity of the flavin reductase ActVB from *Streptomyces coelicolor*. J. Biol. Chem. **278**:296-303.

[161] **Green, N. S., E. Reisler, and K. N. Houk.** 2001. Quantitative evaluation of the lengths of homobifunctional protein cross-linking reagents used as molecular rulers. Protein Sci. **10**:1293-1304.

[162] **Sobrado, P., K. S. Lyle, S. P. Kaul, M. M. Turco, I. Arabshahi, A. Marwah, and B. G. Fox.** 2006. Identification of the binding region of the [2Fe-2S] ferredoxin in stearoyl-acyl carrier protein desaturase: insight into the catalytic complex and mechanism of action. Biochemistry **45**:4848-4858.

[163] **Ingelman, M., S. Ramaswamy, V. Nivière, M. Fontecave, and H. Eklund.** 1999. Crystal structure of NAD(P)H:Flavin oxidoreductase from *Escherichia coli*. Biochemistry **38**:7040-7049.

[164] **Nivière, V., F. Fieschi, J.-L. Décout, M. Fontecave.** 1996. Is the NAD(P)H:flavin oxidoreductase from *Escherichia coli* a member of the ferredoxin-NADP⁺ reductase family? J. Biol. Chem. **271**:16656-16661.

[165] **Bruns, C. M., and P. A. Karplus.** 1995. Refined crystal structure of spinach ferredoxin reductase at 1.7 Å resolution: oxidized, reduced and 2'-phospho-5'-AMP bound states. J. Mol. Biol. **247**:125-145.

[166] **Karplus, P. A., M. J. Daniels, and J. R. Herriott.** 1991. Atomic structure of ferredoxin-NADP⁺ reductase: prototype for a structurally novel flavoenzyme family. Science **251**:60-66.

[167] **Karplus, P. A., and C. M. Bruns.** 1994. Structure function relations for ferredoxin reductase. J. Bioenerg. Biomembr. **26**:89-99.

- [168] **Aliverti, A., C. M. Bruns, V. E. Pandinit, P. A. Karplus, M. A. Vanoni, B. Curti, and G. Zanetti.** 1995. Involvement of serine 96 in the catalytic mechanism of ferredoxin-NADP⁺ reductase: structure-function relationship as studied by site-directed mutagenesis and X-ray crystallography. *Biochemistry* **34**:8371-8379.
- [169] **Medina, M., M. Martínez-Júlvez, J. K. Hurley, G. Tollin, and C. Gómez-Moreno.** 1998. Involvement of glutamic acid 301 in the catalytic mechanism of ferredoxin-NADP⁺ reductase from *Anabaena* PCC 7119. *Biochemistry* **37**:2715-2728.
- [170] **Alfieri, A., F. Fersini, N. Ruangchan, M. Prongjit, P. Chaiyen, and A. Mattevi.** 2006. Structure of the monooxygenase component of a two-component flavoprotein monooxygenase. *Proc. Natl. Acad. Sci.* **104**:1177-1182.
- [171] **Zhan, X., R. Carpenter, and H. R. Ellis.** 2007. Catalytic importance of the substrate binding order for the FMN-dependent alkanesulfonate monooxygenase enzyme (submitted to *Biochemistry*).
- [172] **Nivière, V., M. A. Vanoni, G. Zanetti, and M. Fontecave.** 1998. Reaction of the NAD(P)H:flavin oxidoreductase from *Escherichia coli* with NADPH and riboflavin: identification of intermediates. *Biochemistry* **37**:11879-11887.
- [173] **Gassner, G., L. Wang, C. Batie, and D. P. Ballou.** 1994. Reaction of phthalate dioxygenase reductase with NADH and NAD: kinetic and spectral characterization of intermediates. *Biochemistry* **33**:12184-12193.
- [174] **Sucharitakul, J., P. Chaiyen, B. Entsch, D. P. Ballou.** 2005. The reductase of p-hydroxyphenylacetate 3-hydroxylase from *Acinetobacter baumannii* requires p-hydroxyphenylacetate for effective catalysis. *Biochemistry* **44**:10434-10442.
- [175] **Miles, E. W., S. Rhee, and D. R. Davies.** 1999. The molecular basis of substrate

channeling. *J. Biol. Chem.* **274**:12193-12196.

[176] **Anderson, K. S., E. W. Miles, and K. A. Johnson.** 1991. Serine modulates substrate channeling in tryptophan synthase. A novel intersubunit triggering mechanism. *J. Biol. Chem.* **266**:8020-8033.

[177] **Hyde, C. C., S. A. Ahmed, E. A. Padlan, E. W. Miles, and D. R. Davies.** 1988. Three-dimensional structure of the tryptophan synthase alpha 2 beta 2 multienzyme complex from *Salmonella typhimurium*. *J. Biol. Chem.* **263**:17857-17871.

[178] **Anderson, K. S., A. Y. Kim, J. M. Quillen, E. Sayers, X.-J. Yang, and E. W. Miles.** 1995. Kinetic characterization of channel impaired mutants of tryptophan synthase. *J. Biol. Chem.* **270**:29936-29944.

[179] **Anderson, K. S., E. W. Miles, and K. A. Johnson.** 1991. Serine modulates substrate channeling in tryptophan synthase. A novel intersubunit triggering mechanism. *J. Biol. Chem.* **266**:8020-8033.

[180] **Thoden, J. B., X. Huang, F. M. Raushel, and H. M. Holden.** 2002. Carbamoyl-phosphate synthetase. Creation of an escape route for ammonia. *J. Biol. Chem.* **277**:39722-39727.

[181] **Massant, J., and N. Glansdorff.** 2004. Metabolic channelling of carbamoyl phosphate in the hyperthermophilic archaeon *Pyrococcus furiosus*: dynamic enzyme-enzyme interactions involved in the formation of the channelling complex. *Biochem. Soc. Trans.* **32**:306-309.

[182] **Kim, J., and F. M. Raushel.** 2004. Perforation of the tunnel wall in carbamoyl phosphate synthetase derails the passage of ammonia between sequential active sites. *Biochemistry* **43**:5334-5340.

- [183] **Miles, B. W., and F. M. Raushel.** 2000. Synchronization of the three reaction centers within carbamoyl phosphate synthetase. *Biochemistry* **39**:5051-5056.
- [184] **Huang, X., H. M. Holden, and F. M. Raushel.** 2001. Channeling of substrates and intermediates in enzyme-catalyzed reactions. *Annu. Rev. Biochem.* **70**:149-180.
- [185] **Ovadi, J.** 1991. Physiological significance of metabolic channelling. *J. Theor. Biol.* **152**:1-22.
- [186] **Perham, R. N.** 2000. Swinging arms and swinging domains in multifunctional enzymes: catalytic machines for multistep reactions. *Annu. Rev. Biochem.* **69**:961-1004.
- [187] **Thoden, J. B., H. M. Holden, G. Wesenberg, F. M. Raushel, and I. Rayment.** 1997. Structure of carbamoyl phosphate synthetase: A journey of 96 Å from substrate to product. *Biochemistry* **36**:6305-6316.
- [188] **Stroud, R. M.** 1994. An electrostatic highway. *Nat. Struct. Biol.* **1**:131-134.
- [189] **Knighton, D. R., C.-C. Kan, E. Howland, C. A. Janson, Z. Hostomska, K. M. Welsh, and D. A. Matthews.** 1994. Structure of and kinetic channelling in bifunctional dihydrofolate reductase-thymidylate synthase. *Nat. Struct. Biol.* **1**:186-194.